UNIVERSITAT POLITÈCNICA DE VALÈNCIA

DEPARTAMENTO DE QUÍMICA
INSTITUTO UNIVERSITARIO MIXTO DE
TECNOLOGÍA QUÍMICA (UPV-CSIC)

DOCTORAL THESIS

Photochemistry of 1,3-Dicarbonyl Compounds: DNA Photodamage *vs.* Photoprotection

MARIA ISABEL APARICI ESPERT

Valencia, June 2018

Directors:

Prof. Miguel A. Miranda Alonso

Dr. Virginie Lhiaubet-Vallet

CERTIFICATION

Miguel Ángel Miranda Alonso, full Professor of the Universitat Politècnica de València (UPV) and Virginie Lhiaubet-Vallet, tenured scientist of the ITQ CSIC UPV.

Certify that the Doctoral Thesis entitled “Photochemistry of 1,3-Dicarbonyl Compounds: DNA Photodamage *vs.* Photoprotection” has been developed by María Isabel Aparici Espert under their supervision in the Instituto Universitario Mixto de Tecnología Química (UPV-CSIC).

Prof. Miguel A. Miranda Alonso Dr. Virginie Lhiaubet-Vallet

En primer lugar, quiero agradecer a mis directores de tesis Miguel Ángel Miranda y Virginie Lhiaubet por haberme ofrecido la oportunidad de realizar la tesis con una ayuda económica asociada a un proyecto del CSIC. Asimismo, agradecerles a los dos la dedicación y paciencia que han tenido conmigo de manera incondicional, ya que gracias a ellos he crecido profesional y personalmente. ¡Muchas gracias!

A mi familia, mis padres Fernando y Paqui ya que ellos también han sido un pilar importante durante estos 5 años, ofreciéndome su apoyo incondicional en todo momento. A mis hermanos, Lara y Fernando, que también han estado siempre a mi lado dándome ánimo y fuerza. ¡Gracias!

A mi novio, Fran, gracias a su apoyo incondicional durante estos 3 últimos años. Siempre viendo la parte positiva y aprendiendo día a día. ¡Gracias!

Asimismo, agradecer también a mis compañeros de laboratorio, Gemma, Miguel, Vicky, Paula, Giacomo, Faber, Rebeca y Ana… con los cuales he podido compartir momentos buenos en el laboratorio, escuelas de formación y congresos. ¡Gracias!

Agradecer también a todo el ITQ, centro en el cual he podido llevar a cabo mi tesis doctoral, a todos los técnicos y miembros de este centro de investigación de renombre.

Abbreviations and Symbols

AAA	9-Anthraceneacetic acid
AAA-TEMPO	Intramolecular dyad AAA and 4-OH-TEMPO
AAPH	2,2'-Azobis(2-amidinopropane) dihydrochloride
AB	4-*tert*-Butyl-4'-methoxydibenzoylmethane
AB-KP dyad	Avobenzone-ketoprofen dyad
AB-DF dyad	Avobenzone-diclofenac dyad
ACN	Acetonitrile
AK	Actinic keratosis
BER	Base excision repair
BP	Benzophenone
CH_2Cl_2	Dichloromethane
CD_3CN	Deutered acetonitrile
$CDCl_3$	Deutered chloroform
Cyt	Cytosine
Cyt-Cyt	Cytosine-cytosine dyad
DF	Diclofenac
DNA	Deoxyribonucleic acid
D_2O	Deuterium oxide
DOHThy	5,6-Dihydroxy-5,6- dihydrothymine
DSB	Double-strand break
EPR	Electron paramagnetic resonance
E_T	Triplet excited state energy
EtOH	Ethanol
F	Fluorescence
FapyAde	*N*-(4,6-Diaminopyrimidin-5-yl)formamide
FapyGua	2,6-Diamino-4-hydroxy-5 formamido-pyrimidine
FordU	5-Formyl-2'-deoxyuridine
ForU	5-Formyluracil
FSK	Fibroblast skin
Gua	Guanine
HCl	Hydrochloric acid
HMdUra	5-Hydroxymethyl-2'-deoxyuridine
HOMO, HO	Highest occupied molecular orbital
HPLC	High-performance liquid chromatography
HRMS	High-resolution mass spectroscopy
ICL	Interstrand cross link
IC	Internal conversion
ISC	Intersystem crossing

KP	Ketoprofen
KPMe	Ketoprofen methyl esther
LA	Linoleic acid
LA1	13-Hydroxyperoxide-*cis*-9, *trans*-11-octadecadienoic acid
LA2	9-Hydroxyperoxide-*trans*-10, *cis*-12-octadecadienoic acid
LA3	9-Hydroxyperoxide-*trans*-10, *trans*-12-octadecadienoic acid
LA4	13-Hydroxyperoxide-*trans*-9, *trans*-11-octadecadienoic acid
LFP	Laser Flash Photolysis
LUMO, LU	Lowest unoccupied molecular orbital
MED	Minimal erythemal light dose
MeOH	Methanol
NER	Nucleotide excision repair
NMR	Nuclear magnetic resonance
NSAIDs	Non-steroidal anti-inflammatory drugs
PPG	Photolabile protecting groups
4-OH-TEMPO	4-Hydroxy-2,2,6,6-tetramethylpiperidine-1 oxyl
8-OxoAde	8-Oxo-7,8-dihydroadenine
8-OxodGuo	8-Oxo-7,8-dihydro-2'-deoxyguanosine
P	Phosphorescence
PBS	Phosphate-buffered saline
Ph	Photosensitizer
6-4PP	(6-4) Photoproduct
PPD	Persistent pigment darkening
Pyo	5-Methyl-2-pyrimidone
Pyr	Pyrimidine
Pyr<>Pyr	Cyclobutane pyrimidine dimers (CPDs)
ROS	Reactive oxygen species
SCGE	Single-cell gel electrophoresis
SPF	Sunscreen Protection Factor
SSB	Single-strand break
SSET	Singlet-singlet energy transfer
SSL	Simulated sunlight
TEMP	2,2,6,6-Tetramethylpiperidine
TFA	Trifluoroacetic acid
Thd	Thymidine

TTET	Triplet-triplet energy transfer
Thy	Thymine
Thy-Thy	Thymine-thymine dyad
Thy<>Thy	Cyclobutane thymine dimers
ThyGlycol	5,6-Dihydroxy-5,6-dihydrothymine
UPLC	Ultra performance liquid chromatography
Ura	Uracil
Ura<>Ura	Cyclobutane uracil dimers
UV	Ultraviolet light
τ	Lifetime
Φ	Quantum yield
$^1O_2$	Singlet oxygen
λ	Wavelength

Chapter 1: General Introduction 1
1.1. Photochemistry of 1,3-dicarbonyl compounds 3
1.2. UV light implications in DNA damage and repair mechanisms 14
1.3. Measures for skin cancer prevention 26
1.4. References 31

Chapter 2: General Objectives 41

Chapter 3: A Combined Experimental and Theoretical Approach to the Photogeneration of 5,6-Dihydropyrimidin 5-yl Radicals in Nonaqueous Media 43
1.1. Introduction 43
1.2. Objectives 48
1.3. Results and Discussion 49
1.4. Conclusions 60
1.5. Experimental Section 60
1.6. References 80

Chapter 4: 5-Formyluracil as potential intrinsic DNA photosensitizer 85
1.1. Introduction 85
1.2. Objectives 88
1.3. Results and Discussion 89
1.4. Conclusions 104
1.5. Experimental Section 105
1.6. References 111

Chapter 5: Photocages for protection and controlled release of bioactive compounds: (S)-Ketoprofen and Diclofenac 115
1.1. Introduction 115
1.2. Objectives 123
1.3. Results and Discussion 124
1.4. Conclusions 138
1.5. Experimental Section 139
1.6. References 144

Chapter 6: Photostability and photogenotoxicity studies on AB-KP dyad 149
1.1. Introduction 149
1.2. Objectives 153
1.3. Results and Discussion 153
1.4. Conclusions 161
1.5. Experimental Section 161

1.6. References 164

Chapter 7: Instrumentation 169
1.1. Absorption measurements 169
1.2. Emission measurements 169
1.3. Laser Flash Photolysis (LPF) 169
1.4. Steady-state photolysis 170
1.5. Femtosecond transient absorption spectroscopy 170
1.6. Nuclear Magnetic Resonance (NMR) 171
1.7. Electronic paramagnetic resonance (EPR) experiments using spin trap 171
1.8. UPLC-MS/MS analyses 171
1.9. HPLC analyses 172

Chapter 8: Annex I 173

Chapter 9: General conclusions 179

Chapter 1:

General Introduction

1. Introduction

Photochemistry is the science that studies chemical reactions triggered by the absorption of ultraviolet-visible (200 - 700 nm) and infrared light (700 - 2500 nm) by molecules. Nowadays, photochemistry is present in daily life through technological applications but it is also essential in many biological processes such as vitamin D synthesis in humans, photosynthesis in plants as well as in the appearance of pathologies such as skin cancer.[1]

The whole process starts when a chromophore in its ground state (S_0) is radiatively excited, the incident photons boost one electron from the highest occupied molecular orbital (HOMO, HO) to the lowest unoccupied molecular orbital (LUMO, LU) or even to an upper energy orbital. Thus, unstable singlet excited states (S_n or S_1) are populated and they tend to relax to return to the stable ground state. Deactivation can occur through non-radiative (*ie.* internal conversion, IC) or through radiative processes (*ie.* fluorescence, F) by generation of light emission.

Molecules in their singlet excited state can also undergo another pathway, called intersystem crossing (ISC), that involves forbidden transitions and where a change in the spin multiplicity gives rise to triplet excited state (T_n or T_1). In turn, the generated triplet excited state will deactivate through non-radiative or radiative (*ie.* phosphorescence, P) processes.

As a general rule, IC between successive S_n / S_{n-1} or T_n / T_{n-1} states is so efficient that processes such as emission, ISC, or photochemical reactions cannot compete until reaching the lowest singlet (S_1) or triplet excited state (T_1). In these states, the energy gap to return to S_0 is higher; thus, the IC rate constant is decreased, opening the way to the other processes.

However, relaxation of the excited states does not always lead to the original molecule in its ground state, and unimolecular photoreactions might also take place and yield photoproducts

formation. In this context, the photo-Fries, photo-Claisen, Norrish type I and II are among the most reported photoreactions.[2]

In the presence of other substrates, intermolecular processes could arise. They are for example energy transfer between states with the same multiplicity, *ie.* singlet-singlet or triplet-triplet energy transfer (abbreviated as SSET and TTET, respectively), electron transfer, photocycloaddition, etc.[3], [4]

The molecules in their excited states are unstable and generally relax in a sub-second timescale, being triplet excited states longer-lived (with τ of μs to ms) than singlet excited states (with τ of ns range). However, spectroscopic techniques allow the study of the physical (photophysics) and chemical (photochemistry) changes these states undergo. The Jablonski diagram is universally used to represent the electronic states of a molecule and the possible transitions that they can suffer (Figure 1).

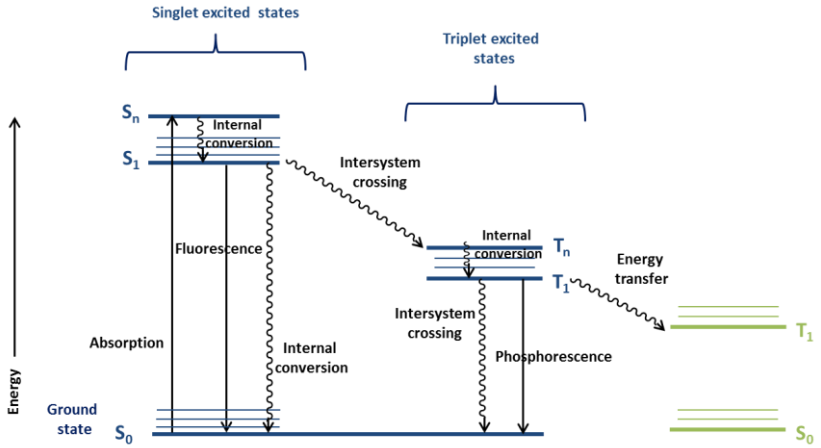

Figure 1. Electronic states of a molecule and the corresponding photochemical processes: Jablonski diagram.

In this context, it is essential to gain knowledge in the physical properties of the different chromophores as well as the photoreactions they can suffer. This doctoral thesis is centered on the role played by 1,3-dicarbonyl compounds as DNA damaging

agents, but also as part of a photolabile molecule designed for a new photoprotection strategy for photosensitizing drugs. For this purpose, it is necessary to detail the photochemistry of the carbonyl and 1,3-dicarbonyl derivatives and more concretely the reactions undergone by this chromophore in the presence of UV light.

1.1. Photochemistry of 1,3-dicarbonyl compounds

The presence of two carbonyl functional groups in β position confers to these compounds interesting features in the ground state, especially when a hydrogen is present in α position allowing the keto-enol equilibrium to take place.[5] Thus, 1,3-dicarbonyl derivatives can exist, in theory, under the form of different isomers, which include a hydrogen-bonded enol (chelated enol, CE), non-hydrogen bonded enols (non chelated enols, NCEs) and diketones (Figure 2).

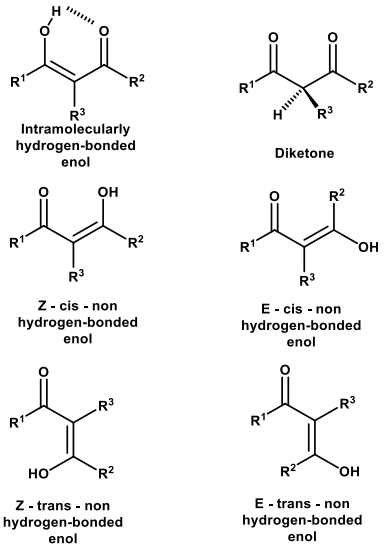

Figure 2. Possible isomers of 1,3-dicarbonyl compounds.

The intramolecular hydrogen bonding stabilizes the keto-enol isomer (chelated enol, CE); therefore, it is largely favored over the diketo non-chelated forms. The nature of the substituents R^1, R^2 and R^3 is the main factor that determines the composition of isomers mixture. Thus, bulky substituents such as phenyl groups at R^1 and R^2 positions favor the keto-enol form over the diketone tautomer.[6]

The solvent is also an important factor in the keto-enol equilibrium of 1,3-dicarbonyl compounds. Polar solvents tend to stabilize the diketo tautomer *vs.* the keto-enol form.[7] Indeed, in the latter, the electron density is partially delocalized around the chelated ring. The diketo isomer has a higher polarity, and is stabilized in polar solvents by solvation of the oxygen atoms of the two carbonyls; therefore, the content of diketo tautomer in solution increases with the polarity and hydrogen-bond ability of solvents. The ratio between diketo and keto-enol tautomers also varies with temperature as an increase of the temperature causes a slight shift in favor of the diketo form in the solid state.[5]

A remarkable property of the chelated isomer relies on its strong UV absorption in the 250-350 nm region that is due to the β-hydroxyvinyl carbonyl system. The position of the highest absorption band is independent of the type of aliphatic substituents R^1, R^2, and R^3. However, the presence of a benzyl substituent (R^1 = PhCH), produces a bathochromic shift in the absorption maximum. Aromatic substituents in R^2 and R^3 give rise to a new absorption band in the 250-260 nm range that can be assigned to the aroyl group of the diketonic form. [5]

The photochemistry of 1,3-dicarbonyl compounds includes characteristic intramolecular transformations. Typical photoreactivity for non enolizable derivatives is Norrish Type I photoreaction, decarbonylation, 1,3-shift and conformational changes (Scheme 1).[5] Concerning enolizable 1,3-dicarbonyl compounds, the main pathway is photoisomerization to the diketo tautomer, which is the reactive

form and can suffer subsequent α-cleavage *ie.* a Norrish Type I reaction (Scheme 2). An nπ* triplet state is believed to be responsible for this photoreactivity .[5]

Intermolecularly, keto enol form can react with alkenes by means of the typical De Mayo reaction (Scheme 2). In this case, a [2+2] photocycloaddition occurs between the double bond of the keto enol isomer and that of a nearby olefin; this leads to a cyclobutanol intermediate, which after a retro aldol condensation yields a 1,5-dicarbonyl compound.[8]

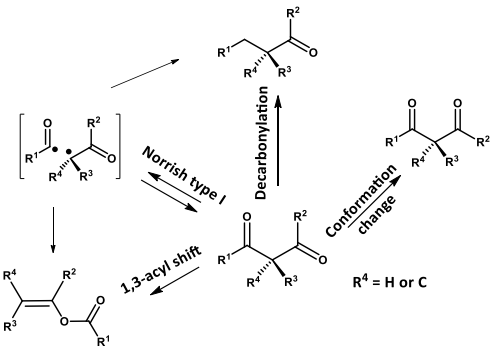

Scheme 1. Photoreactions of non enolizable 1,3-dicarbonyl compounds.

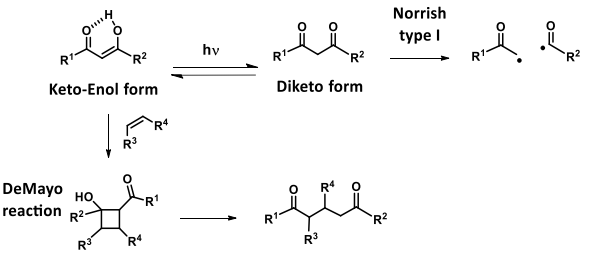

Scheme 2. Photoreactions of enolizable 1,3-dicarbonyl compounds.

In the late 70s, flash photolysis studies performed on 1,3-dicarbonyl compounds reported their facile photoisomerization from the CE to a non chelated and short lived enol that might return to the initial form and/or evolve to the diketo isomer. [6] More recently, the photophysics of 1,3-dicarbonyl derivatives have been addressed by means of ultrafast spectroscopy in order to shed some light on the results previously obtained.[9],[10] These studies have proposed the initial cleavage of the intramolecular H-bond to yield different non

chelated conformers from a singlet excited state, whereas formation of the diketo isomer might result from the triplet excited state after intersystem crossing. [9],[10]

1.1.1. The role of 1,3-dicarbonyl compounds in photoprotection: dibenzoylmethane and its derivatives

Dibenzoylmethane (DBM) structures have largely been used in the cosmetic industry as solar filters (Figure 3) since they present large UVA absorption properties.[11],[12],[13],[14] Both in solid and in solution, these dibenzoylmethanes exist mainly as the chelated keto-enol form; this has been attributed to the electron withdrawing ability and the bulky nature of the phenyl ring substituent.

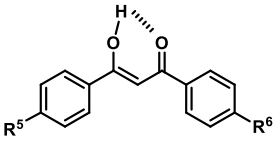

R^5	R^6	
H	H	Dibenzoylmethane
OMe	*t*-Bu	Parsol 1789 - Avobenzone (AB)
H	*t*-Bu	Eusolex 8020
OMe	OMe	Parsol DAM

Figure 3. Dibenzoylmethane structures used as UVA solar filters.

The chelated enol form of DBMs shows strong absorption bands in the UVA region (315–380 nm) due to the $\pi\pi^*$ transition of the chelated π-electron system.[15] DBMs are non-fluorescent in solution, which indicates the presence of efficient and ultrafast non-radiative processes from the singlet excited states.

The most important representative of the DBM family is avobenzone (AB, 4-*tert*-butyl-4'-methoxydibenzoylmethane, also known as Parsol 1789), which is one of the most widely used UVA sunscreens. It exhibits a large absorbance at 350 nm due to its chelated enol form, largely favored in the ground state. After UV light absorption, extensive photoisomerization to the β-diketone occurs

(band absorption at 260 - 280 nm) (Scheme 3 and Figure 4). However, this change is reversible, and the enol form is slowly recovered in the dark.[16]

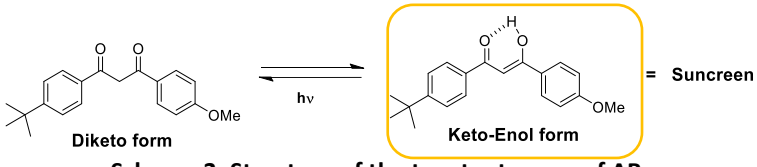

Scheme 3. Structure of the two tautomers of AB.

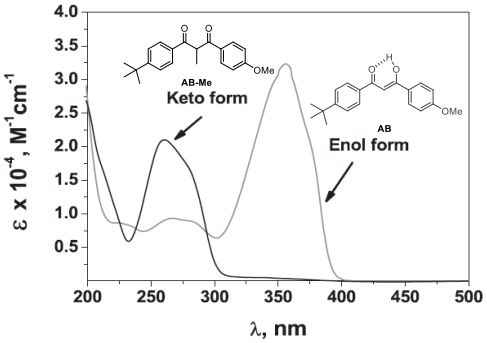

Figure 4. UV-Vis absorption spectra of the two AB tautomers, enol form, grey line and diketo (obtained from AB-Me model compound) form black line.

The photochemistry of DBM derivatives has been widely studied and their sensitivity to light is dependent on experimental conditions. They are photolabile towards UVA light in non-polar solvents, whereas in polar solvents photodegradation is slowed down.[14],[16],[17] Photodegradation involves a Norrish Type I photoreaction followed by radical recombination or H abstraction and/or oxidation (Scheme 4).[14]

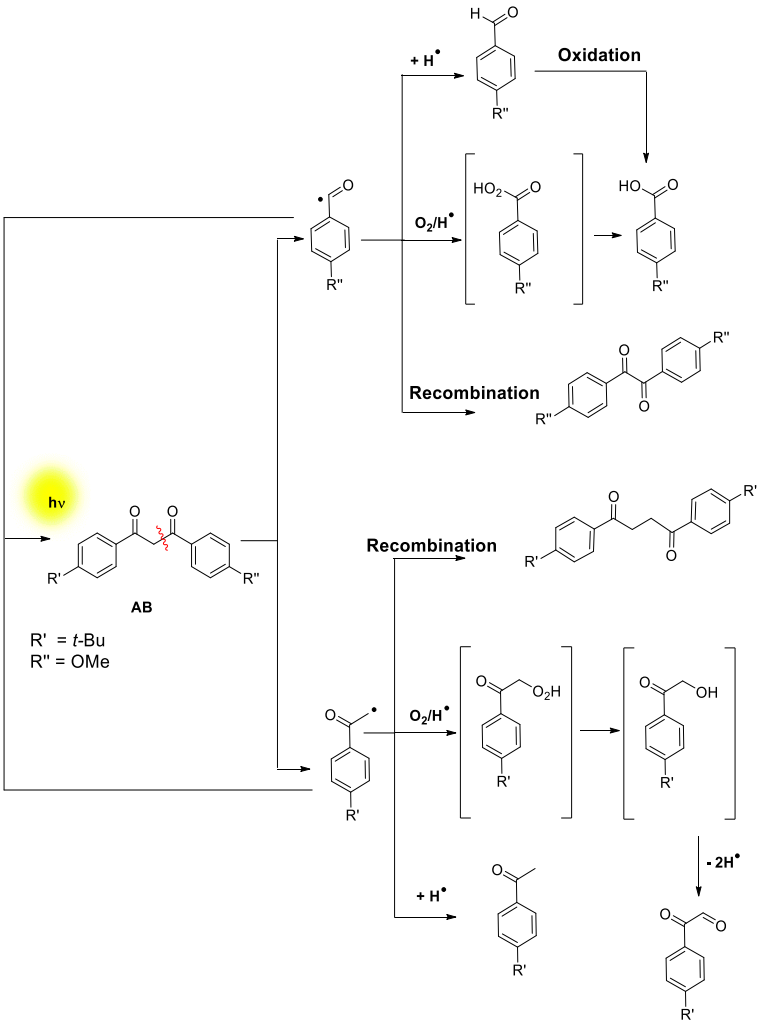

Scheme 4. Photodegradation of 4-*tert*-butyl-4'-methoxydibenzoylmethane (AB) in solutions (R and R´´ are mutually exchangeable).

From a photophysical point of view, the triplet excited state of AB has been observed by means of phosphorescence experiments in ethanol at 77 K; and an energy of 244.1 kJ/mol has been determined for this state. [15] Nanosecond laser flash photolysis of AB (λ_{exc} = 355 nm) leads to absorbance changes in the UV region with a peak at 300 nm and bleaching of the ground state at *ca.* 360 nm.[13],[15],[18],[19],[20] Careful analyses of the kinetics under different

conditions have evidenced that excitation of the CE isomer leads to the formation of different NCEs.[13],[19],[21] In this context, a first isomer NCE1 has been observed as a result of *cis*/*trans* isomerization of CE.[13],[19] The other isomers NCE2 and NCE3 are formed through rotation of single bonds, but fast relaxation does not allow their detection under the experimental time window.[19],[21] Formation of the diketo isomer has been proposed to result from NCE1; however, it has been observed only in acetonitrile solutions due to a potential stabilization of CE by protic solvents.[19]

More details on the isomerization have been obtained through the study of the AB dynamics in the picosecond timescale [22] (Scheme 5). This study reveals a complex evolution of the CE excited state that leads, at least, to a vibrationally excited CE (CE_{vib}) and three NCEs. Kinetics have shown that CE_{vib}, NCE2 and NCE3 relax in the picosecond time range, while NCE1 is longer lived. Moreover, the fractional population of each NCE isomer (ϕ_{NCE}, Scheme 5) has been estimated from the amplitude of the fitting of their time evolution. Unfortunately, no clear conclusion about the formation of the diketo form has been drawn.

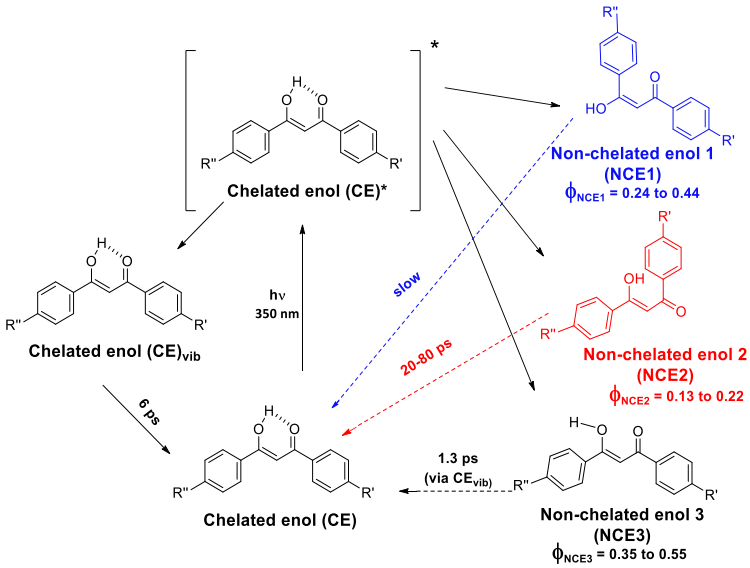

Scheme 5. Evolution of AB after excitation at 350 nm at the picosecond timescale.

The study of photochemistry and photophysics of the diketo form is complex due to its instability and to the slow recovering of the chelated keto-enol form. Preliminary results have been obtained by registering the transient absorption spectra of a pre-irradiated solution of AB, where part of the CE isomer was transformed into the diketo tautomer.[13]

Recently, our group has synthesized a pure blocked diketo form of AB by methylation at the α-carbonyl position (AB-Me). [23] As expected, AB-Me does not show the UVA absorption band but exhibits a maximum at 260 nm (Figure 4). Phosphorescence experiments, in ethanol at 77 K, have evidenced a spectrum with the vibrational levels of the carbonyl progression; a triplet energy of 295.5 kJ/mol was determined from its 0-0 band.[15] Nanosecond laser flash photolysis experiments for AB-Me derivative have shown a broad transient absorption spectrum with a maximum at 380 nm, which decays with a lifetime of $\tau \sim 0.9$ μs. Quenching studies in the presence of β-carotene have revealed the appearance of the typical β-carotene triplet excited state at 520 nm concomitantly with the decay of the 380 nm signal, as expected from a triplet-triplet energy transfer.[23] Thus, this 380 nm signal has been assigned to the triplet excited state of AB-Me.

As abovementioned, the photoinduced diketo form is the main player in DBM photodegradation (Scheme 4). Photostability is an important issue when talking about photoprotection because the Norrish Type I process, occurring from the diketone triplet state, induces radicals that can be potentially reactive towards skin components or biological substrates. Indeed, the photosensitizing effect of AB has been attributed to this diketo isomer as an intermediate in the formation of allergens such as arylglyoxals.[24] Moreover, studies in the presence of biologically relevant targets have evidenced the AB damaging potential through strand breaks formation of plasmid DNA[25], oxidative modification of albumin[26], decreased survival of yeast cells[27], cytotoxicity to human keratinocytes[28] and lipid peroxidation.[29]

To overcome this instability, sunscreens contain other components aimed at stabilizing AB. Indeed, its combination with triazine UV-B filter decreased its undesirable effects by an efficient quenching of AB triplet excited state in its the diketo form.[23] Filter–filter interactions have been examined as well using octyl methoxycinnamate, bis-ethylhexyloxyphenol methoxyphenyl triazine, octocrylene, diethylamino hydroxybenzoyl hexyl benzoate, octyl triazone and dioctyl butamido triazone.[30] Moreover, AB has also been stabilized by the use of antioxidants such as vitamin C, vitamin E, and ubiquinone. This latter has shown the most effective photostabilization together with an increase in the sun protection factor (SPF).[31]

In this thesis, we will take advantage of another feature of the diketo form of AB to propose a new strategy for photoprotection based on the presence in its structure of two phenacyl moieties, which are well known photolabile groups (see Chap. 5).

1.1.2. 1,3-Dicarbonyl compounds derived from DNA pyrimidine nucleobases

The photoreactivity of the 1,3-dicarbonyl compounds has also been exploited to shed light on the chemical fate of 5,6-dihydropyrimidin-5-yl radicals within DNA. In this context, introduction of *tert*-butyl (or isopropyl) ketone as substituent at C5 of dihydropyrimidines has led to the regioselective generation of C5 radicals.[32], [33], [34] This reaction occurs through a Norrish Type I mechanism where the photocleavage in position α of the ketone yields the purported radical formation. Moreover, absorption of the *tert*-butyl (or isopropyl) ketone substituent at λ>300 nm allows a selective UVB/UVA excitation of the photolabile moiety without irradiating the canonical nucleobases (Scheme 6).

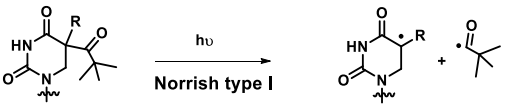

Scheme 6. Norrish Type I photoreaction for 1,3-dicarbonyl pyrimidine compounds.

Before the development of these photolabile compounds, conclusions were obtained from analysis of mixtures resulting from γ-radiolysis of pyrimidines, where radicals are generated without any selectivity.[35],[36] Thus, synthesis and steady-state photolysis of these 1,3-dicarbonyl derivatives have represented an important advance in the study of the radical fate in pyrimidine nucleobases. Indeed, it has been shown that the 5,6-dihydrothymidin-5-peroxyl radical produced under aerobic conditions leads to direct strand breaks by H abstraction at C1' o C2' of the sugar moiety of the 5'-adjacent nucleoside [32]. Concerning the 5,6-dihydrouridin-5-yl radical, its generation under anaerobic conditions has evidenced its ability to yield direct strand breaks in an intranucleotidyl and internucleotidyl manner in single and double stranded oligonucleotides. [34]

A more detailed description of the radical reactivity will be provided in Chapter 3, where we have addressed the photochemistry in non aqueous media of a C5 dihydropyrimidine radical precursor belonging to the 1,3-dicarbonyl family.

Interestingly, 1,3-dicarbonyl compounds have also found application in DNA photodamage as for 5-formyl-2'-deoxyuridine (FordU), which is the major oxidatively generated lesion in pyrimidine bases. The presence of the formyl electron-withdrawing group in the C5-position confers it particular properties. On the one hand, this yields a more acidic N3-hydrogen and thus pK_a values are decreased. A pK_a value of *ca.* 8.12 has been experimentally determined for FordU, which is significantly higher than that measured for the corresponding free base (uracil) but lower than that of 2′-

deoxyuridine nucleoside (pK_a of *ca.* 9.69).[37] This finding has been related to changes in the H-bonding capability affecting the base pairing with its complementary counterpart, which could result in miscoding during replication. [38],[39] Moreover, FordU is able to form covalent cross-links with proteins through the particular chemistry of the aldehyde functional group with amino or thiol-containing amino acids, leading to a Schiff base formation.[40]

On the other hand, keto–enol equilibrium is occurring in a pH-independent way (Scheme 7), with the diketo form favored over the keto-enol tautomer. Conversion of this diketo tautomer to an ionized (anionic) form increases with the pH (Scheme 7)[39] inducing changes in the UV absorption spectrum, which suffers a bathochromic shift.[37] Therefore, these changes could extend the active fraction of sunlight making possible excitation of this damaged DNA at longer wavelengths than that of the parent base.

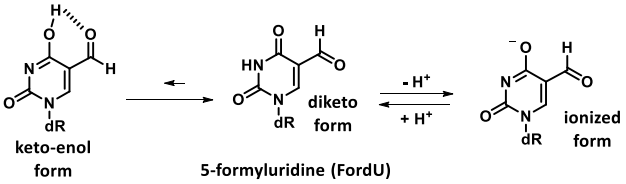

Scheme 7. Two tautomeric forms of FordU and its ionized form in high pH conditions.

Thus, FordU might play the role of an intrinsic photosensitizer as it fulfills the first basic requirement for a photosensitizing compound *ie.* UVB/UVA absorption. Since up to now there is no photophysical or photobiological data available in the literature, the photochemistry 5-formyluracil and its ability to behave as an endogenous DNA photodamaging agent will be discussed in Chapter 4.

2. UV Light implications in DNA damage and repair

Interaction between solar light and biological compounds is a matter of concern because the resulting photochemical reactions might originate important pathologies. In this context, it is now well-established that DNA is the key cellular macromolecule involved in the carcinogenic effects due to solar radiation.[41],[42] Furthermore, DNA is highly susceptible to chemical modifications by endogenous and exogenous agents. In fact, UV radiation emanating from the sun, considered an exogenous physical agent, is responsible for skin cancers in humans.[43]

Among the different regions of sunlight radiation reaching the Earth surface, the ultraviolet (UV) light is the main deleterious agent for DNA. It is subdivided in UVC (100-290 nm), UVB (290-320 nm) and UVA (320-400 nm).

Fortunately, the ozone layer of the atmosphere is capable of filtering almost all the UVC radiation. Indeed, UVC is the most energetic and the most damaging radiation for biological components because DNA or proteins generally present their main absorption band in this range. The UVB is also blocked to a large extent (90-95%); however, the remaining component is of paramount importance as it can be directly absorbed by biomolecules, or it can activate endogenous or exogenous chemicals (photosensitizers). Finally, UVA radiation is not significantly blocked by the atmosphere, but it is barely absorbed by DNA or other biomolecules. However, by contrast with the other wavelengths, UVA is capable of reaching the skin dermis, and hence, it can activate chemicals that can be at the origin of biomolecular damage. Both UVB and UVA are considered as relevant biological radiations (Figure 5).

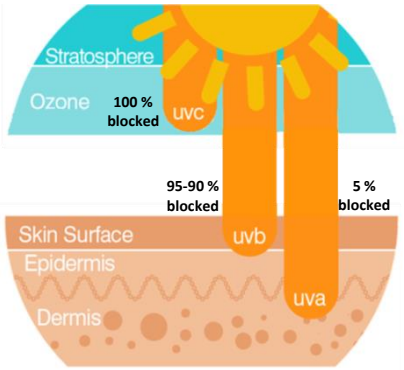

Figure 5. Ozone layer UV light blocking ability and UV light penetration into the skin surface.

Thus, the photochemical damages produced on biomolecules are divided in two types of processes depending on the involvement or not of an additional molecule. Direct damages are formed, principally in the UVC and UVB, after light absorption by the macromolecule. The radiation can also be absorbed by an external agent that will be the responsible for the photoreaction with the biomolecule. This latter process is called photosensitization and generally takes place for UVA/UVB irradiations (Figure 6). The distribution of DNA lesions depends on the type of process. For direct irradiation, thymine (Thy) is the most UV sensitive nucleobase and leads to the formation of cyclobutane pyrimidine dimers (CPDs), (6-4) photoproducts (6-4PPs), Dewar valence isomers. Recent results have established that 2´-deoxyguanosine can be damaged to 8-oxo-7,8-dihydro-2´-deoxyguanosine (8-OxodGuo) by direct irradiation. Photosensitization becomes an important pathway of reaction in the UVA, where light is not directly absorbed by DNA components. Excitation of the endogenous or exogenous photosensitizer can lead to a huge variety of photoproducts arising from processes such as energy transfer, electron transfer or production of reactive oxygen species (ROS) (Figure 6).[43], [44]

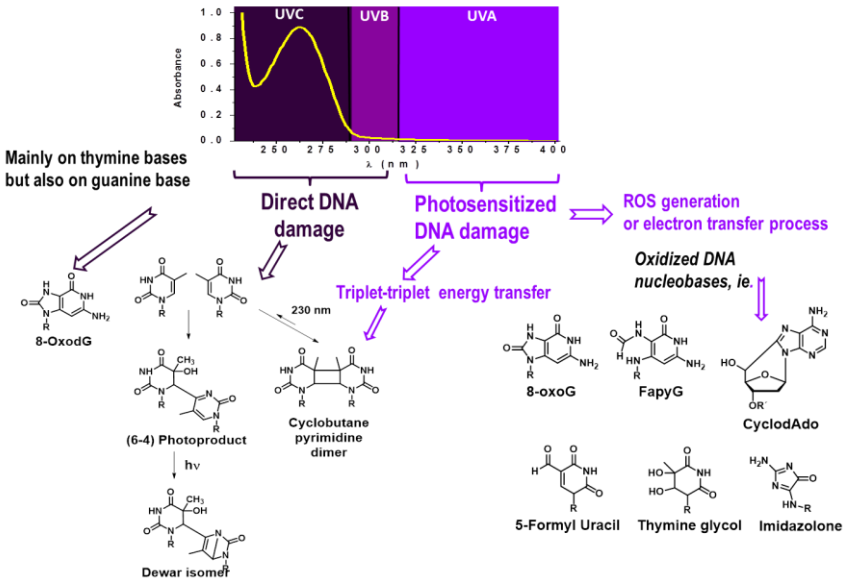

Figure 6. Direct and photosensitized damage.

Nonetheless, cells are equipped with complex and sophisticated systems such as DNA repair, damage tolerance, cell cycle checkpoints, and cell death pathways, which work altogether to reduce the undesirable consequences of DNA damage.

More concretely, cell responds to DNA damage by triggering DNA repair pathways, which are base excision repair (BER), nucleotide excision repair (NER), mismatch repair (MMR), homologous recombination (HR), and nonhomologous end joining (NHEJ).[43] In humans, the UV-induced DNA damages are repaired by the excision of the damaged portion, followed by the resynthesis using the undamaged strand as template and final ligation. For instance, BER helps to excise small oxidized bases, strand breaks and abasic sites [4], [44], [45] and NER excises bulky photoproducts (CPDs and 6-4PPs). [4],[45]

When there is a low level of DNA damage, DNA repair is activated whereas at high DNA damage levels DNA repair is saturated and unrepaired DNA damage persists activating one of the death programs, including apoptosis, regulated necrosis and autophagy in order to get rid of cells with extensive genome instability.[46] Even if

death programs prevent in a high rate mutations and cancer spread, these programs can be altered as people become older or in certain circumstances, allowing then the propagation of mutations.

Hence, when DNA repair fails, damage tolerance is carried out by a specific type of polymerase. This enzyme bypasses the damage and enables the continuation of replication, but with the possibility of an introduction of an incorrect base that can be fixed into a mutation in the subsequent round of replication. It is well-established that an important part of the cancer etiology lies in the accumulation of DNA mutations that lead to aberrant RNA and protein, with widespread deregulation of transcription during oncogenesis.[43],[46],[47] Hence, altogether the repair processes are key to maintaining genetic stability in cells.

2.1. Direct DNA damage induced by UVC and UVB light

Until few years ago, it was described that the directly induced DNA damage in UVC/UVB was centered on the pyrimidine bases generating the dimeric photoproducts, *ie.* cyclobutane pyrimidine dimers (CPDs), (6-4) photoproducts (6-4PPs) and their Dewar valence isomers. However, a recent study has shown that guanine might also be a reactive base under these conditions.

2.1.1. Cyclobutane Pyrimidine Dimers

The cyclobutane pyrimidine dimers (CPDs) arise from a fast [2+2] cycloaddition reaction, occurring in few picoseconds, between the C5-C6 double bond of two adjacent pyrimidines. Their formation involves the ππ* excited states; however, the scientific community is still debating the excited state involved in this reaction, whether a localized or delocalized singlet or the triplet state (Figure 7A). [44]

In naked and cellular DNA, four possible CPDs have been isolated, they correspond to the TT (T<>T), CT (C<>T), TC (T<>C) and CC (C<>C) bipyrimidine sequences. A large number of isomers can be produced in function of the orientation of the two nucleobases, the different conformation being *cis, syn; trans, syn; trans, anti; cis, anti*. Due to structural features and natural constraints of the double DNA helix in B conformation, which is the most common in Nature, the predominant isomer is the *cis, syn* (Figure 7B). [4], [44], [45]

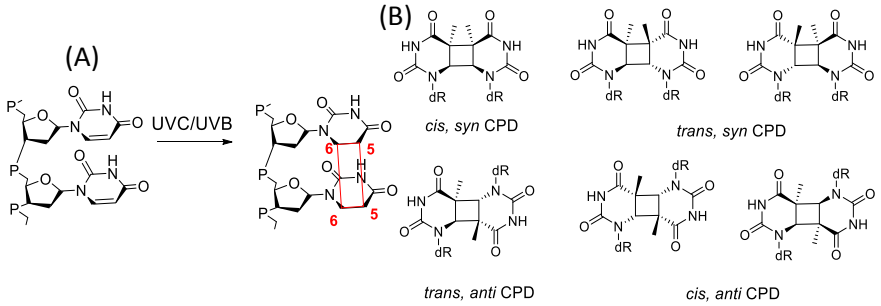

Figure 7. A) [2+2] photocycloaddition of C5-C6 double bonds of two adjacent pyrimidines. (B) Different thymine CPDs isomers.

CPDs account for 2% of the total of DNA photodamage in humans and their distribution in isolated and cellular DNA for TT, TC, CT and CC is in a 10:5:2:1 ratio.[45] These lesions exhibit a low repair rate by NER contributing to mutagenesis.[4] The CPDs containing a cytosine are the most mutagenic since they may undergo a further dark chemical modification known as deamination by reacting with water. In fact, the exocyclic amino group is substituted by a hydroxyl group, converting the cytosine nucleobase into a uracil. The original cytosine should lead to the incorporation of guanine upon replication; but, uracil would miscode for an adenine. This means that homocytosine CPDs generate a characteristic CC → TT transition; the so-called UV signature mutation.[45],[48]

2.1.2. 6-4PPs and their Dewar valence isomers

The (6-4) photoproducts are produced in few milliseconds through a Paternò-Büchi reaction. This photochemical reaction consists of a [2+2] cycloaddition between de C5-C6 double bond of the 5'-end pyrimidine base and the C4 carbonyl group of a 3'-end thymine (Figure 8). It has been proposed that the photoreaction occurs through the nπ* singlet excited states as 6-4PPs are only observed by direct irradiation of DNA, and not by photosensitization as CPDs do (see section 2.3.3. CPDs por TTET).[44], [4]

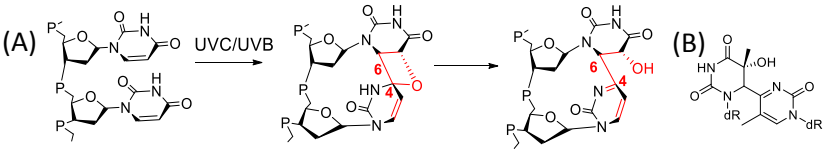

Figure 8. [2+2] cycloaddition between C5-C6 double bond and C4 carbonyl group of two adjacent pyridimines. B) TT 6-4PPs structure.

The 6-4PPs have been observed in TT, TC, CT and CC bipyrimidine sequences.[44] The intermediates of the photocycloaddition are oxetanes or azetidines depending on the presence of a thymine or cytosine at the 3´-end (Figure 8A). Both intermediates are highly unstable and are consequently converted into their respective 6-4PPs. By contrast with CPDs, these photoproducts exhibit a strong absorption at 315 nm for TC and CC sequences or at 325 nm in TT and CT, which is due to the presence of the pyrimidone ring at the 3´-end. [44], [4]

The 6-4PPs are produced in lower yields than CPDs, the ratio being of 1:2 or 1:8 depending on the bipyrimidine sequences and the detection methods. Although 6-4PPs are quite mutagenic, they are repaired by NER mechanism much faster than CPDs. Thereby, they contribute to a lesser extent to UV mutagenesis.[45]

Once the pyrimidone ring is formed, it can absorb light around 320 nm triggering a 4π electrocyclization through singlet excited state intermediates leading to the Dewar valence isomer

(Figure 9). It has been demonstrated that irradiation with a combination of UVB and UVA, such as simulated sunlight radiation or sequential exposure to UVB and UVA, is more efficient in producing Dewar valence isomer than pure UVB at high doses. This is explained by the fact that UVB is absorbed by the unreacted bases whereas UVA is more efficiently absorbed by 6-4PPs. [4],[44],[45]

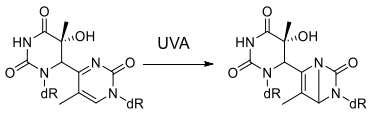

Figure 9. 4π electrocyclization of pyrimidone ring of 6-4PPs leading to its Dewar valence isomer.

2.1.2. DNA oxidative damage.

It has been recently reported that direct UVC and UVB irradiation of DNA induces formation of 8-OxodGuo.[49] Mechanistic insights have been obtained through trapping experiments in the presence of a polyamine called spermine. The formation of spermine – guanine adduct at C8 and the inhibition of the 8-OxodG formation point toward the involvement of the guanine radical cation generated through photoionization of the nucleobase. Moreover, this guanine-centered reactivity is in complete agreement with its ionization potential (IP) that is the lowest among the DNA bases.[49]

2.2. Direct DNA damage induced by UVA light

2.2.1. Cyclobutane Pyrimidine Dimers (CPDs)

As abovementioned, DNA barely absorbs in the UVA region of sunlight. Indeed, the absorption spectrum of an oligomeric duplex dA_{20}:dT_{20} has revealed a long tail reaching the UVA region that might afford its direct irradiation. However, it is important to underline that

the maximum molar absorption coefficient of the oligonucleotide (duplex) in this region is of *ca.* 10 M^{-1} cm^{-1}. [50]

UVA irradiations performed in more complex systems such as calf thymus DNA and keratinocytes samples, where an extreme caution was made to avoid the presence of photosensitizer, have revealed that the only photoproducts observed are TT, TC and CT CPDs (TT > TC > CT). [50] These experiments have shown that the UVA carcinogenic potential was underestimated and this recent discovery claims for a complete blocking of the incident photons by the use of photoprotection.

2.3. DNA photosensitized damage by UVA light

In relation with the poor DNA absorption in the UVA, photoproducts predominantly arise from photosensitization processes. These processes are generally triggered by the triplet excited state of the photosensitizer (^{3}Ph), which is longer lived than the singlet excited state, and thus, allows the reaction to occur in a longer dynamic range. Indeed, photosensitization is a matter of concern for the public health because the presence of exogenous photosensitizers could extend the active fraction of sun spectrum having a carcinogenic potential.[51],[52],[53]

DNA photosensitization might be principally divided into two parts, the first one addresses the oxidation of DNA nucleobases by ROS and electron transfer, and the second one deals with the formation of CPDs by an energy transfer process.

2.3.1. Photosensitized DNA oxidative damage

Oxidation of biological substrates generally takes place through two types of mechanisms, the so-called Type I and Type II processes [54] (Scheme 8 and Figure 10).

The Type I photosensitization is linked to radical formation and electron transfer reactions. In this context, the canonical DNA bases are poor substrates for photoreduction, but they are known to be oxidized by a wide number of Ph. Guanine nucleobase is the main target, since this purine base exhibits by far the lowest oxidation potential among DNA nucleobases [55]; its photooxidation leads to the formation of 8-oxo-7,8-dihydro-2'-deoxyguanosine (8-OxodGuo) and 2,6-diamino-4-hydroxy-5-formamido-pyrimidine (FapyGua).[44] 8-OxodGuo exhibits an even lower oxidation potential, being 100-fold more reactive, than guanine [56] (Table 1). Nonetheless, the other nucleobases can also be oxidized in the presence of Ph with appropriate redox potential in the excited state.[57],[58]

Molecule	**Oxidation potential (**vs NHE**)**
dGuo	1.29 V
8-oxodGuo	0.64 V

Table 1. Oxidation potential of the redox pair, dGuo and 8-OxodGuo.

Radical-mediated reactions occur in the nucleobase or the sugar moiety. These radicals might arise from hydroxyl radical formation in the medium and its subsequent attack onto DNA. Indeed, these OH radicals could be produced from different sources such as ionizing radiation, Fenton chemistry, etc. Moreover, UVA irradiation is at the origin of the release of significant amounts of superoxide anion in cells, either as a response of mitochondria or upon reaction of the radical anion of Type I photosensitizers with molecular oxygen. Superoxide radical anion can be converted into hydrogen peroxide, a precursor of OH radical, by the action of the superoxide dismutase enzyme. UVA has also been shown to induce the release of large amounts of iron from ferritin inside the cells that can originate OH radical through a Fenton chemistry.[59] By contrast with the electron transfer processes, the reactivity of OH radicals does not exhibit target selectivity; therefore, it reacts with all components of DNA at diffusion-controlled rates.[60] Its reaction with purine bases yields 8-OxodGuo, FapyGua for guanine, and 8-Oxo-7,8-

dihydroadenine (8-OxoAde) and *N*-(4,6-diaminopyrimidin-5-yl)formamide (FapyAde) for adenine. Regarding pyrimidine bases, OH radical adds at the C5–C6 double bond, leading to the formation of 5,6-dihydroxy-5,6-dihydrothymine (DOHThy) and 5,6-dihydroxy-5,6-dihydrocytosine. Moreover, the main hydroxyl radical-mediated methyl oxidation products of thymine are 5-hydroxymethyl-uracil (HmUra) and 5-formyluracil (ForU). [4], [12]

Regarding Type II photosensitization, it involves an energy transfer process from the sensitizer to molecular oxygen leading to singlet oxygen $^1O_2$ formation (Scheme 8). In DNA, this species exclusively oxidizes guanine to 8-OxodGuo, which suffers further oxidation as it is more prone to react with $^1O_2$ than the parent molecule. [4], [12]

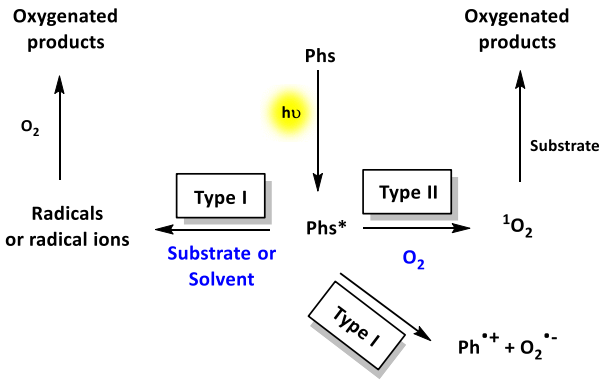

Scheme 8. The two different photosensitization mechanisms involved in DNA photooxidation.

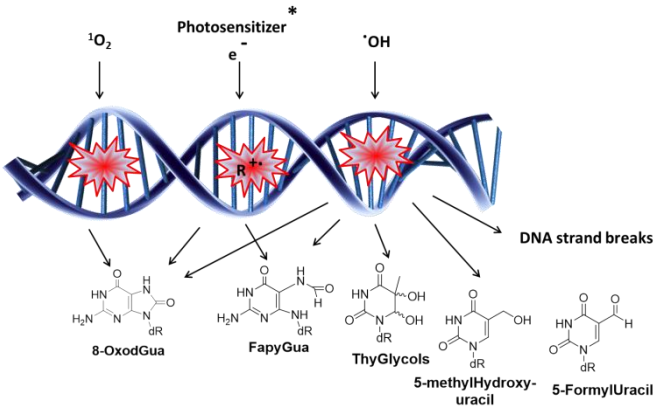

Figure 10. Photosensitized oxidative DNA photoproducts.

It is noteworthy that in addition to the exogenous photosensitizers, such as xenobiotics,[61] the organism contains a number of endogenous compounds that can photoinduce DNA lesions. Porphyrins, which are the non-amino acidic moiety of chromoproteins (hemoglobin, myoglobin…), take importance in this part of photooxidatively induced damage. These compounds are well-known Type II photosensitizers that, moreover, exhibit fluorescence emission. Because of these features, they have been extensively used in photodynamic therapy and tumor diagnosis.[62] The therapeutic effect consists in the formation of ROS, especially singlet oxygen, by means of light excitation. The systemic administration of porphyrins generally results in accumulation in cancer tissues rather than in the surrounding tissues, then a selective irradiation with visible light triggers $^1O_2$ formation that will destroy tumor cells.[63]

Other molecules such as pterins are also important endogenous compounds. More concretely, pterins are present in human epidermis and they act as cofactors in the hydroxylation of aromatic amino acids (5,6,7,8-tetrahydrobiopterin). When the metabolism of 5,6,7,8-tetrahydrobiopterin is altered, for instance in

vitiligo disease, unconjugated oxidized pterins are accumulated in the skin (biopterin, formylpterin and carboxypterin). These oxidized forms of pterins have been recently studied and reported to act through both Type I and Type II mechanisms leading to the degradation of guanosine[64],[65], adenosine[66] and pyrimidine nucleotides,[67] but also to that of proteins[68] and membranes.[69]

2.3.3. Photosensitized CPDs formation

Triplet-triplet energy transfer (TETT) from a photosensitizer to DNA nucleobases is another process that originates DNA damages. Therefore, after excitation the photosensitizer undergoes intersystem crossing that leads to the population of long-lived triplet excited states. If the energy of this latter is higher than that of thymine (or cytosine) in DNA, a triplet-triplet energy transfer (TTET) process can take place and lead to CPDs formation (Figure 11). [4], [44], [45]

Interestingly, this process only occurs between the excited Ph and pyrimidine DNA bases giving rise to the formation of CPDs, as the only photoproducts. As abovementioned, no 6-4PPs have been detected in the presence of Ph able to act by TETT, this has led to the conclusion that 6-4PPs are formed from the singlet excited state.

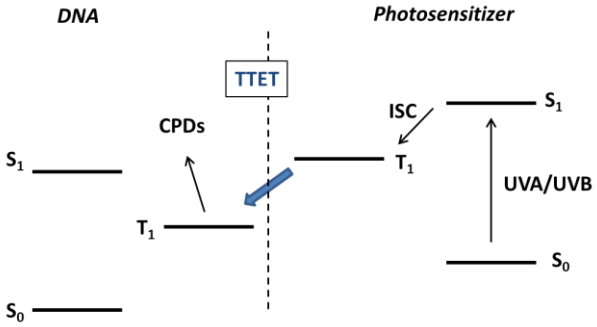

Figure 11. Photosensitized TTET involved in the formation of CPDs.

In fact, benzophenone and drugs containing this chromophore, fluoroquinolones and other pharmaceutical agents have been evidenced to efficiently induce CPDs formation through TTET process. [61] However, the ratio between photosensitized CPDs and oxidative damage depends on the triplet energy and redox potentials of the photosensitizer and DNA nucleobases.[4]

Recently, delayed formation of CPDs has been discovered and attributed to a peculiar reactivity of melanin.[70] The mechanism involves different steps. After UV exposure, superoxide and nitric oxide are produced and are at the origin of increasing levels of peroxynitrite, which degrades melanin and produces a short-lived dioxetane. This intermediate undergoes then a spontaneous thermolysis yielding formation of two carbonyl functional groups, one of them as a triplet excited state. This triplet excited state is high enough to transfer its energy to thymine and produce CPDs. Indeed, the delay observed between the initial irradiation and the appearance of CPDs (hours after UV exposure) is due to the induction time needed for dioxetane to be formed and decomposed.

3. Measures for skin cancer prevention

The large amount of data that relates UV skin exposure with skin cancer[42],[43],[48] has raised awareness on the harmful effect of excessive sunlight exposure. Thus, skin cancer preventive strategies are now widespread. These primary measures consist in (*i*) avoiding sun exposure during midday sun hours, from 12 p.m. to 16 p.m., (*ii*) using protective clothes such as caps and hats, sunglasses or long-sleeved clothes and (*iii*) regular application of sunscreens especially during outdoor activities. Efficient sunscreens must have a minimum sunscreen factor of 30 or greater and they are required to cover a broad absorption spectrum, protecting against UVB and UVA radiation.[71]

Secondary preventive strategies are regular self-examinations in order to detect any skin changes that must be complemented with

annual full-body skin examination performed by a specialized dermatologist. The early diagnosis by skin cancer screening techniques and treatment are determining to reduce further possible complications and to improve the cancer prognosis.[48]

However, the best strategy for skin cancer prevention is still the avoidance of mutations due to UV-induced DNA damage. Even if DNA repair could reduce the number of DNA lesions, it is wiser to reduce damage formation by sun protective measures, such as sunscreen application early in life.

An important characteristic of the sunscreen is its Sun Protection Factor (SPF) that establishes the effectiveness of protection against UVB radiation. More concretely, it corresponds to the ratio between the amount of UV radiation required to provoke an erythema on protected skin (with sunscreen) and that required to induce it on the same unprotected skin (eq. 1). In this way, high SPFs provide more protection against the dangerous effects of sunlight than low SPF. In the European Union sunscreens are classified according to their SPF into low (SPF 6, 10), medium (SPF 15, 20, 25), high (SPF 30, 50), and very high (SPF 50+).[71]

SPF = MED of protected skin / MED of unprotected skin eq. 1
where, MED is the minimal erythemal light dose.

The effectiveness of a sunscreen agent to protect against UVA is measured by the Persistant Pigment Darkening (PPD, *in vivo*) or COLIPA (*in vitro*) must be at least one-third of the SPF *in vivo* value. Sunscreens are as well classified in the European Union according to their PPD into low (PPD 2), medium (PPD 4), high (PPD 8) and very high (PPD 14). Another *in vitro* approach for protection in Europe against UVA is represented by a star system for easier understanding of customers. The measure is based on Diffey's UVA/UVB ratio and classifies products into five classes of protection level; 1-minimum sun protection, 2-moderate, 3-good, 4-superior and 5-ultra. [71]

There are two general types of sunscreens, physical and chemical, depending on the absorbing molecules. Physical sunscreens protect skin from the sun by reflecting or scattering the sun's rays and preventing them to penetrate in the skin. They are inorganic sunscreens such as zinc oxide (ZnO), titanium dioxide (TiO_2), etc. They are generally stable and protect against UVB and UVA, and do not produce free radicals. However, an important drawback is their heavy, white and hard to apply formulations. In order to overcome this inconvenient, nanoparticles of TiO_2 and ZnO are currently introduced in formulations in order to increase their efficacy and reduce whitening on the skin. However, they are newer technologies and studies have shown that these nanoparticles may promote the generation of free radicals and cause cytotoxicity, genotoxicity and photocarcinogenesis.[71] A recent study has been able to mitigate the potential risk of free radical generation associated with TiO_2 nanoparticles by coating them with a lignin antioxidant shell that scavengs free radicals before they can exit the TiO_2-lignin composites.[72]

Regarding chemical sunscreens (Figure 12), they are organic filters capable of absorbing high-energy UV rays and they ideally should remain unchanged after UV irradiation and return to their ground state by dissipating the energy as thermal energy.[73] However, most chemical filters exhibit some photoreactivity as it is the case for the 4-*tert*-butyl-4'-methoxydibenzoylmethane (AB, avobenzone), which is probably the most representative UVA chemical sunscreen with a broad spectral protection and a high power of absorption. As previously introduced, it has a maximum absorption at *ca.* 340-350 nm in its ground state due to its keto-enol tautomer; however, this protection is lost during irradiation due to formation of the diketo form and its subsequent photodegradation.[16], [74] The AB photoinstability has been successfully overcome by combinations with other sunscreens like cinnamates, benzylidene malonates, benzylidiene camphor or triazines.[23] Indeed, avobenzone is currently the UVA filter most used together with Tinosorb S (Bemotrizinol, Figure 12).[75] This latter presents a broad-spectrum

absorption with two peaks in the UVA/UVB region at 310 and 340 nm. It is highly photostable and is capable of preventing AB photodegradation when used in combination.[75]

Besides avobenzone, there are many other UVA organic filters commercially available such as Benzophenones (Oxybenzone, Sulisobenzone), Meradimate, Bisdisulizole disodium, etc (Figure 12).

Regarding chemical filters affording protection in the UVB range, some examples are represented in Figure 12. Octinoxate is the most commonly used UV-B filter in sunscreens. Its application has proven to be effective in preventing sunburns; however, studies have shown that it behaves like an endocrine disruptor.[76] Other UVB filters commonly used are Octocrylene and Ensulizole.

Likewise Bemotrizinol, Ecamsule, a benzylidene camphor derivative with a broad spectral protection, exhibits high photostability and dissipates energy through a thermal process without penetrating into the skin. Studies have proven that Ecamsule is capable of preventing skin alterations leading to photoageing.[77] Other broad spectrum filters are Silatriazole and Bisoctrizole (Figure 12).

Nevertheless, chemical filters offer more protection against UVA and UVB rays than physical sunscreens, but their range of protection strongly depends on the particular chromophore and its stability. [71]

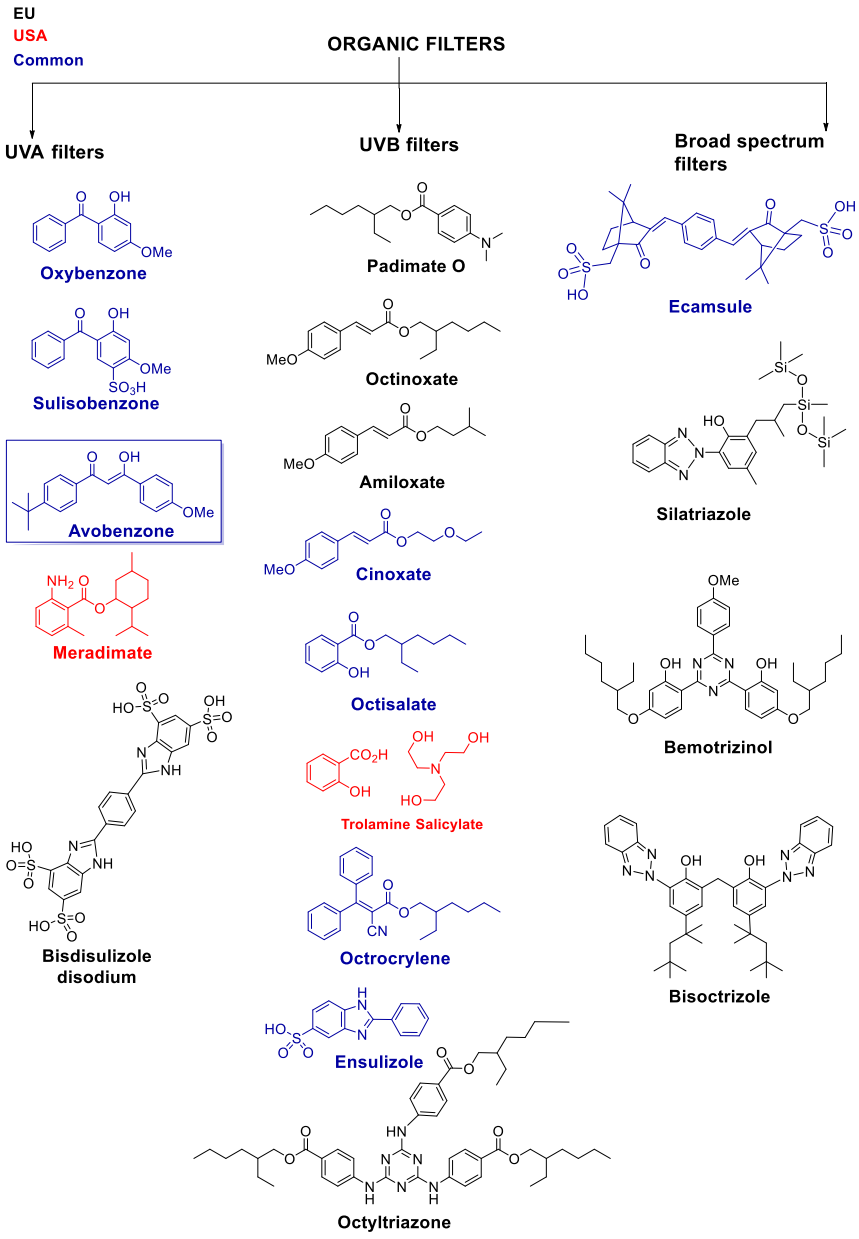

Figure 12. Structures of some organic filters.

Moreover, nowadays, organic sunscreens combined with repair enzymes are also commercially available.[78] Antioxidants could also be considered as a primary strategy in the prevention of skin cancer and they can be topically and systemically administered.[79]

4. References

[1] C. Young, "Solar ultraviolet radiation and skin cancer," *Occup. Med.*, **2009**, 59, 82–88.

[2] N. J. Turro, V. Ramamurthy and J. C. Scaiano, "Photochemistry of carbonyl compounds" "Photochemistry olefins" and "Photochemistry of aromatic compounds, " In *Modern Molecular Photochemistry of Organic Molecules*, Editor: J. Stiefel, **2010**, 629-704, 705-800, and 847-924.

[3] B. J. Michl, "Photophysics of organic molecules in solution," In *CRC Handbook of Photochemistry Third Ed., Editors:* Marco Montalti, Alberto Credi, Luca Prodi, M. Teresa Gandolfi, **2006**, Chapter 1, 1–47.

[4] T. Douki, "Formation and repair of UV-induced DNA damage," In *CRC Handbook Organic Photochemistry and Photobiology, Third Ed. - Two Vol. Set*, Editors: A. Griesbeck, M. Oelgemöller, F. Ghetti **2012**, 1349–1392.

[5] P. Markov, "Light-induced tautomerism of β-dicarbonyl compounds", *Chem. Soc. Rev.*, **1984**, 1, 69-96.

[6] D. Veierov, T. Bercovici, E. Fischer, Y. Mazur, and A. Yogev, "Photoisomerization of the enol form of 1,3-dicarbonyl compounds," *J. Am. Chem. Soc.*, **1977**, 99, 2723–2729.

[7] P. Markov, I. Petkov and D. Jeglova "Photochemistry of enolizable β-dicarbonyl compounds: study on the photoketonization of some esters of aroylacetic acids,"*J. Photochem.*, **1978**, 8, 277-284.

[8] Z. Wang, "de Mayo reaction," In *Comprehensive Organic*

Name Reactions and Reagents, **2010**, 858-861.

[9] P. K. Verma, F. Koch, A. Steinbacher, P. Nuernberger, and T. Brixner, "Ultrafast UV-induced photoisomerization of intramolecularly H-bonded symmetric β-diketones," *J. Am. Chem. Soc.*, **2014**, 136, 14981−14989.

[10] P. K. Verma, A. Steinbacher, F. Koch, P. Nuernberger, and T. Brixner, "Monitoring ultrafast intramolecular proton transfer processes in an unsymmetric β-diketone," *Phys. Chem. Chem. Phys.*, **2015**, 17, 8459–8466.

[11] F. Wetz, C. Routaboul, D. Lavabre, J. C. Garrigues, I. Rico-Lattes, I. Pernet, and A. Denis "Photochemical behavior of a new long-chain UV absorber derived from 4-*tert*-butyl-4 methoxydibenzoylmethane," *Photochem. Photobiol.*, **2004**, 80, 316–321.

[12] J. C. Hubaud, I. Bombarda, L. Decome, J. C. Wallet, and E. M. Gaydou, "Synthesis and spectroscopic examination of various substituted 1,3-dibenzoylmethane, active agents for UVA/UVB photoprotection," *J. Photochem. Photobiol. B, Biol.*, **2008**, 92, 103–109.

[13] A. Cantrell and D. J. Mc Garvey, "Photochemical studies of 4-*tert*-butyl-4'-methoxydibenzoylmethane," *J. Photochem. Photobiol. B, Biol.,* **2001***,* 64, 117–122.

[14] S. P. Huong, E. Rocher, J. D. Fourneron, L. Charles, V. Monnier, H. Bun, and V. Andrieu, "Photoreactivity of the sunscreen butylmethoxydibenzoylmethane (DBM) under various experimental conditions," *J. Photochem. Photobiol. A Chem.*, **2008**, 196, 106–112.

[15] M. Yamaji, C. Paris, and M. A. Miranda, "Steady-state and laser flash photolysis studies on photochemical formation of 4-*tert*-butyl-4'-methoxydibenzoylmethane from its derivative via the Norrish Type II reaction in solution," *J. Photochem. Photobiol. A Chem.*, **2010**, 209, 153–157.

[16] W. Schwack and T. Rudolph, "Photochemistry of dibenzoyl methane UVA filters Part 1," *J. Photochem. Photobiol. B, Biol.*, **1995**, 28, 229-234.

[17] G. J. Mturi and B. S. Martincigh, "Photostability of the sunscreening agent 4-*tert*-butyl-4'-methoxydibenzoylmethane (avobenzone) in solvents of different polarity and proticity," *J. Photochem. Photobiol. A, Chem.*, **2008**, 200, 410–420.

[18] I. Andrae, A. Bringhen, F. Böhm, H. Gonzenbach, T. Hill, L. Mulroy and T. G. Truscott, "A UVA filter (4-*tert*-butyl-4'-methoxydibenzoylmethane : photoprotection reflects photophysical properties," *J. Photochem. Photobiol. B, Biol.*, **1997**, 37, 147–150.

[19] M. Yamaji and M. Kida, "Photothermal tautomerization of a UV sunscreen (4-*tert*-butyl-4'- methoxydibenzoylmethane) in acetonitrile studied by steady-state and laser flash photolysis," *J. Phys. Chem. A*, **2013**, 117, 1946−1951.

[20] A. Aspée, C. Aliaga, and J. C. Scaiano, "Transient enol isomers of dibenzoylmethane and avobenzone as efficient hydrogen donors toward a nitroxide pre-fluorescent probe," *Photochem. Photobiol.*, **2007**, 83, 481–485.

[21] S. Tobita, J. Ohba, K. Nakagawa, and H. Shizuka, "Recovery mechanism of the reaction intermediate produced by photoinduced cleavage of the intramolecular hydrogen bond of dibenzoylmethane," *J. Photochem. Photobiol. A, Chem.,* **1995***,* 92, 61-67.

[22] A. D. Dunkelberger, R. D. Kieda, B. M. Marsh, and F. F. Crim, "Picosecond dynamics of avobenzone in solution," *J. Phys. Chem. A*, **2015**, 119, 6155–6161.

[23] C. Paris, V. Lhiaubet-Vallet, O. Jiménez, C. Trullas, and M. A. Miranda, "A blocked diketo form of avobenzone: Photostability, photosensitizing properties and triplet quenching by a triazine-derived UVB-filter," *Photochem. Photobiol.*, **2009**, 85, 178–184.

[24] I. Karlsson, L. Hillerström, A. L. Stenfeldt, J. Mårtensson, and A. Börje, "Photodegradation of dibenzoylmethanes: Potential cause of photocontact allergy to sunscreens," *Chem. Res. Toxicol.*, **2009**, 22, 1881–1892.

[25] E. Damiani, L. Greci, R. Parsons, and J. Knowland, "Nitroxide

radicals protect DNA from damage when illuminated in vitro in the presence of dibenzoylmethane," *Free Radic. Biol. Med.*, **1999**, 26, 809–816.

[26] E. Damiani, P. Carloni, C. Bondi and L. Greci, "Increased oxidative modification of albumin when illuminated in vitro in the presence of a common sunscreen ingredient: protection by nitroxide radicals," *Free Radic. Biol. Med.*, **2000**, 28, 193–201.

[27] J. Knowland, E. A. McKenzie, P. J. McHugh and N. A. Cridland, "Sunlight-induced mutagenicity of a common sunscreen ingredient," *FEBS Lett.*, **1993**, 324, 309–313.

[28] T. Armeni, E. Damiani, M. Battino, L. Greci, and G. Principato, "Lack of *in vitro* protection by a common sunscreen ingredient on UVA-induced cytotoxicity in keratinocytes," *Toxicology*, **2004**, 203, 165–178.

[29] E. Damiani, W. Baschong, and L. Greci, "UV-Filter combinations under UV-A exposure : concomitant quantification of over-all spectral stability and molecular integrity," *J. Photochem. Photobiol. B, Biol.*, **2007**, 87, 95–104.

[30] V. Lhiaubet-Vallet, M. Marin, O. Jimenez, O. Gorchs, C. Trullas, and M. A. Miranda, "Filter–filter interactions. Photostabilization, triplet quenching and reactivity with singlet oxygen," *Photochem. Photobiol. Sci.*, **2010**, 9, 552–558.

[31] S. Afonso, K. Horita, J. P. Sousa e Silva, I. F. Almeida, M. H. Amaral, P. A. Lobao, P. C. Costa, M. S. Miranda, J. C. G. Esteves da Silva and J. M. Sousa Lobo, "Photodegradation of avobenzone: stabilization effect of antioxidants," *J. Photochem. Photobiol. B, Biol.*, **2014**, 140, 36–40.

[32] M. R. Barvian and M. M. Greenberg, "Independent generation of 5,6-dihydrothymid-5-yl in single-stranded polythymidylate. O_2 is necessary for strand scission," *J. Am. Chem. Soc.*, **1995,** 117, 8291-8292.

[33] M. M. Greenberg, M.R. Barvian, G. P. Cook, B. K. Goodman, T. J. Matray, C. Tronche, and H. Venkatesan, "DNA damage induced via 5,6-dihydrothymid-5-yl in single-stranded

oligonucleotides," *J. Am. Chem. Soc.*, **1997**, *119,* 1828-1839.

[34] M. J. E. Resendiz, V. Pottiboyina, M. D. Sevilla, and M. M. Greenberg, "Direct strand scission in double stranded RNA via a C5-pyrimidine radical," *J. Am. Chem. Soc.*, **2012,** 134, 3917–3924.

[35] D. J. Deeble, S. Das, and C. Von Sonntag, "Uracil derivatives: sites and kinetics of protonation of the radical anions and the UV spectra of the C(5) and C(6) H-atom adducts," *J. Phys. Chem.*, **1985**, 89, 5784–5788.

[36] T. Ito, H. Shinohara, H. Hatta, S. Fujita, and S. Nishimoto, "Radiation-induced and photosensitized splitting of C5-C5'-linked dihydrothymine dimers. 2. Conformational effects on the reductive splitting mechanism," *J. Phys. Chem. A*, **2000**, 104, 2886–2893.

[37] E. J. Privat and L. C. Sowers, "A proposed mechanism for the mutagenicity of 5-formyluracil," *Mutat. Res.*, **1996**, 354, 151-156.

[38] D. K. Rogstad, J. Heo, N. Vaidehi, W. A. I. Goddard, A. Burdzy, and L. C. Sowers, "5-Formyluracil-induced perturbations of DNA function," *Biochemistry*, **2004**, 43, 5688–5697.

[39] H. Ånensen, F. Provan, A. T. Lian, H.S. Reinertsen, Y. Ueno, A. Matsuda, E. Seeberg and S. Bjelland, "Mutations induced by 5-formyl-2'-deoxyuridine in Escherichia coli include base substitutions that can arise from mispairs of 5-formyluracil with guanine, cytosine and thymine," *Mutat. Res.*, **2001**, 476, 99–107.

[40] T. Sugiyama, A. Kittaka, H. Takayama, M. Tomioka, Y. Ida, and R. Kuroda, "Chemical cross-linking of peptides derived from RecA with single-stranded oligonucleotides containing 5-formyl-2'-deoxyuridine," *Nucleosides, Nucleotides Nucleic Acids*, **2001**, 20, 1079–1083.

[41] J. Cadet, C. Anselmino, T. Douki and L. Voituriez "Photochemistry of nucleic acids in cells," *J. Photochem. Photobiol. B, Biol.*, **1992**, 277–298.

[42] G. P. Pfeifer, A. Besaratinia, "UV wavelength-dependent DNA

damage and human non-melanoma and melanoma skin cancer ," *Photochem. Photobiol. Sci.*, **2012**, 11, 90–97.

[43] N. Chatterjee, G. C. Walker, "Mechanisms of DNA damage, repair, and mutagenesis," *Environ. Mol. Mutagen.*, **2017**, 58, 235-263.

[44] J. Cadet, S. Mouret, J. Ravanat, and T. Douki, , "Photoinduced damage to cellular DNA: direct and photosensitized," *Photochem. Photobiol.*, **2012**, 88, 1048–1065.

[45] J. Ravanat , and T. Douki, "UV and ionizing radiations induced DNA damage, differences and similarities," *Radiat. Phys. Chem.*, **2016**, 128, 92–102.

[46] W. P. Roos, A. D. Thomas, and B. Kaina, "DNA damage and the balance between survival and death in cancer biology," *Nat. Publ. Gr.*, **2015**, 16, 20–33.

[47] B. Sadikovic, K. Al-Romaih, J. A. Squire, and M. Zielenska, "Cause and consequences of genetic and epigenetic alterations in human cancer," *Curr. Genomics,* **2008***, 9,* 394-408.

[48] C. Seebode, J. Lehmann, and S. Emmert, "Photocarcinogenesis and skin cancer prevention strategies," *Anticancer Res.,* **2016**, 36, 1371-1378.

[49] M. Gomez-Mendoza, A. Banyasz, T. Douki, D. Markovitsi, and J. L. Ravanat, "Direct oxidative damage of naked DNA generated upon absorption of UV radiation by nucleobases," *J. Phys. Chem. Lett.*, **2016**, 7, 3945−3948.

[50] S. Mouret, C. Philippe, J. Gracia-Chantegrel, A. Banyasz, S. Karpati, D. Markovitsi, and T. Douki "UVA-induced cyclobutane pyrimidine dimers in DNA : a direct photochemical mechanism," *Org. Biomol. Chem.*, **2010**, 8, 1706–1711.

[51] V. Lhiaubet-Vallet, M. C. Cuquerella, J. V. Castell, F. Bosca, and M. A. Miranda, "Triplet excited fluoroquinolones as mediators for thymine cyclobutane dimer formation in DNA," *J. Phys. Chem. B*, **2007**, 111, 7409–7414.

[52] M. C. Cuquerella, V. Lhiaubet-Vallet, J. Cadet, and M. A.

Miranda, “Benzophenone photosensitized DNA damage,” *Acc. Chem. Res.*, **2012**, 45, 1558–1570.

[53] M. C. Cuquerella, V. Lhiaubet-Vallet, F. Bosca, and M. A. Miranda, “Photosensitised pyrimidine dimerisation in DNA,” *Chem. Sci.*, **2011**, 2, 1219-1232.

[54] C. S. Foote, “Definition of Type I and Type II,” *Photochem. Photobiol.*, **1991**, 54, 659.

[55] S. Steenken and S. V. Jovanovic, “How easily oxidizable is DNA? One-electron reduction potentials of adenosine and guanosine radicals in aqueous solution,” *J. Am. Chem. Soc.*, **1997**, 119, 617–618.

[56] K. D. Sugden, C. K. Campo, and B. D. Martin, “Direct oxidation of guanine and 7,8-dihydro-8-oxoguanine in DNA by a high-valent chromium complex: a possible mechanism for chromate genotoxicity,” *Chem. Res. Toxicol.*, **2001**, 14, 1315–1322.

[57] T. Delatour, T. Douki, C. D’Ham, and J. Cadet, “Photosensitization of thymine nucleobase by benzophenone through energy tranfer, hydrogen abstraction and one-electron odidation,” *J. Photochem. Photobiol. B, Biol.*, **1998**, 44, 191–198.

[58] T. Douki and J. Cadet, “Modification of DNA bases by photosensitized one-electron oxidation,” *Int. J. Rad. Biol.*, **1999**, 75, 571-581.

[59] C. Pourzand, R. D.Watkin, J. E. Brown, and R. M. Tyrell, “Ultraviolet A radiation induces immediate release of iron in human primary skin fibroblasts: the role of ferritin,” *Proc. Natl. Acad. Sci. USA*, **1999**, 96, 6751–6756.

[60] G. M. Rodríguez-Muñiz, M. L. Marin, V. Lhiaubet-Vallet, and M. A. Miranda, “Reactivity of nucleosides with a hydroxyl radical in non-aqueous medium,” *Chem. Eur. J.*, **2012,** 18, 8024–8027.

[61] V. Lhiaubet-Vallet, M. A. Miranda, “Phototoxicity of drugs”, In *CRC Handbook of Organic Photochemistry and Photobiology*, *Third Ed. - Two Vol. Set*, Editors: A. Griesbeck, M. Oelgemöller,

F. Ghetti, **2012***,* 66, 1541-1556.

[62] K. Berg, P. K. Selbo, A. Weyergang, A. Dietze, L. Prasmickaite, A. Bonsted, B. Ø. Engesaeter, E. Angellpetersen, T. Warloe, N. Frandsen, and A. Hogset "Porphyrin-related photosensitizers for cancer imaging and therapeutic applications," *J. Microsc.*, **2005**, 218, 133–147.

[63] R. Bonnett, "Photosensitizers of the porphyrin and phthalocyanine series for photodynamic therapy," *Chem. Soc. Rev.*, **1995**, 19-33.

[64] G. Petroselli, M. L. Dantola, F. M. Cabrerizo, A. L. Capparelli, C. Lorente, E. Oliveros, and A. H. Thomas, "Oxidation of 2'-deoxyguanosine 5'-monophosphate photoinduced by pterin: type I versus type II mechanism," *J. Am. Chem. Soc.*, **2008**, 130, 3001-3011.

[65] M. P. Serrano, S. Estebanez, M. Vignoni, C. Lorente, P. Vicendo, E. Oliveros, and A. H. Thomas, "Photosensitized oxidation of 2'-deoxyguanosine 5'-monophosphate: mechanism of the competitive reactions and product characterization," *New J. Chem.,* **2017**, 41, 7273-7282.

[66] M. P. Serrano, C. D. Borsarelli, and A. H. Thomas, "Type I photosensitization of 2'-deoxyadenosine 5'-monophosphate (5'-dAMP) by biopterin and its photoproduct formylpterin," *Photochem. Photobiol.*, **2013**, 89,1456–1462.

[67] M. P. Serrano, M. Vignoni, C. Lorente, P. Vicendo, E. Oliveros, and A. H. Thomas, "Thymidine radical formation via one-electron transfer oxidation photoinduced by pterin : Mechanism and products characterization," *Free Radic. Biol. Med.*, **2016**, 96, 418–431.

[68] M. L. Dántola, B. N. Zurbano, A. H. Thomas, "Photoinactivation of tyrosinase sensitized by folic acid photoproducts," *J. Photochem. Photobiol. B, Biol.*, **2015**, 149, 172–179.

[69] X. L. Warnet, M. Laadhari, A. A. Arnold, I. Marcotte, and D. E. Warschawski, "A ^{2}H magic-angle spinning solid-state NMR characterisation of lipid membranes in intact bacteria,"

Biochim. Biophys. Acta, **2016**, 1858, 146–152.

[70] S. Premi, S. Wallisch, C. M. Mano, A. B. Weiner, A. Bacchiocchi, K. Wakamatsu, E. J. H. Bechara, R. Halaban, T. Douki, and D. E. Brash "Chemiexcitation of melanin derivatives induces DNA photoproducts long after UV exposure," *Science*, **2015**, 347, 842–847.

[71] M. S. Latha, J. Martis, S. V, R. Sham, S. Bangera, B. Krishnankutty, S. Bellary, S. Varughese, Prabhakar, and B. R. N. Kumar, "Sunscreening agents," *J. Clin. Aesthet. Dermatol.*, **2013**, 6, 16–26.

[72] M. Morsella, N. D'Alessandro, A. E. Lanterna, and J. C. Scaiano, "Improving the sunscreen properties of TiO_2 through an understanding of its catalytic properties," *ACS Omega*, **2016**, 1, 464–469.

[73] J. Kockler, M. Oelgemöller, S. Robertson, and B. D. Glass, "Photostability of sunscreens," *J. Photochem. Photobiol. C Photochem. Rev.*, **2012**, 13, 91–110.

[74] N. M. Roscher , M. K.O. Lindemann, S. B. Kong, C. G. Cho, and P. Jiang, "Photodecomposition of several compounds commonly used as sunscreen agents," *J. Photochem. Photobiol. A, Chem.,* **1994***, 180*, 417-421.

[75] E. Chatelain, and B. Gabard, "Photostabilization of butyl methoxydibenzoylmethane (avobenzone) and ethylhexyl methoxycinnamate by bis-ethylhexyloxyphenol methoxy-phenyl triazine (tinosorb S), a new UV broadband filter," *Photochem. Photobiol.*, **2001**,74, 401–406.

[76] M. Lorigo, M. Mariana, and E. Cairrao, "Photoprotection of ultraviolet-B filters: Updated review of endocrine disrupting properties," *Steroids*, **2018**, 131, 46–58.

[77] S. Scite, D. Moyal, S. Richard, J. De Rigal, J. L. Lévêque, C. Hourseau, and A. Fourtanier, "Mexoryl SX : a broad absorption UVA filter protects human skin from the effects of repeated suberythemal doses of UVA,"*J. Photochem. Photobiol. B, Biol.*, **1998**, 44, 69-76.

[78] E. Berardesca, M. Bertona, K. Altabas, V. Altabas, and E.

Emanuele, "Reduced ultraviolet-induced DNA damage and apoptosis in human skin with topical application of a photolyase containing DNA repair enzyme cream: clues to skin cancer prevention," *Mol. Med. Rep.*, **2012**, 5, 570-574.

[79] A. Godic, B. Poljšak, M. Adamic, and R. Dahmane, "The Role of antioxidants in skin cancer prevention and treatment," *Oxid. Med. Cell. Longev.*, **2014**, 2014, 1-6.

Chapter 2:

General Objectives

As mentioned in the introduction, the 1,3-dicarbonyl moiety is present in a large variety of chemical compounds that encompass from UVA filters, such as dibenzomethane derivatives, to DNA nucleobase derivatives.

Thus, the main goal of this thesis is to contrast the role of these 1,3-dicarbonyl compounds as DNA damaging agents with respect to their photoprotective potential. First, the properties of β-dicarbonyl compounds as part of the DNA structure will be addressed through the study of C5-pivaloyl substituted dihydropyrimidines as photolabile precursors of carbon centered radicals, but also through the evaluation of the DNA oxidatively generated damage, 5-formyl uracil, as a potential intrinsic DNA photosensitizing agent. Additionally, the diketo isomer of the most representative UVA filter, the well-known avobenzone, which contains two photoremovable phenacyl groups, will be used in order to develop a new strategy for photoprotection based on the photorelease of a photosensitizing topical drugs together with its protecting UVA filter.

More concretely, the following specific objectives have to be addressed:

1) To characterize the photophysical properties of the species involved in the SSB production in DNA and RNA by a photogenerated pyrimidin-5-yl radical in non-aqueous medium. For that purpose, a lipophilic precursor, *tert*-butyl ketone, together with a profluorescent radical trap (AAA-TEMPO) have been selected to perform trapping experiments and laser flash photolysis studies.

2) To evaluate the potential photosensitizing behavior of an oxidatively generated DNA damage, 5-formyluracil, in order to get insight into its ability to exacerbate DNA damage during a second UV light exposure producing cluster lesions.

In this context, model pyrimidine dyads as well as plasmid DNA are the target molecules proposed for the study.

3) To design and evaluate photoactivatable dyads for the controlled release of photosensitizing pharmaceutical active principles under the photoprotective action of a solar filter. In this context, (*S*)-Ketoprofen and Diclofenac are the selected drugs and avobenzone the UVA protecting shield.

4) To assess the photosafety of the new photoactivable dyads mentioned in the third objective in order to guarantee their harmlessness towards the DNA.

Chapter 3:

A Combined Experimental and Theoretical Approach to the Photogeneration of 5,6-Dihydropyrimidin 5-yl Radicals in Nonaqueous Media

1. Introduction

Ionizing radiation is one of the environmental factors that endangers the integrity of cells producing double strand breaks in DNA. During this process, a large family of reactive species such as nucleobase radicals is produced. Consequently, the chemical fate of these species is relevant to understand the biological effects of radiation and to explain formation of DNA lesions.

Radicals are capable of producing DNA strand breaks and, these require a transfer of the radical from the nucleobase to the sugar skeleton. The dihydropyrimidine radicals and / or their respective peroxyl radicals are inducers of strand breaks by H abstraction from the nucleotide sugar, in RNA (uridine) and to a lesser extent in DNA (thymidine)[1], [2].

However, elucidating the chemistry of a specific radical is challenging because of the limitations imposed by the unselective nature of the involved processes. This problem has been overcome through independent generation of the putative reactive intermediates by means of photolabile groups inserted in isolated nucleosides as well as in synthetic oligonucleotides[1], [2], [3], [4], [5], [9].

These modified DNA fragments have been a powerful tool for mechanistic studies aimed at elucidating the role of individual nucleobase and osidic reactive intermediates in the formation of DNA lesions since they are selectively excited in the UVB/UVA region, where canonical DNA nucleobases do not absorb.

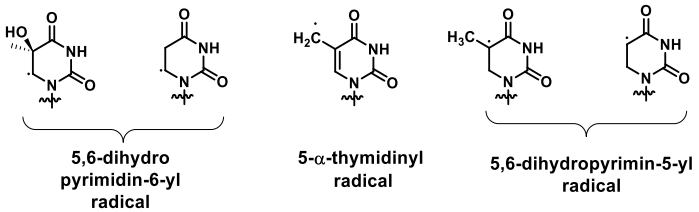

Figure 1. Examples of reported pyrimidinyl DNA and RNA radicals.

In this chapter, radicals centered in pyrimidine bases are the object of study. More concretely, some DNA and RNA radicals such as 5,6-dihydropyrimidin-6-yl radical, 5-α-thimidinyl radical and 5,6-dihydropyrimidin-5-yl radical (Figure 1) have been generated by means of photolysis at UVB/UVA wavelengths using the photolabile protecting group methodology (Figure 2).

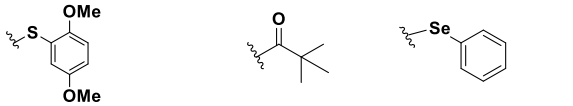

2,5-dimethoxy-phenylsulfide | ***tert*-butyl ketone (pivaloyl group)** | **phenyl selenide**

Figure 2. Examples of photolabile protecting groups (PPGs).

The 5-hydroxy-5,6-dihydrothymidin-6-yl radical and 5,6-dihydrouridin-6-yl radical have been generated from a photolabile precursor bearing the 2,5-dimethoxyphenylsulfide[2],[6] moiety. Steady-state photolysis studies in anaerobic conditions of these precursors incorporated in oligodeoxynucleotides revealed that none of them produce direct strand-breaks. However, when the radical is generated under aerobic conditions, it can react with oxygen yielding a peroxyl radical that can, in turn, be the hydrogen abstracting species. The studies evidenced that 5,6-dihydro-5-hydroxythymidine perox-6-yl is less reactive than the unsubstituted analogue derived from uridine (5,6-dihydrouridine perox-6-yl radical) and does not yield measurable levels of hydrogen atoms abstraction products due to the increased hindrance of the C5-substituents. In the case of 5,6-dihydrouridine perox-6-yl radical, it was demonstrated to abstract H from C2'-carbohydrate from a 5'-adjacent uridine inducing strand breaks. It is thought that steric hindrance could play a significant role here.

On the other hand, photogeneration of 5-α-thymidinyl radical and its respective carbocation, using phenyl selenide and 2,5-dimethoxyphenylsulfide moiety[3], [4], [7], has been studied to shed light on their interstrand cross link (ICL) formation ability by means of aerobic and anaerobic irradiation. However, in order to distinguish if

the ICL aroused from the radical (formed during direct heterolysis) or from the carbocation (coming from an electron transfer from the radical) a competition study using methoxyamine and 4-hydroxy-TEMPO was carried out. The addition of 4-hydroxy-TEMPO had no effect on ICL formation in duplex DNA, indicating that 5-(α-deoxyuridinyl)methyl radical is not responsible for ICL formation. In contrast, methoxyamine competed with ICL formation since the ratio of trapped carbocation to ICL varied linearly with respect to the methoxyamine concentration independently of the presence of oxygen. Therefore, the species involved in ICL is the carbocation centered in the methylene part.

Finally, in the study of 5,6-dihydropyrimidin-5-yl radical using *tert*-butyl ketone moiety as precursor, 5,6-dihydrothymidin-5-yl radical did not induce direct strand breaks under anaerobic conditions; however, in aerobic conditions where 5,6-dihydrothymidin-5-peroxyl radical is produced, direct strand breaks by a H abstraction in C1' o C2' of the sugar moiety at the 5'-adjacent nucleoside were evidenced[8]. Kinetic isotopic experiments revealed that H abstraction occurred at C1' sugar moiety in an internucleotidyl manner[5]. In addition to this, detection of a single strand break at three nucleosides units in 5'- direction is relevant of a migration of the radical.

In the RNA case, anaerobic photogeneration of 5,6-dihydro-uridin-5-yl radical, using *tert*-butyl ketone moiety as precursor, has revealed its capability to produce direct strand breaks by abstracting hydrogen atoms from its own sugar moiety (intranucleotidyl) and from the C2-hydrogen atom of the 5'-adjacent nucleotide (internucleotidyl). These direct strand breaks are induced both in single and double stranded chains but more efficiently in the last case. Moreover, it has been demonstrated that radicals generated in RNA nucleobases are more reactive and prone to induce direct strand breaks than those generated in DNA nucleobases due to their low carbon-hydrogen bond dissociation energy at C2' [9].

Few spectroscopic experiments have been run in aqueous media to investigate the formation and fate of pyrimidinyl radicals. Nonetheless, the obtained spectra corresponded to mixtures of several species, and usually the transient absorption spectrum of the radical of interest was obtained through mathematical treatment of the whole signals. This way, it has been deduced that 5,6-dihydrothymin-5-yl and related radicals exhibit weak (ε *ca.* 1000 M^{-1} cm^{-1}) transient absorption spectra with broad maxima ranging from 380 nm to 460 nm and lifetimes of hundreds of microseconds.

Thus, "clean" selective generation and spectroscopic study of this C5-centered radical should be of interest to confirm the abovementioned data. For this purpose, a photolabile group such as the *tert*-butyl ketone appears to be a useful option since it contains a nπ* transition, which can be populated via direct irradiation at λ > 300 nm and can generate the desired radical via Norrish type I photocleavage.

Concerning radical detection, one of the methods widely used is based on radical trapping by paramagnetic species such as nitroxides. In this context, profluorescent nitroxides represent a powerful analytical tool to detect free radicals and it is among the most sensitive methods currently available to follow thermooxidative, photophysical and other radical-based chemical processes.[10], [11], [12] These profluorescent radical probes consist of a nitroxide moiety covalently linked via a spacer to a fluorophore. Interaction of the unpaired spin of the nitroxide radical with the electrons of the fluorophore conjugated π system results in the loss of fluorescence emission. But, when the radical character from the molecule is removed (through either radical trapping or redox processes) fluorescence is completely restored. Thus, the fluorescence increase is a direct measurement of the free radical formation allowing study of its kinetics. A large variety of these

profluorescent probes have been synthesized by combining commercially available nitroxides to fluorophores via ester, amine, amide or sulfonamide linkages. [10]

In this context, trapping of carbon centered radical of nucleosides has been achieved using paramagnetic compounds such as TEMPO[3] and characterization of the obtained adduct has been performed by UPLC measurements followed by enzymatic digestion. Thus, the profluorescent nitroxide trapping methodology appears to be useful to detect the photogenerated C-centered radicals.

With this background, we will focus on the independent generation of 5,6-dihydropyrimidin-5-yl radicals in non-aqueous medium by means of the spectroscopic study of a lipophilic precursor, using the *tert*-butyl ketone as photolabile protecting group. Indeed, UVB/UVA irradiation (at $\lambda > 300$ nm) allows selective excitation of the $n\pi^*$ excited state of the ketone in a range where DNA barely absorbs, and yields radical formation through a Norrish type I photoreaction.[13] Up to now, photolabile precursors of nucleoside radicals have been used to establish the chemical fate in aqueous solution of thymidine and uridine C5 radicals integrated into synthetic oligonucleotides.[5],[8],[9] Nonetheless, production of these radicals in non-aqueous media would also be of interest to study since the microenvironment provided by the DNA structure and its complexes with proteins like histones may not be fully reproduced in aqueous media. Despite this fact, information on nucleic acid reactivity in non-aqueous media is lacking, except for the recently reported oxidation of DNA bases through one electron transfer or hydroxyl radical attack.[14],[15]

Hence, the main purpose of the work is to obtain transient absorption data of high value for subsequent time-resolved experiments in non-aqueous solutions, as well as to provide a new

tool for future assessment of the possible modulating effect of organic solvents on the secondary reactions mediated by peroxyl radicals.

2. Objectives

The main goal of this chapter is to characterize the photophysical properties of the species involved in the SSB production in DNA and RNA, pyrimidin-5-yl radical, in non-aqueous medium.

For this purpose, the following objectives have been pursued:

- To design and synthesize pyrimidin-C5-yl radical precursors making use of *tert*-butyl ketone photolabile group.

- To characterize the photophysical properties of the *tert*-butyl ketone radical precursor in order to confirm that it absorbs at $\lambda > 300$ nm where DNA barely absorbs and, as well, to confirm the presence of the radical by time-resolved spectroscopy.

- To design and synthesize an appropriate profluorescent radical trap that allows selective excitation at 365 nm and displays a structured fluorescence emission when trapping is produced. This will allow to perform further radical trapping experiments between the pyrimidin-5-yl radical precursors and the profluorescent probe.

- To corroborate the obtained experimental data with theoretical calculations.

3. Results and discussion

3.1. Synthesis of the 5,6-dihydropyrimidine-5-yl radical precursors

For the study of pyrimidin-C5-yl radicals, C5-pivaloyl derivatives precursors **1** (uridine) and **2** (thymidine) have been designed and synthesized as described in the literature for similar compounds[9] (Scheme 1). In a first step C5-C6 double bond of uridine or thymidine was reduced by hydrogenation using Rh/Al_2O_3 as catalyst. This was followed by the protection of the C5' and C3' hydroxyl by the *tert*-butyldimethylsilyl group (TBDMS) as well as nitrogen protection in position 3 by the *N*-2-trimethylsilylethyoxymethyl moiety (SEM). These derivatizations were also useful in order to increase the solubility in organic media. Finally, deprotonation of C5 by lithium diisopropylamide (LDA) and subsequent reaction with pivaloyl chloride led to the desired compounds.

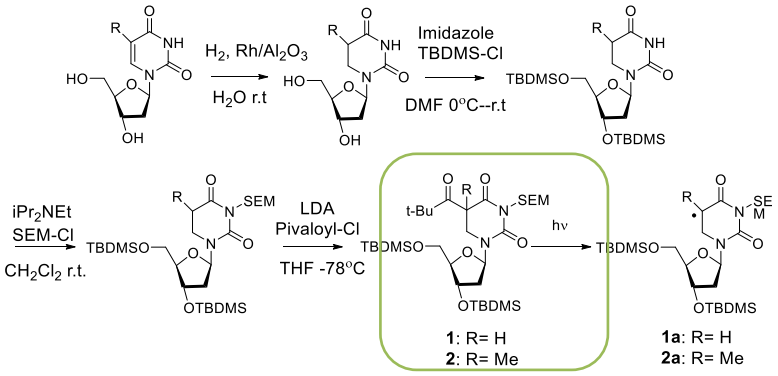

Scheme 1. Synthetic procedure of the C5-radical precursors derived from uridine and thymidine.

3.2. Photophysical characterization and steady-state photolysis of radical precursors with radical trapping

The UV-Vis absorption of the precursors has been measured in acetonitrile in order to determine the functional excitation range

required to trigger photodeprotection. The absorption spectra showed a band with absorption maxima at 285 or 315 nm for **1** and **2**, respectively (Figure 3). This absorption, assigned to the nπ* singlet excited state of the pivaloyl moiety, is relevant because it confers the possibility of performing selective UVA/UVB excitation of the radical precursor when inserted in DNA.

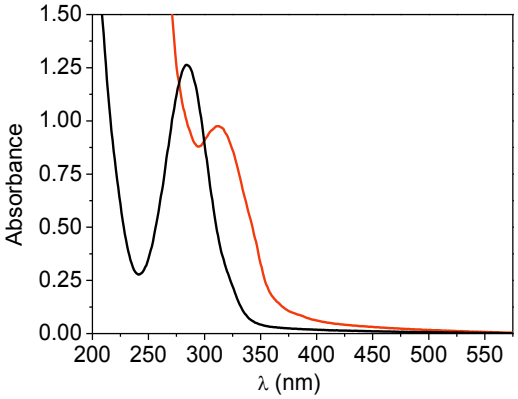

Figure 3. UV-Vis absorption spectra of compounds 1 (black) and 2 (red) in acetonitrile.

The photofragmentation of the radical precursors **1** and **2** was first investigated by using a new nitroxide-based fluorescent probe to confirm carbon-centered radical formation via its trapping. Thus, to design the probe, its two active parts have to be carefully chosen.

For the nitroxide moiety, TEMPO was selected based on its previously reported reactivity with carbon-centered radical of thymidine nucleoside.[3] Concerning the fluorescent moiety, several points need to be taken into account. The fluorophore has to (i) exhibit a strong and unambiguous fluorescence emission; (ii) be efficiently quenched by TEMPO paramagnetic species; (iii) have an absorption at long wavelength, higher than 350 nm, where DNA does not absorb and (iv) show little if any absorption in the 260−330 nm range, so that there is no interference with the absorbance of the *tert*-butyl ketone moiety.

In this context, 9-anthraceneacetic acid (AAA) was selected as a convenient fluorophore because it fulfills all the requirements mentioned above. AAA was synthesized following the procedure described by J. R. Shah et *al.*[16] (Scheme 2) where 9-hydroxy-methylanthracene was used as the starting material, and suffered a bromination followed by a nucleophilic substitution with potassium cyanide. Finally, 9-nitrilemethylanthracene was hydrolyzed with potassium hydroxide to yield 9-anthraceneacetic acid (AAA).

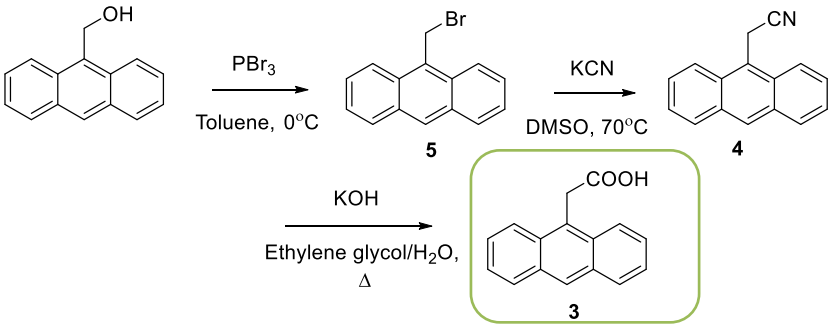

Scheme 2. Organic synthesis of AAA fluorophore.

Indeed, AAA has an absorption spectrum that allows selective excitation at 365 nm and displays a structured fluorescence emission. (Figure 5). In order to verify if its fluorescence emission can be affected by the presence of a paramagnetic species, preliminary steady-state and time-resolved fluorescence emission measurements (Figure 4A and 4B) were performed with AAA in the presence of 4-hydroxy-2,2,6,6-tetramethylpiperidine-1 oxyl (4-OH-TEMPO).

For both steady state and time-resolved quenching experiments, the excitation wavelengths (λ_{exc}) were 365 and 375 nm, respectively. A solution of 2-(anthracen-9-yl)acetic acid AAA in acetonitrile (2.6×10^{-5} M) and a stock solution of 4-OH-TEMPO (0.1 M) were prepared for the experiments. The rate constants for the reaction of AAA with 4-OH-TEMPO were obtained from the Stern–Volmer plots following equation (eq.) 1 or 2 for steady-state and time-resolved measurements, respectively.

$$I_0/I = 1 + K_{SV} \times [\text{4-OH-TEMPO}]$$
$$= 1 + k_q \times \tau_0 \times [\text{4-OH-TEMPO}], \text{ where } K_{SV} = k_q \times \tau_0 \quad \text{eq. 1}$$

where I_0 is the fluorescence intensity of AAA in the absence of quencher, I is the emission intensity after addition of a quencher concentration [4-OH-TEMPO] in molar, and K_{SV} is the Stern-Volmer constant (M^{-1}). A value of 109.4 M^{-1} was obtained for K_{SV} (Figure 4A).

$$1/\tau = 1/\tau_0 + k_q \times [\text{4-OH-TEMPO}] \quad \text{eq. 2}$$

where τ is the lifetime (s) after addition of a quencher concentration [4-OH-TEMPO] and τ_0 is the lifetime for AAA in the absence of quencher. A τ_0 value of 4.7 ns was measured (Figure 4B), and a bimolecular quenching rate constant k_q of *ca*. 2×10^{10} M^{-1} s^{-1} was obtained from the Stern−Volmer plot (Figure 4B, inset). Moreover, it appears from eq. 1 that k_q can be determined from K_{SV}. A similar k_q value of 2.3×10^{10} M^{-1} s^{-1} was thus obtained for the steady-state experiment, which rules out the occurrence of static quenching.

In consequence, an efficient quenching of the AAA singlet excited state by 4-OH-TEMPO was observed with bimolecular rate constant of *ca.* 10^{10} M^{-1} s^{-1}. As a whole, these data support the choice of AAA as the emissive species of the profluorescent probe.

The next step was the synthesis of the new AAA-TEMPO intramolecular dyad (Scheme 4), which was performed following a procedure given in the literature by Scaiano *and coll.* for similar compounds.[17] In agreement with the expectations, the obtained probe exhibited only a very weak emission (Figure 5).

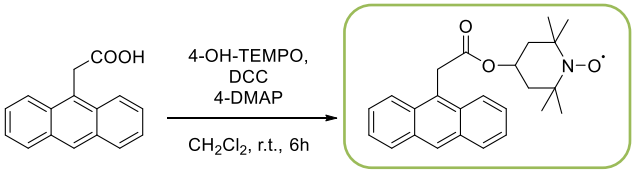

Scheme 4. Organic synthesis of the profluorescent probe AAA-TEMPO.

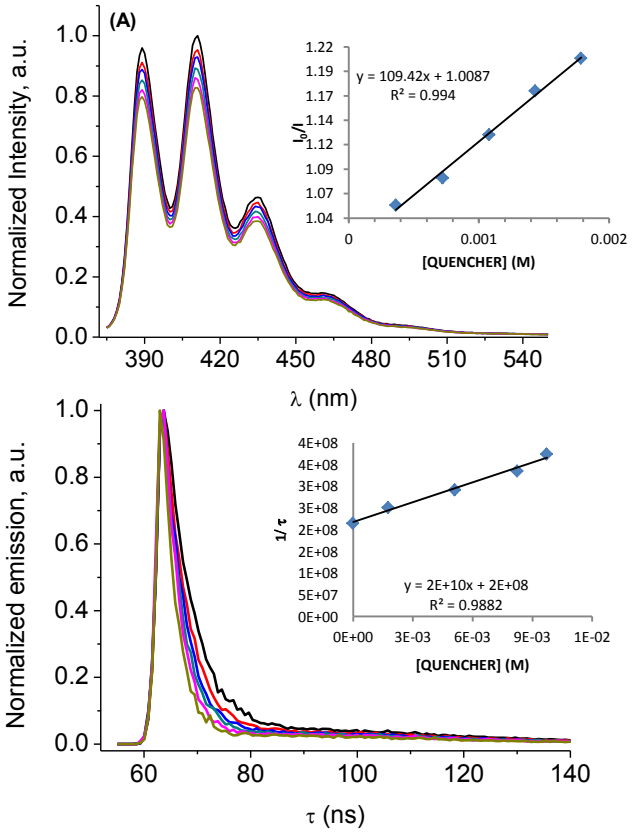

Figure 4. (A) Steady state fluorescence of an acetonitrile solution of AAA in the presence of increasing amounts of 4-OH-TEMPO (from 0 to 1.8 mM), λ_{exc}= 365 nm. Inset: Stern-Volmer plot. (B) Kinetic curves of an acetonitrile solution of AAA in the presence of increasing amounts of 4-OH-TEMPO (from 0 to 9.7 mM), λ_{exc}= 375 nm. Inset: Stern-Volmer plot.

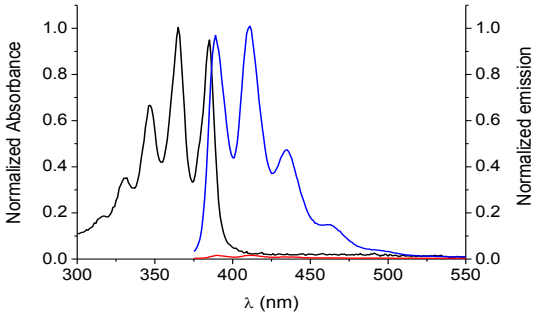

Figure 5. Absorption (black) and emission spectra of AAA (blue) and AAA-TEMPO (red) in acetonitrile, λ_{exc}= 365 nm.

Then, the ability of AAA-TEMPO to trap C-centered radicals was assessed by experiments in the presence of 2,2'-azobis(2-amidinopropane) dihydrochloride (AAPH) as thermolabile radical initiator.[12] A time-dependent enhancement of the emission was observed when the azo compound was heated at 100°C in the presence of the profluorescent probe (Figure 6).

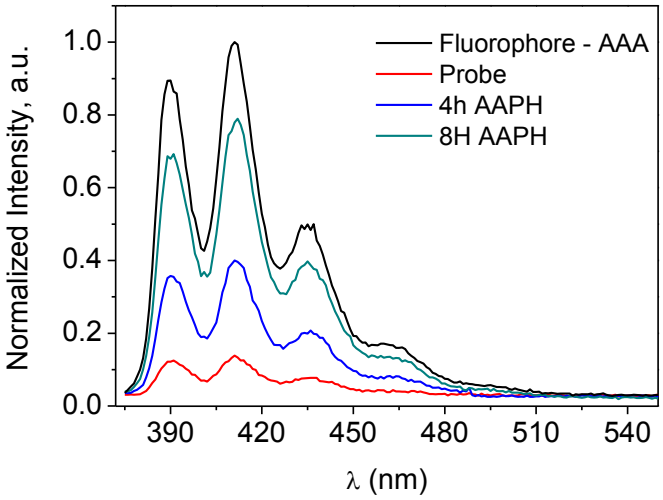

Figure 6. Steady state fluorescence of AAA-TEMPO in the presence of the radical initiator 2,2'-azobis(2-amidinopropane) dihydrochloride (0.032mM) at 100°C, λ_{exc}= 365 nm.

Thus, AAA-TEMPO was confirmed to behave as a typical nitroxide-based fluorescent probe, and it was used to investigate the formation of C5 centered radical by irradiation of **1** and **2** precursors. When a deaerated acetonitrile solution of **1** or **2** (0.15 mM) was irradiated at 300 nm in the presence of AAA-TEMPO (0.032 mM), the anthracene emission increased substantially as a function of irradiation time (Figure 7). Unfortunately, the profluorescent probe was photolabile to irradiation at 300 nm as a fluorescence enhancement was observed in the control sample, which contained solely the probe. Nonetheless, the generated fluorescence was consistently higher in the presence of **1** or **2**. In addition to this, the resultant covalent adduct of AAA-TEMPO with C5 radical of **1** and **2** was evidenced by a UPLC-HRMS analysis. The values of exact mass *m/z* 978.5503 and 992.5699 were determined and correspond to the molecular ion [M + H^+] with formula $C_{52}H_{84}N_3O_9Si_3$ for **1a** adduct and $C_{53}H_{86}N_3O_9Si_3$ for **2a** adduct, respectively. A control experiment performed under the same conditions but using a solution of uridine (or thymidine)/AAA-TEMPO helped to rule out the occurence of a H-abstraction process and supported the trapping of the C5-centered radical.

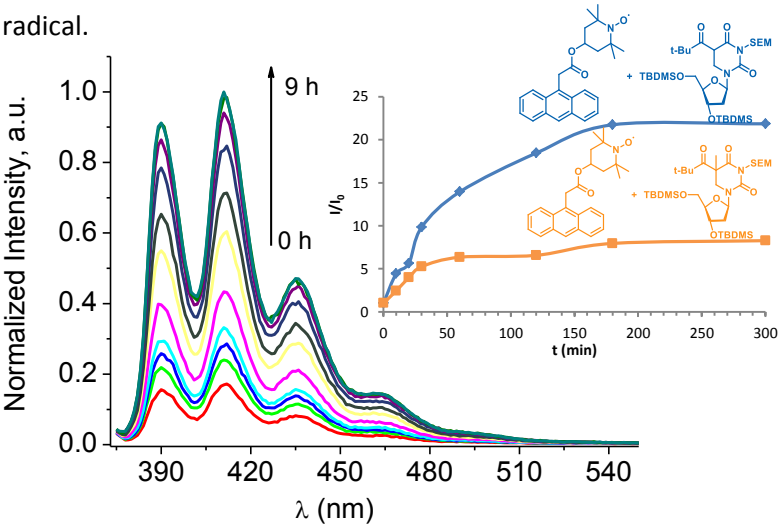

Figure 7. Emission spectra of N_2-bubbled acetonitrile solution of AAA-TEMPO in the presence of 1 (1:5), irradiated at λ_{irr}= 300 nm. Inset: I/I_0 ratio as a function of irradiation time for 1 (blue) and 2 (orange); the value obtained for the probe alone has been subtracted.

Further evidence supporting generation of the 5,6-dihydropyrimidin-5-yl radical has been obtained by laser flash photolysis in the nanosecond timescale. Experiments were useful to characterize the photogenerated C5 radical using 308 nm as excitation wavelength. Solutions of compounds **1** and **2** in acetonitrile (1.24 mM and 2.23 mM, respectively) were degassed under nitrogen atmosphere. The transient absorption spectrum was registered 4 μs after the laser pulse in order to avoid the presence of misleading short-lived components such as the triplet excited state. Indeed, this delay was selected because of the long lifetime of the radicals that are being studied, which do not decay in a window of tens of microseconds.[18],[19] In addition to this, the transient absorption spectra registered were noisy, due to the low ε of the radical species; however, **1** exhibited a maximum at ca. 400-420 nm, whereas in the case of **2** a blue shifted maximum peaking at ca. 350-400 nm was observed (Figure 8). Since these data are in agreement with previous pulse radiolysis experiments, the obtained transients were assigned to the C5-radicals. [18]

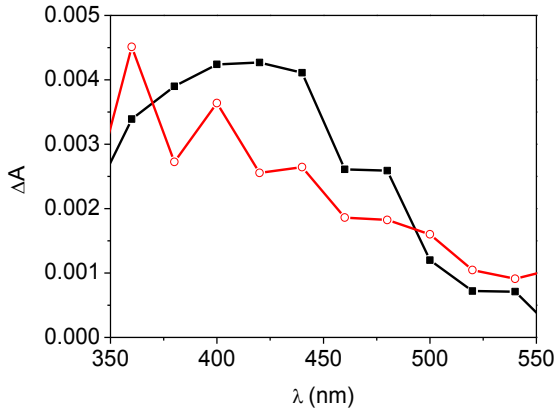

Figure 8. Transient absorption spectra for a deaerated acetonitrile solution of 1 (black line) and 2 (red line) obtained 4 μs after the 308 nm laser pulse.

3.3. Theoretical approach for photogeneration of 5,6-dihydropyrimidin-5-yl radicals

These experimental data were compared to theoretical calculations performed in collaboration with the research group of Dr. Roca-Sanjuán. Studies were carried out considering the chromophore structures **I**, **II**, **Ia**, and **IIa** (Figure 9) using the multiconfigurational CASPT2//CASSCF protocol[20], [21] in combination with the atomic natural orbital L-type (ANO-L) basis set contracted to C, N, O [4s3p1d]/H [2s1p],[22] as implemented in the MOLCAS 8 suite of programs,[23] to compute the vertical absorption energies and the oscillator strengths of the first eight excited states of the four species.

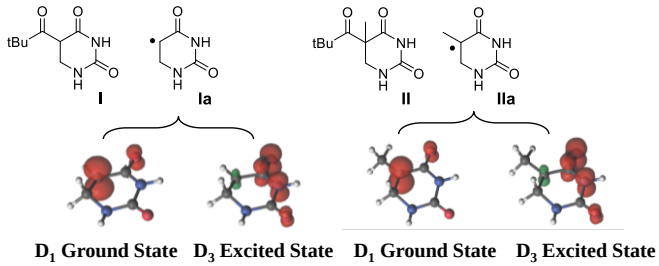

Figure 9. Structures of the models used in the theoretical calculations, I and II are singlet molecules, whereas Ia and IIa are doublet species. Representation of the difference between the α and β spin densities obtained from the computed CASSCF wave functions for the ground D_1 and excited D_3 states of Ia and IIa using an isovalue of 0.01, red and green colors indicate positive and negative spin densities, respectively.

The theoretical results are compiled in Table 1, where only data of the three lowest-energy excited states are shown. Absorption of UVB light by compounds **I** and **II** at low energies corresponds to the population of the relatively dark S_1 state, which mainly involves the $n_{CO1} \rightarrow \pi_1^*$ excitation localized in the C=O bond of the pivaloyl fragment. Such excited state was computed vertically at 4.11 eV (302 nm) and 3.93 eV (315 nm) for **I** and **II**, respectively. These theoretical predictions are in reasonable agreement with the experimental band maxima recorded at 4.35 eV (285 nm) for **1** and 3.93 eV (315 nm) for **2** (see Figure 3). Since the computed values were obtained

for the molecules *in vacuo* while in the experimental measurements the compounds were in an acetonitrile solution, the change of the module of the dipole moments between the excited and ground states were also analyzed; negligible solvatochromic shifts are expected for the low-lying excited-states of **I** and **II**, according to the small Δ_μ values (see Table 1). Although the agreement between theory and experiments for the absorption properties of the pivaloyl derivatives of uracil and thymine was not fully satisfactory, the trend was indeed coincident. Lower absorption energies were obtained for the compound with the methyl group. A parallel behavior has also been found when comparing the absorption spectra of the canonical nucleobases uracil and thymine.

For radical **Ia**, three excited states (D_2, D_3, and D_4) were computed at the energy range between 2.5 and 4.0 eV (see Table 1). Since the oscillator strength (*f*) associated with the $D_1 \rightarrow D_3$ transition is much higher than that of the D_2 and D_4 states, the D_3 state is predicted as the main responsible for the broad experimental band peaking at 2.95 – 3.10 eV (400-420 nm). The vertical absorption energy of the state, computed at 3.21 eV (386 nm), is in quite good agreement with the recorded absorption maximum. Regarding the solvent effects, negligible impact on the absorption energy of the bright D_3 state is expected on the basis of its relatively small Δ_μ value.

Changes in the localization of the unpaired electron after excitation were tracked by analyzing the spin densities of the ground and excited states (see Figure 9). The **Ia** species in the D_1 ground state has the unpaired electron in a π singly occupied natural orbital (SONO) mainly localized at the C5 atom (see orbitals in Figure 10). The excitation process implies a redistribution of the spin density over the molecule, changing the radical position to other parts of the molecular structure. Thereby, in the D_3 state, the unpaired electron is in the π_1 natural orbital (NO) that is now mainly localized over the OCN atoms, as shown in the spin-density representations displayed in Figure 9.

The UV-Vis absorption properties of the radical **IIa** are also summarized in Table 1. No significant differences in the electronic nature of the ground and excited states were found with respect to those of **Ia**. Nonetheless, as a consequence of the methyl group at the C5 position, the vertical absorption energies are somewhat higher than those of **Ia**. This blue shift of around 0.1-0.2 eV is also observed in the experiments.

Compound	State	Nature of the transition	Vertical absorption energy/ eV(nm)	Oscillator Strength (*f*) gs → es	Δμ / D	Experimental / eV(nm)
I	S_1	$n_{CO1} \rightarrow \pi_1^*$ (pivaloyl group)	**4.11 (302)**	**0.00004**	**-0.02**	**4.35 (285)**
II	S_1	$n_{CO1} \rightarrow \pi_1^*$ (pivaloyl group)	**3.93 (315)**	**0.00004**	**-0.32**	**3.93 (315)**
Ia	D_2	$n_{CO1} \rightarrow \pi_{SONO}$	**2.57 (482)**	**0.00019**	**-1.42**	
	D_3	$\pi_1 \rightarrow \pi_{SONO}$	**3.21 (386)**	**0.02173**	**-2.84**	**2.95-3.10 (400-420)**
	D_4	$\pi_2 \rightarrow \pi_{SONO}$	**3.62 (342)**	**0.00290**	**5.82**	
IIa	D_2	$n_{CO1} \rightarrow \pi_{SONO}$	**2.74 (453)**	**0.00024**	**-1.20**	
	D_3	$\pi_1 \rightarrow \pi_{SONO}$	**3.35 (370)**	**0.02372**	**-3.04**	**3.54-3.10 (350-400)**
	D_4	$\pi_2 \rightarrow \pi_{SONO}$	**3.82 (325)**	**0.00235**	**5.06**	

Table 2. **Nature of the electronic transition, CASPT2 vertical absorption energies, oscillator strengths, and module of the CASSCF dipolar moments relative to the ground state (Δμ = $|\vec{\mu}|_{ES} - |\vec{\mu}|_{GS}$) for the low-lying excited states of the studied species. The experimental absorption band maxima associated with the corresponding excited state are also shown. Abbreviations: gs = ground state, es = excited state.**

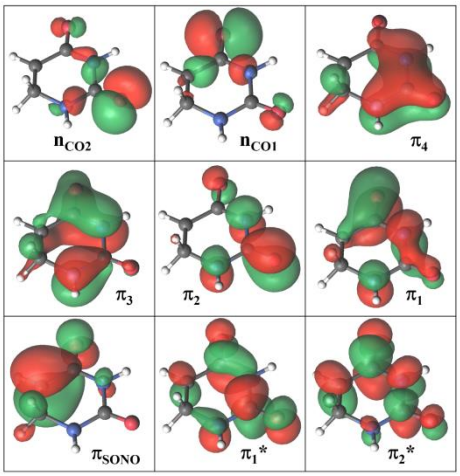

Figure 10. Natural orbitals included in the active space of the CASSCF/CASPT2 calculations for Ia. Similar orbitals have been obtained for IIa.

4. Conclusions

To summarize, synthesis of lipophilic C5 radical precursors **1** and **2** and their photogeneration in non-aqueous medium has been established by radical trapping experiments using TEMPO-based profluorescent probe. Finally, laser flash photolysis experiments evidenced their transient absorption spectra in a clean process. These experimental data, have been supported by multiconfigurational *ab initio* CASPT2//CASSCF protocol.

5. Experimental Section

5.1. Synthesis and characterization

5.1.1. General procedures for synthesis of 1 and 2

5.1.1.1. 2'-Deoxy-5,6- dihydrouridine (1Sa) and 5,6-dihydrothymidine (2Sa). Synthesis was performed following the method described by Greenberg *et al.*;[5] 0.25 g of the Rh/Al_2O_3 catalyst was added to 5 g of 2'-deoxyuridine or 2'-deoxythymidine in 50 mL of water under 30 bar

of H_2. After purification, 4.4 g (96%) of **1Sa** and 4.3 (85%) of **2Sa** were obtained as a colorless oil.

Characterization of 1Sa:

^{1}H NMR (300 MHz, D_2O) δ: 6.26 (t, J = 7 Hz, 1H), 4.37 (m, 1H), 3.91 (m, 1H), 3.75 (m, 2H), 3.55 (m, 2H), 2.74 (t, J = 6 Hz, 2H), 2.31 (m, 1H), 2.13 (m, 1H).

^{13}C NMR (75 MHz, D_2O) δ: 173.8 (CO), 154.2 (CO), 85.2 (CH), 84.0 (CH), 70.8 (CH), 61.6 (CH_2), 35.7 (CH_2), 35.2 (CH_2), 30.0 (CH_2). HMRS (ESI-TOF): *m/z*, $C_9H_{14}N_2O_5Na$ $[M + Na]^+$ calculated for 253.0800; found: 253.0799.

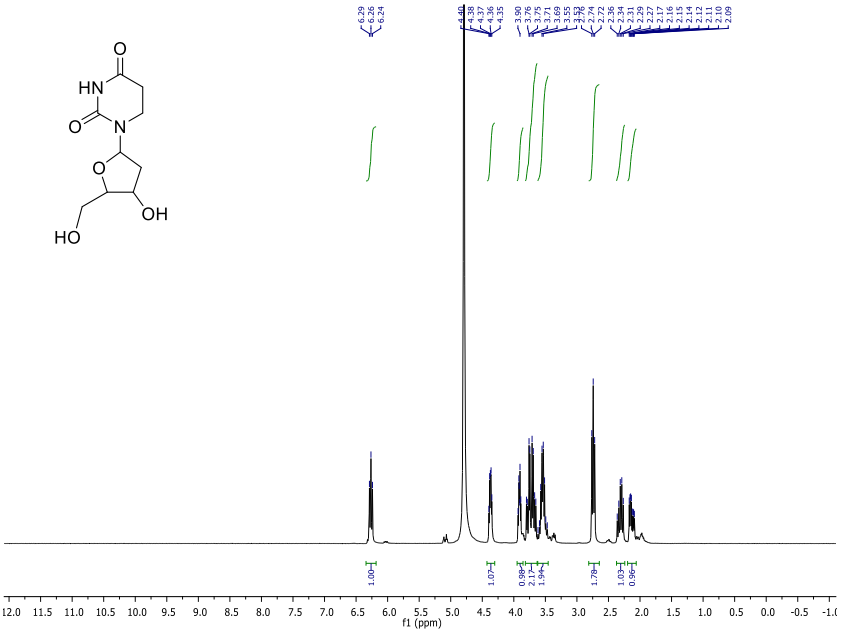

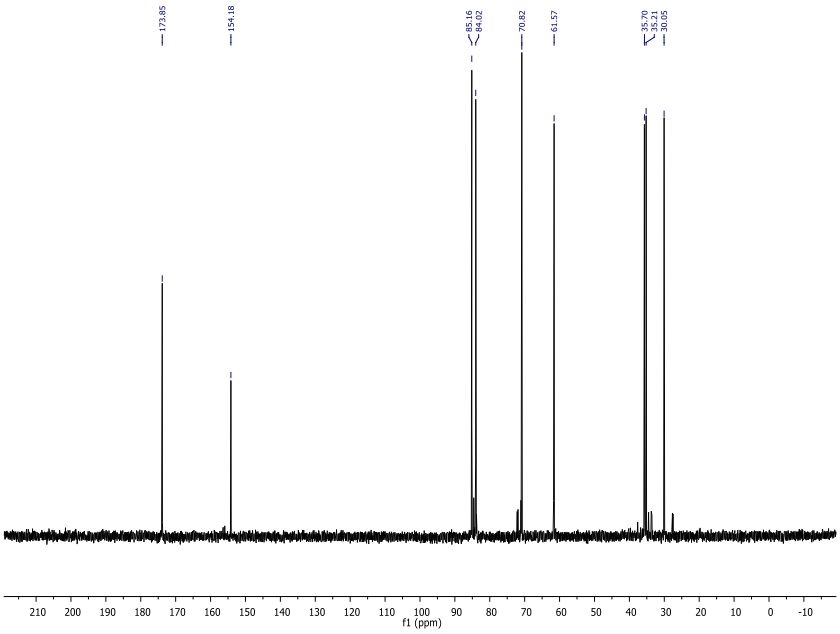

Characterization of 2Sa:

^{1}H NMR (300 MHz, D_2O) δ: 6.27 (t, J = 6 Hz, 1H), 4.35 (m, 1H), 3.88 (m, 1H), 3.71 (m, 2H), 3.56 (dd, J = 12.9, 5.6 Hz, 1H), 3.25 (m, 1H), 2.83 (m, 1H), 2.30 (m, 1H), 2.14 (m, 1H), 1.21 (d, J = 7.1 Hz, 3H).

^{13}C NMR (75 MHz, D_2O) δ: 176.7 (CO), 154.3 (CO), 85.1 (CH), 83.8 (CH), 70.8 (CH), 61.6 (CH_2), 42.0 (CH_2), 35.4 (CH_2), 34.6 (CH), 12.1 (CH_3).

HMRS (ESI-TOF): *m/z* $[M + H]^+$ calculated for $C_{10}H_{17}N_2O_5$: 245.1137; found: 245.1131.

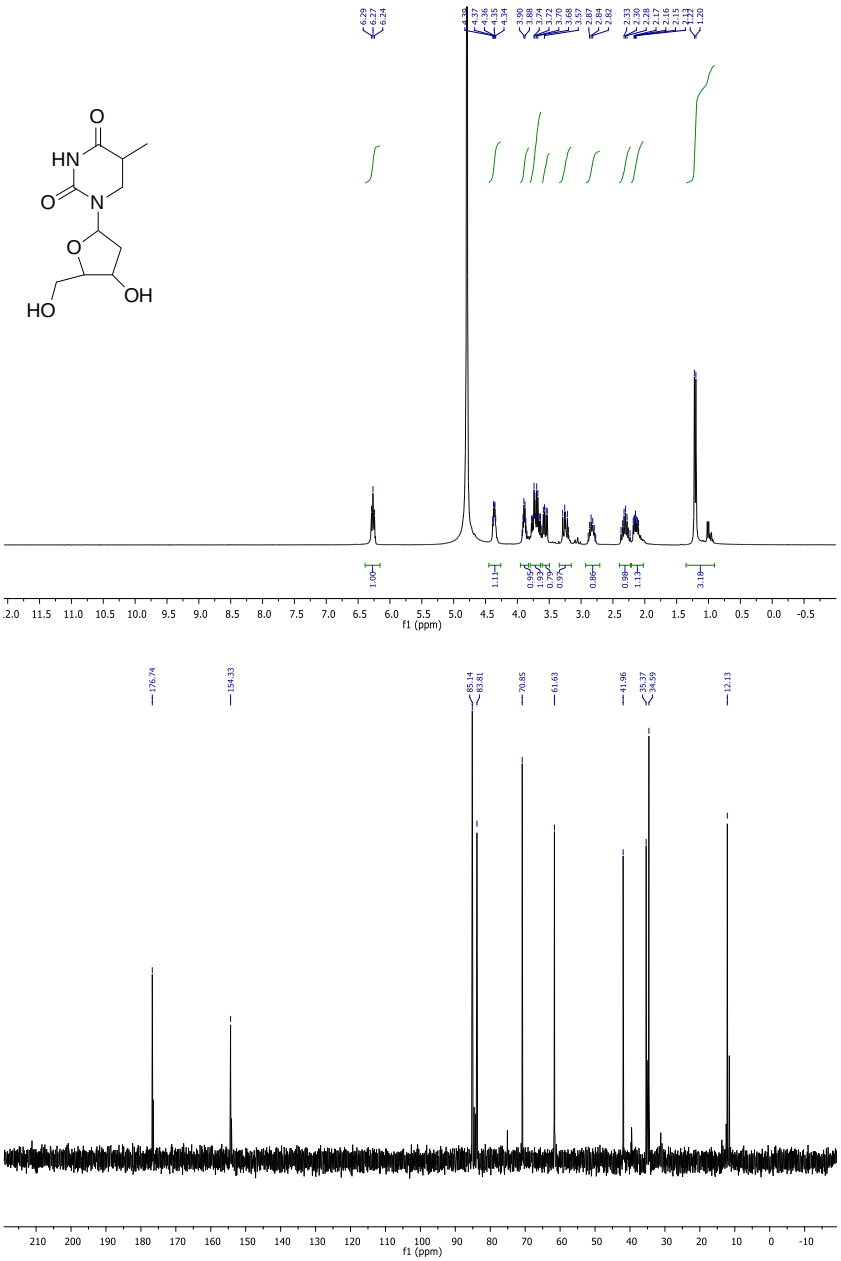

5.1.1.2. 2'-Deoxy-3',5'-bis-o-[(*tert*-butyl)dimethylsilyl]-5,6-dihydrouridine (1Sb). 4.4 g (0.021 mol) of **1Sa**, 8.55 g (0.126 mol) of imidazole, and 11.4 g (0.076 mol) of *tert*-butyldimethylsilyl chloride were diluted in 35 mL

of dimethylformamide at 0 °C. The mixture was allowed to reach room temperature and stirred overnight. Then, 250 mL of water were added, and extraction was performed with diethyl ether. The aqueous phase was further washed with diethyl ether (3 × 180 mL). The combined organic phases were mixed, washed with brine, dried with $MgSO_4$, and evaporated to dryness under reduced pressure. Purification was performed by flash column chromatography using hexane/ethyl acetate, (6:1, v:v), as eluent, and 7.2 g (76%) of **1Sb** were obtained as a white solid.

3',5'-Bis-o-[(*tert*-butyl)dimethylsilyl]-5,6-dihydrothymidine (2Sb).
4.3 g (0.018 mol) of **2Sa**, 7.2 g (0.106 mol) of imidazole, and 9.5 g (0.063 mol) of *tert*-butyldimethylsilyl chloride were diluted in 30 mL of dimethylformamide at 0 °C. The mixture was allowed getting to room temperature and stirred overnight. After addition of 250 mL of water and extraction with diethyl ether, the aqueous phase was further washed with diethyl ether (3 × 180 mL). The combined organic phases were mixed, washed with brine, dried with $MgSO_4$, and evaporated under reduced pressure. Purification was performed by flash column chromatography using hexane: ethyl acetate, (6:1, v:v), as eluent. Compound **2Sb** (6.2 g) was obtained in 75% yield as a white solid.

Characterization of 1Sb:
^{1}H NMR (300 MHz, $CDCl_3$) δ: 7.62 (br s, 1H), 6.28 (t, J = 7.0 Hz, 1H), 4.36 (m, 1H), 3.77 (m, 1H), 3.71 (m, 2H), 3.65 (m, 1H), 3.31 (m, 1H), 2.59 (m, 2H), 2.01 (m, 2H), 0.89 (m, 18H), 0.06 (m, 12H).
^{13}C NMR (75 MHz, $CDCl_3$) δ: 169.9 (CO), 152.2 (CO), 86.5 (CH), 84.0 (CH), 72.1 (CH), 63.0 (CH_2), 37.8 (CH_2), 35.4 (CH_2), 31.3 (CH_2), 26.0 ($3CH_3$), 25.9 ($3CH_3$), 18.4 (C), 18.1 (C), −4.5 (CH_3), −4.7 (CH_3), −5.3 (CH_3), −5.4 (CH_3).
HMRS (ESI-TOF) *m/z* $[M+Na]^+$ calculated for $C_{21}H_{42}N_2O_5Si_2Na$: 481.2530; found: 481.2531.

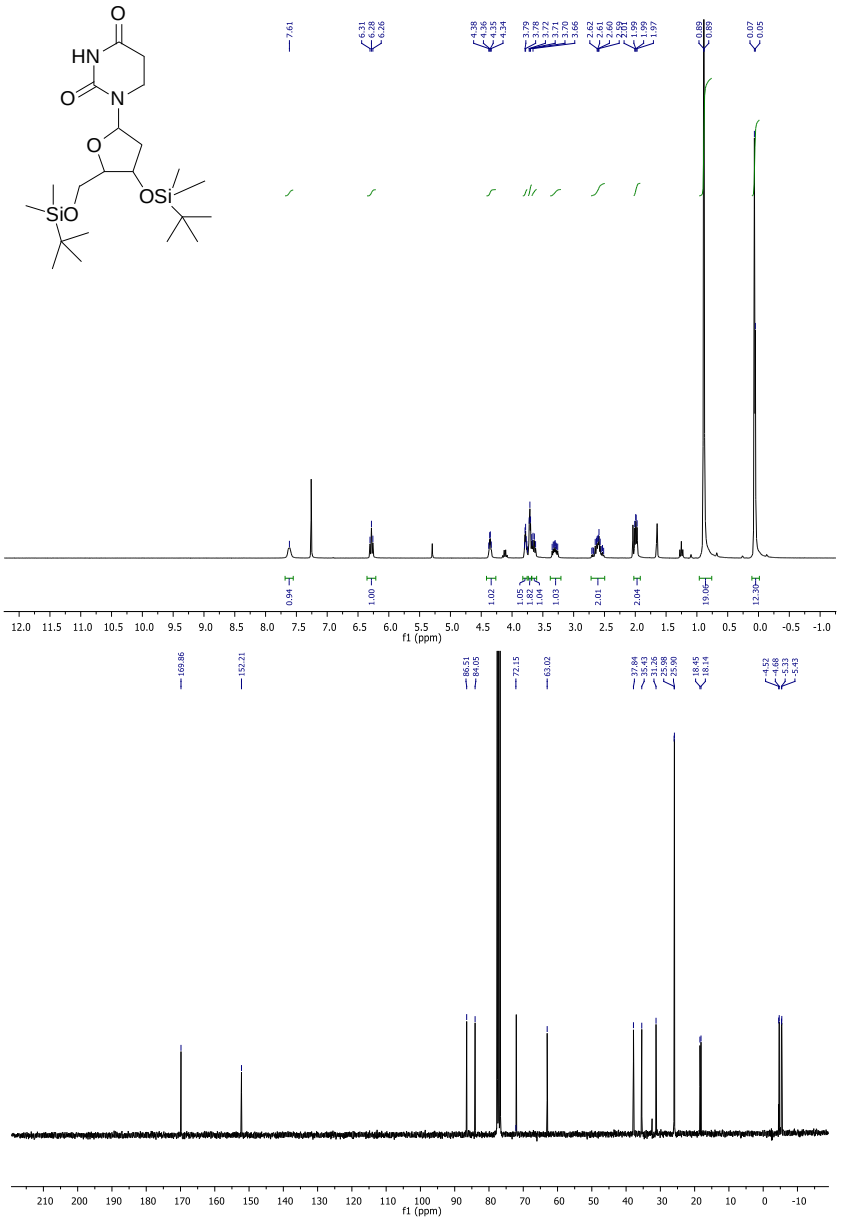

Characterization of 2Sb:

^{1}H NMR (300 MHz, $CDCl_3$) δ: 7.44 (br s, 1H), 6.30 (t, J = 7 Hz,1H), 4.36 (m, 1H), 3.80 (m, 1H), 3.71 (m, 2H), 3.37 (m, 1H), 3.27 (m, 1H), 2.61 (m, 1H), 1.98 (m, 2H), 1.25 (d, J = 9 Hz, 3H), 0.89 (s + s, 18H), 0.06 (br s, 12H).

^{13}C NMR (75 MHz, $CDCl_3$) δ: 172.8 (CO), 152.5 (CO), 86.6 (CH), 83.8 (CH), 72.2 (CH), 63.1 (CH_2), 42.1 (CH_2), 38.1 (CH_2), 35.6 (CH), 26.0 ($3CH_3$), 25.9 ($3CH_3$), 18.5 (C), 18.1 (C), 13.2 (CH_3), −4.5 (CH_3), −4.7 (CH_3), −5.3 (CH_3), −5.4(CH_3).

HRMS (ESI-TOF) *m/z* $[M+ H]^+$ calculated for $C_{22}H_{45}N_2O_5Si_2$: 473.2867; found: 473.2862.

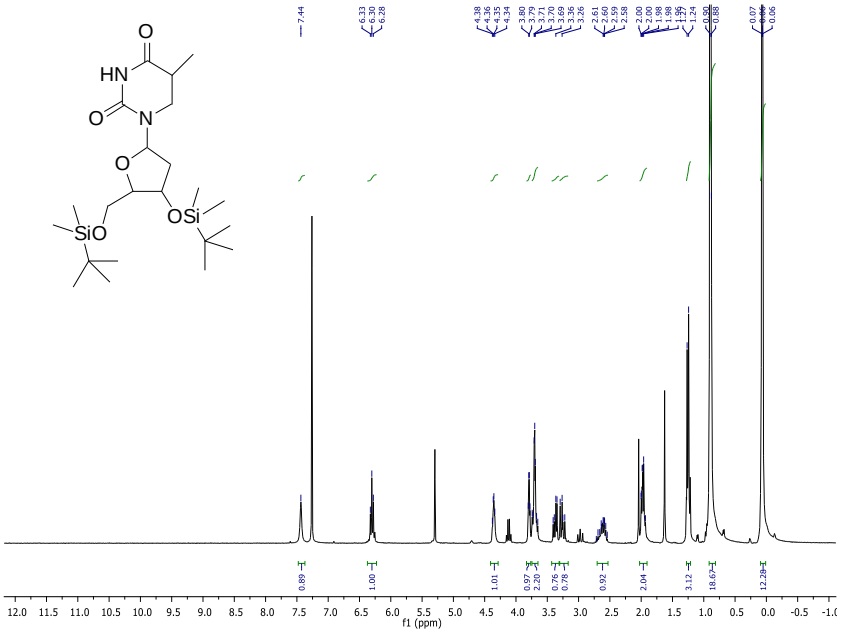

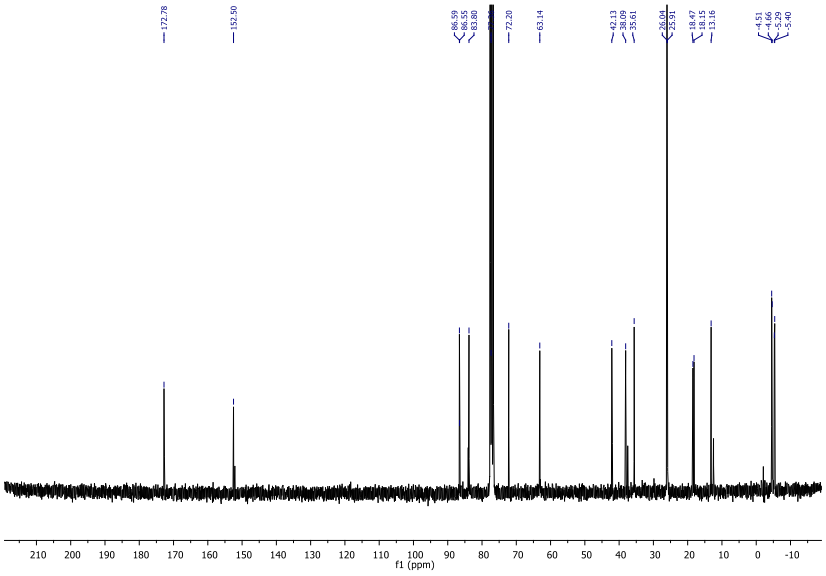

5.1.1.3. 2'-Deoxy-3',5'-bis-o-[(*tert*-butyl)dimethylsilyl]-3-[[2-(trimethylsilyl) ethoxy]methyl]-5,6-dihydrouridine (1Sc).

A solution of **1Sb** (7.23g, 0.016 mol) in 11 mL of *N,N*-diisopropylethylamine was mixed with 4.2 mL (0.024 mol) of 2-(trimethylsilyl)ethoxymethyl chloride diluted in 10 mL of CH_2Cl_2, and the mixture was stirred overnight at room temperature. Then, CH_2Cl_2 and a saturated solution of $NaHCO_3$ were added, and the organic phase was extracted, dried with $MgSO_4$, and concentrated under reduced pressure. Purification was performed by flash column chromatography using hexane:ethyl acetate (10:1, v:v) as eluent, and 5.3 g (57%) of **1Sc** were obtained as a colorless oil.

3',5'-Bis-o-[(*tert*-butyl)dimethylsilyl]-3-[[2-(trimethylsilyl)ethoxy]-methyl]-5,6-dihydrothymidine (2Sc).

A solution of **2Sb** (4.3 g, 0.0091 mol) in 16 mL of *N,N*-diisopropylethylamine was mixed with 3.5 mL (0.02 mol) of 2-(trimethylsilyl)ethoxymethyl chloride diluted in 10 mL of CH_2Cl_2, and the mixture was stirred overnight at room temperature. Then, CH_2Cl_2 and a saturated solution of $NaHCO_3$ were added, and the organic phase was extracted, dried with $MgSO_4$, and concentrated under reduced pressure. Purification was performed by flash column

chromatography using hexane: ethyl acetate (10:1, v:v) as eluent, and 4.2 g (53%) of **2Sc** were obtained as colorless oil.

Characterization of 1Sc.

^{1}H NMR (300 MHz, $CDCl_3$) δ: 6.32 (t, J = 7 Hz, 1H), 5.21 (m, 2H), 4.34 (m, 1H), 3.83−3.56 (m, 6H), 3.25 (m, 1H), 2.68 (m, 2H), 1.99 (m, 2H), 0.95−0.88 (m, 20H), 0.05 (brs, 12H), −0.02 (brs, 9H).

^{13}C NMR (75 MHz, $CDCl_3$) δ 169.7(CO), 152.9 (CO), 86.4 (CH), 84.8(CH), 72.0 (CH), 69.9 (CH_2), 67.0 (CH_2), 63.0 (CH_2), 37.9 (CH_2), 34.3 (CH_2), 32.0 (CH_2), 25.9 ($3CH_3$), 25.8 ($3CH_3$), 18.4 (CH_2), 18.2 (2C), −1.3 ($3CH_3$), −4.5 (CH_3), −4.7 (CH_3), −5.4 (CH_3), −5.5 (CH_3).

HMRS (ESI-TOF) *m/z* $[M+ Na]^+$ calculated for $C_{27}H_{56}N_2O_6Si_3Na$: 611.3344; found: 611.3326.

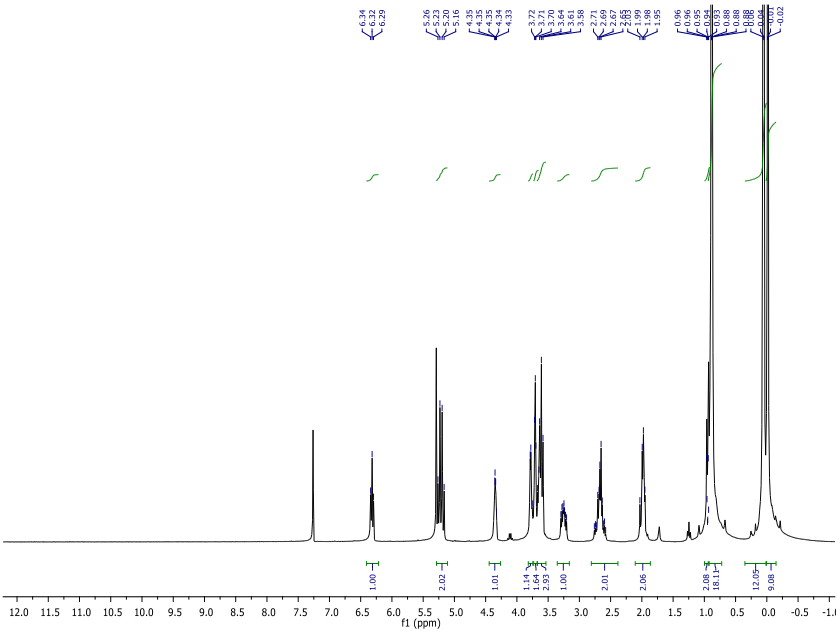

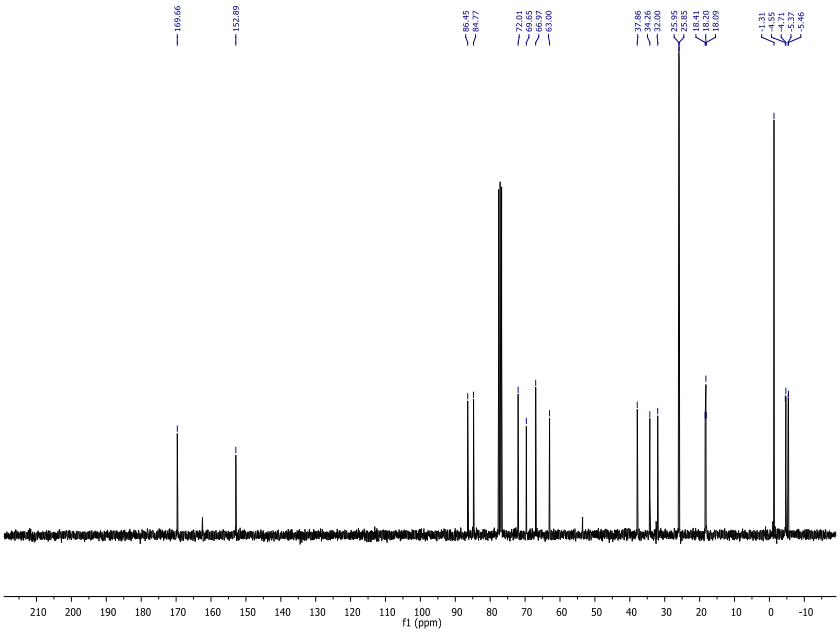

Characterization of 2Sc.

^{1}H NMR (300 MHz, $CDCl_3$) δ: 6.35 (t, J = 9 Hz, 1H), 5.20 (s, 2H), 4.35 (m, 1H), 3.79 (m, 1H), 3.70 (m, 2H), 3.61 (m, 2H), 3.29 (m, 2H), 2.66 (m, 1H), 1.95 (m, 2H), 1.25 (d, J = 9 Hz, 3H), 0.90 (m, 20H), 0.06 (brs, 12H), −0.01 (s, 9H).

^{13}C NMR (75 MHz, $CDCl_3$) δ: 172.8 (CO), 153.1 (CO), 86.5 (CH), 84.5 (CH), 72.2 (CH), 69.9 (CH_2), 66.9 (CH_2), 63.1 (CH_2), 40.8 (CH_2), 38.1 (CH_2), 36.0 (CH), 26.0 ($3CH_3$), 25.9 ($3CH_3$), 18.5 (2C), 18.2 (CH_2), 13.6 (CH_3), −1.3 ($3CH_3$), −4.5 (CH_3), 4.7 (CH_3), −5.3 (CH_3), −5.4 (CH_3).

HMRS (ESI-TOF) *m/z* $[M + Na]^+$ calculated for $C_{28}H_{58}N_2O_6Si_3Na$: 625.3500; found: 625.3484.

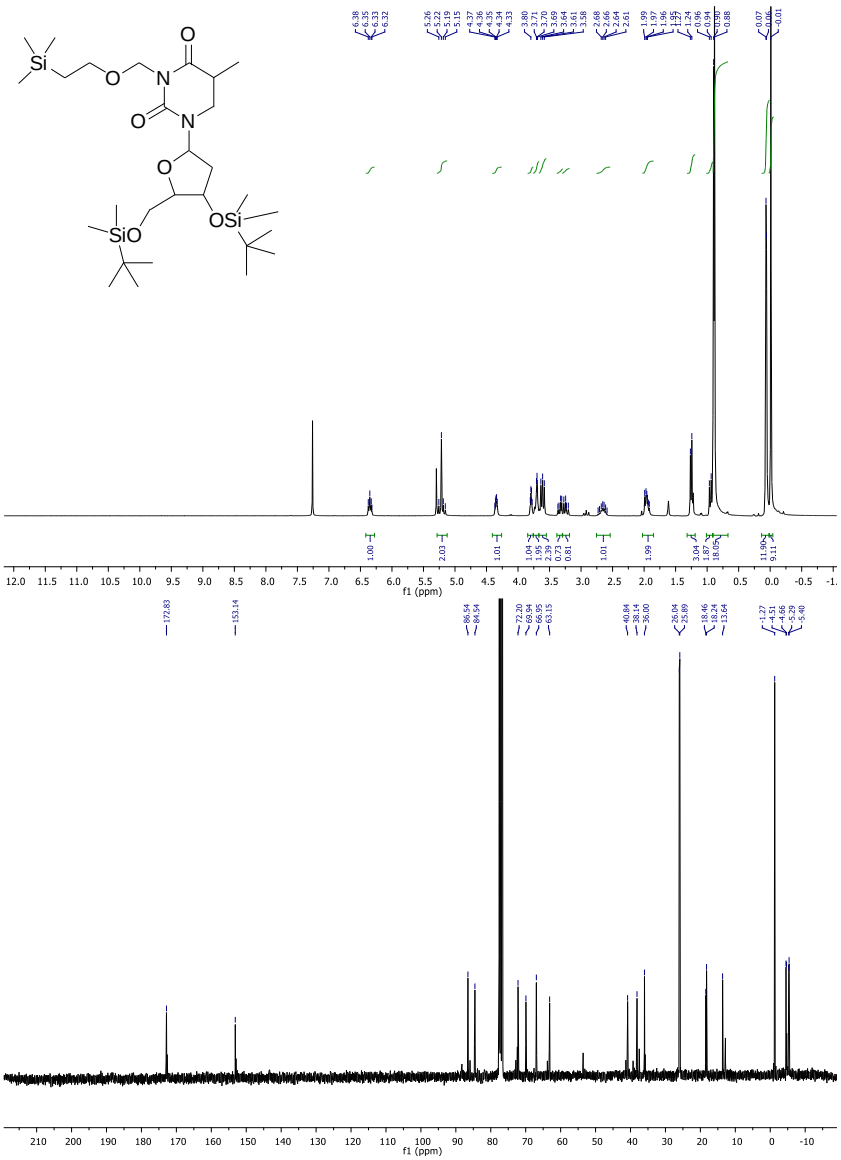

5.1.1.4. 2'-Deoxy-3',5'-bis-o-[(*tert*-butyl)dimethylsilyl]-3-[[2-(trimethylsilyl) ethoxy]methyl]-5-(2,2-dimethyl-1-oxopropyl)-5,6-dihydrouridine (1).

The final compound **1** was obtained as a diastereomeric mixture following the methodology described in the literature by Greenberg *et al.* for related compounds.[5] Briefly, a solution of **1Sc** (0.1 g, 1.7 × 10^{-4} mol) in tetrahydrofuran was stirred during 30 min with 0.85 mL of 2 M LDA at 78 °C. Then, pivaloyl chloride (0.02 mL, 1.6 × 10^{-4} mol)

was added dropwise, and the mixture was kept at this temperature for 30 min. The organic phase was extracted after addition of a saturated solution of NH_4Cl and ethyl acetate (3 × 75 mL), washed with brine, dried with $MgSO_4$, and evaporated to dryness under reduced pressure. The purification was performed by preparative liquid chromatography (PLC) using hexane: ethyl acetate (5:1, v:v) as eluent to afford compound **1** as a yellowish oil (0.06 g, 53%).

3',5'-Bis-o-[(*tert*-butyl)dimethylsilyl]-3-[[2-(trimethylsilyl)ethoxy]-methyl]-5-(2,2-dimethyl-1-oxopropyl)-5,6-dihydrothymidine (2).

The final compound **2** was obtained following the methodology described in the literature by Greenberg *et al.* for related compounds.[5] Briefly, a solution of **2Sc** (0.1 g, 1.7 × 10^{-4} mol) in tetrahydrofuran was stirred for 3 h with 0.83 mL of 2 M LDA at -78 °C. Then, pivaloyl chloride (0.02 mL, 1.6 × 10−4 mol) was added dropwise, and the mixture was kept at this temperature for 1 h 30 min, allowed to reach room temperature, and stirred for additional 3 hours. The organic phase was extracted after addition of a saturated solution of $NaHCO_3$ and ethyl acetate (3 × 75 mL), washed with brine, dried with $MgSO_4$, and evaporated to dryness under reduced pressure. The purification was performed by preparative liquid chromatography (PLC) using hexane: ethyl acetate (5:1, v:v) as eluent to afford compound **2** as a transparent oil (0.07 g, 61%).

Characterization of 1.

^{1}H NMR (300 MHz, $CDCl_3$) δ: 6.34 (dd, J = 9 Hz, J = 6 Hz, 1H), 5.28 (d, J = 9 Hz, 1H), 5.15 (d, J = 9 Hz, 1H), 4.31 (m, 1H), 4.17 (m, 1H), 3.82 (m, 1H), 3.67−3.57 (m, 5H), 3.47 (m, 1H), 1.93 (m, 2H), 1.25− 1.21 (m, 9H), 0.89 (m, 20H), 0.07 to −0.01 (m, 21H).

^{13}C NMR (75 MHz, $CDCl_3$) δ: 209.1 (CO), 207.6 (CO), 168.1 (CO), 167.9 (CO), 152.7 (CO), 152.2 (CO), 86.8 (CH), 86.7 (CH), 85.1 (CH), 84.8 (CH), 77.4 (C), 72.7 (CH), 72.4 (CH), 70.0 (CH_2), 67.1 (CH_2), 67.0 (CH_2), 63.6 (CH_2), 63.3 (CH_2), 47.9 (CH), 47.7 (CH), 45.5 (C), 38.2 (CH_2), 37.6 (CH_2), 37.4 (CH_2), 26.0 ($3CH_3$), 25.9 ($3CH_3$), 25.7 ($3CH_3$), 18.4 (C), 18.1 (CH_2), −1.3 ($3CH_3$), −4.5 (CH_3), −4.7 (CH_3), −5.3 (CH_3), −5.4 (CH_3).

HRMS (ESI-TOF) *m/z* $[M + Na]^+$ calculated for $C_{32}H_{64}N_2O_7Si_3Na$: 695.3919; found: 695.3903.

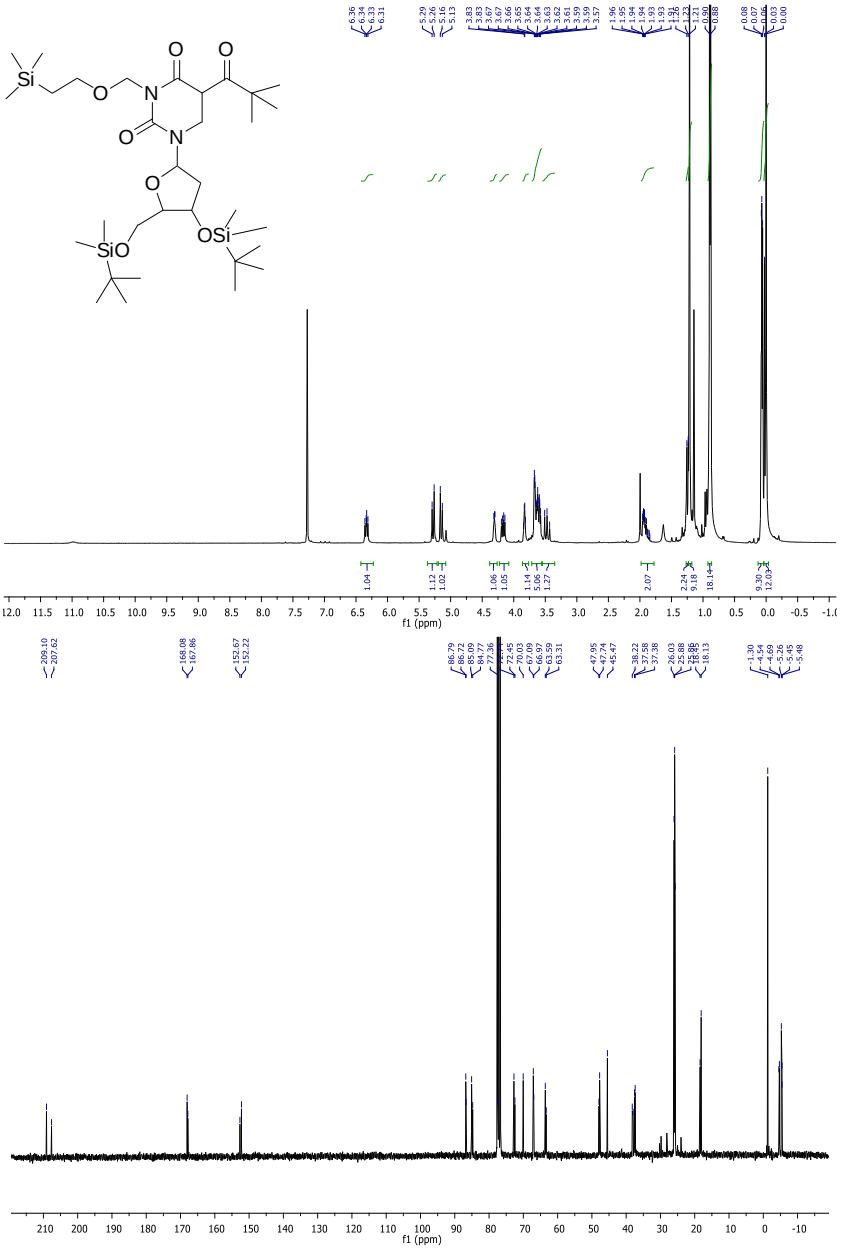

Characterization of 2.

^{1}H NMR (300 MHz, $CDCl_3$) δ: 6.39 (t, J = 6 Hz, 1H), 4.93 (m, 2H), 4.33 (m, 1H), 3.94 (d, J = 12 Hz, 1H), 3.75−3.63 (m, 4H), 3.50 (t, J = 6 Hz, 2H), 2.09 (m, 1H), 1.89 (m, 1H), 1.49 (s, 3H), 1.30 (s, 9H), 0.89 (m, 20H), 0.06 (br s, 12H), −0.02 (s, 9H).

^{13}C NMR (75 MHz, $CDCl_3$) (corresponds to the enol ester 2' resulting from 1,3 acyl shift inside the NMR tube) δ: 174.6 (CO), 153.8 (CO), 134.3 (CO), 94.1 (C), 86.0 (CH), 84.4 (CH), 72.1 (CH), 71.2 (CH_2), 65.0 (CH_2), 63.0 (CH_2), 42.1 (CH_2), 39.2 (C), 36.2 (CH_2), 27.1 ($3CH_3$), 26.1 ($3CH_3$), 25.9 ($3CH_3$), 18.5 (C), 18.1 (C), 18.0 (CH_2), 12.8 (CH_3), −1.2 ($3CH_3$), −4.5 (CH_3), −4.7 (CH_3), −5.2 (CH_3), −5.4 (CH_3).

HMRS (ESI-TOF) *m/z* $[M + H]^+$ calculated for $C_{33}H_{67}N_2O_7Si_3$: 687.4256; found: 687.4271.

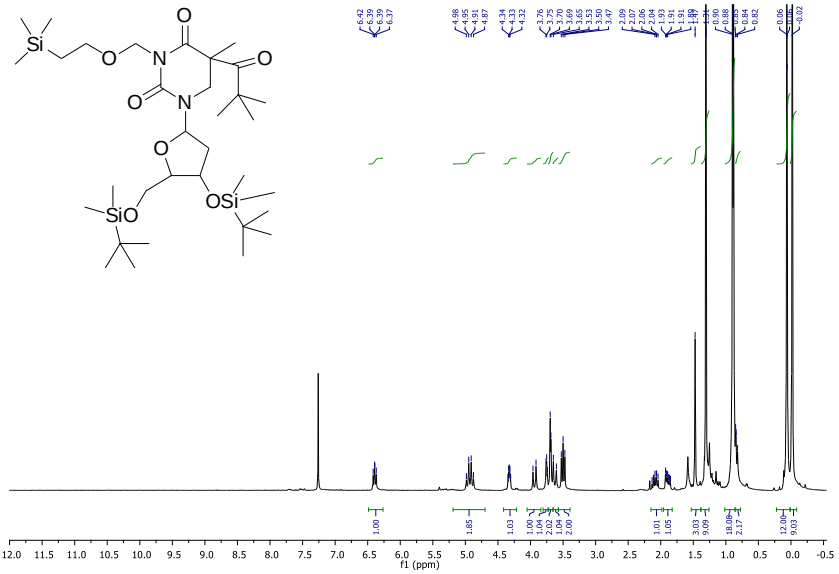

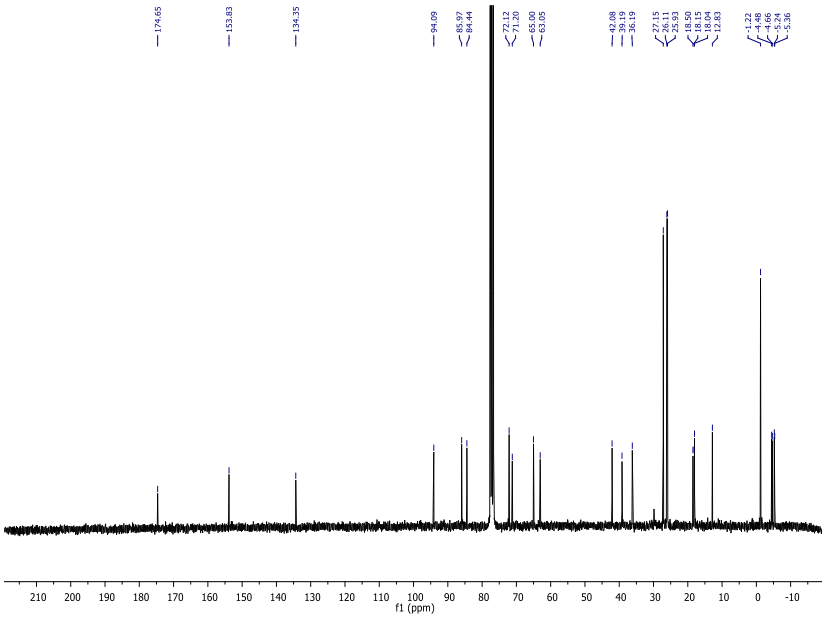

5.1.2. General procedure for synthesis of AAA and AAA-TEMPO.

5.1.2.1. Synthesis of AAA fluorophore.

5.1.2.1.1. Synthesis of 9-(bromomethyl)anthracene (5).

The synthetic procedure was performed as described in the literature,[16] phosphorus tribromide (8.43 mmol, 0.8 mL) was added via syringe to a suspension of 9-hydroxymethylanthracene (7.2 mmol, 1.5 g) in dry toluene (0.18 M) at 0°C. The mixture was stirred for 1 hour at 0°C and then allowed to reach room temperature, when the reaction turned homogeneous. A saturated solution of Na_2CO_3 (15 mL) was slowly added to the reaction mixture. For the work up, the phases were separated and the organic phase was rinsed with H_2O (10 mL) and then with brine and finally dried with $MgSO_4$. Compound **5** was obtained as a yellowish crystalline powder with a 100 % yield (2.08 g).

Characterization of 5.

^{1}H NMR (300 MHz, $CDCl_3$) δ: 8.50 (s, 1H), 8.32 (d, J=9Hz, 2H), 8.05 (d, J=6Hz, 2H), 7.65 (ddd, J=12Hz, J=6Hz, J=3Hz, 2H), 7.51 (m, J=6Hz, 2H), 5.55 (s, 2H). 1.56 traces of water present in $CDCl_3$.

^{13}C NMR (75 MHz, $CDCl_3$) δ: 131.75 (C), 129.88 (2C), 129.42 (2CH), 129.34 (CH), 128.02 (2C), 126.94 (2CH), 125.53 (2CH), 123.66 (2CH), 27.09 (CH_2).

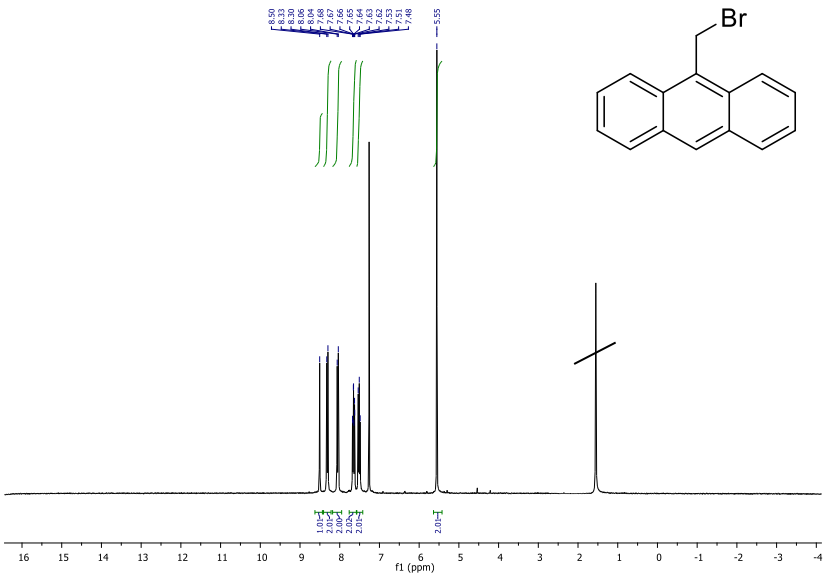

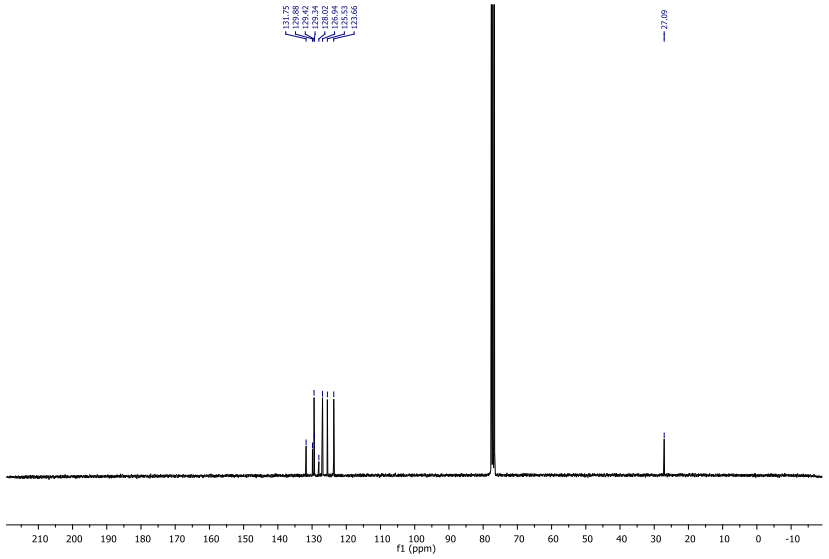

5.1.2.1.2. Synthesis of 2-(anthracen-9-yl)acetonitrile (4).

A solution of **5** (7.67 mmol, 2.08 g) in DMSO (0.37 M) was added during 10 minutes to a stirring suspension of potassium cyanide (11.53 mmol, 0.751 g) in DMSO (0.27 M) at 70ºC under inert atmosphere. The mixture was stirred for 40 minutes and was allowed to reach room temperature, then it was diluted with H_2O.

For the work up, the unique phase was satured with NaCl and extracted with ether (3 x 25 mL). The organic phase was washed with H_2O and dried with $MgSO_4$. An orange crystalline powder was obtained (**4**) with a 100 % yield (1.67 g).

Characterization of 4.

^{1}H NMR (300 MHz, $CDCl_3$) δ: 8.47 (s, 1H), 8.13 (d, J=6Hz, 2H), 8.04 (d, J=9Hz, 2H), 7.62 (m, J=9Hz, J=6Hz, 2H), 7.50 (dd, J=9Hz, J=6Hz, 2H), 4.57 (s, 2H). 2.5 residual DMSO.

^{13}C NMR (75 MHz, $CDCl_3$) δ: 131.50 (2C), 129.87 (C), 129.60 (2CH), 128.94 (2CH), 127.36 (2CH), 125.41 (2CH), 123.04 (CH), 120.84 (2C), 117.82 (CN), 16.29 (CH_2). 40.76 residual DMSO.

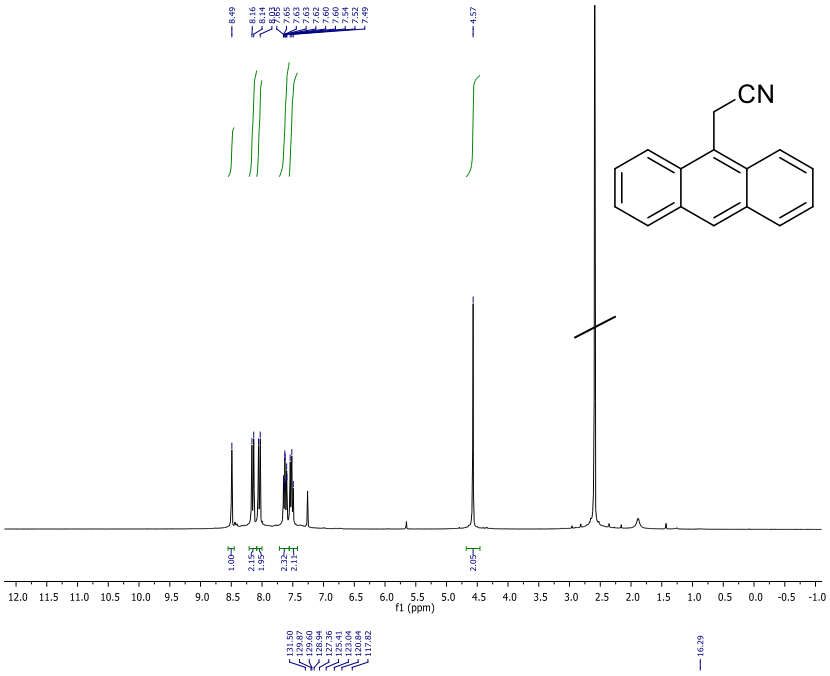
8.49
8.16
8.14
7.65
7.65
7.63
7.63
7.62
7.60
7.54
7.52
7.49
4.57
CN
1.00
2.19
1.95
2.32
2.11
2.05
12.0 11.5 11.0 10.5 10.0 9.5 9.0 8.5 8.0 7.5 7.0 6.5 6.0 5.5 5.0 4.5 4.0 3.5 3.0 2.5 2.0 1.5 1.0 0.5 0.0 -0.5 -1.0
f1 (ppm)

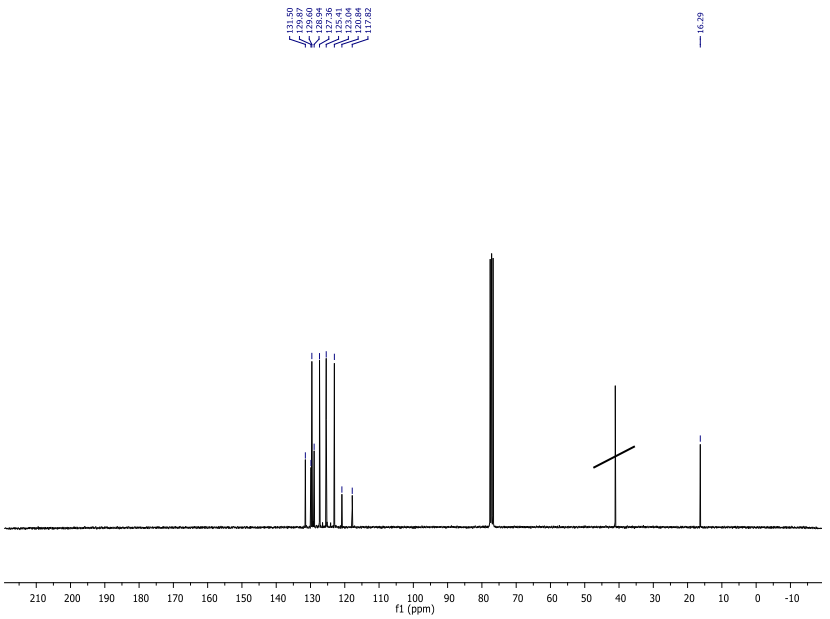
131.50
130.87
129.60
128.94
127.36
125.41
123.04
120.84
117.82
16.29
210 200 190 180 170 160 150 140 130 120 110 100 90 80 70 60 50 40 30 20 10 0 -10
f1 (ppm)

5.1.2.1.3. Synthesis of 2-(anthracen-9-yl)acetic acid (AAA fluorophore) (3).

A hydroxide potassium (34.3 mmol, 1.93 g) solution in H_2O (1.7 M) was added to a suspension containing **4** (7.7 mmol, 1.67 g) in ethylene glycol (0.087 M). The reaction mixture was heated at reflux temperature for 24 hours until it became homogeneous. The warm solution was filtered and the liquid was acidified with diluted HCl in order to obtain product **3** as a precipitate. It was purified by means of flash chromatography using a mixture of hexane: ethyl acetate (4:1, v:v) as eluent phase. 0.46 g of a crystalline yellowish powder was obtained (23 % yield).

Characterization of 3.

^{1}H NMR (300 MHz, $CDCl_3$) δ: 8.44 (s, 1H), 8.22 (d, J=9Hz, 2H), 8.01 (d, J=9Hz, 2H), 7.50 (m, 4H), 4.64 (s, 2H).

^{13}C NMR (75 MHz, $CDCl_3$) δ: 175.31 (COOH), 131.60 (C), 130.61 (C), 129.30 (CH), 127.60 (CH), 126.42 (CH), 125.90 (C), 125.11 (CH), 124.31 (CH), 33.81 (CH_2).

HMRS (ESI-TOF) *m/z* $[M+ Na]^+$ calculated for $C_{16}H_{12}O_2Na$: 259.0735 found: 259.0741.

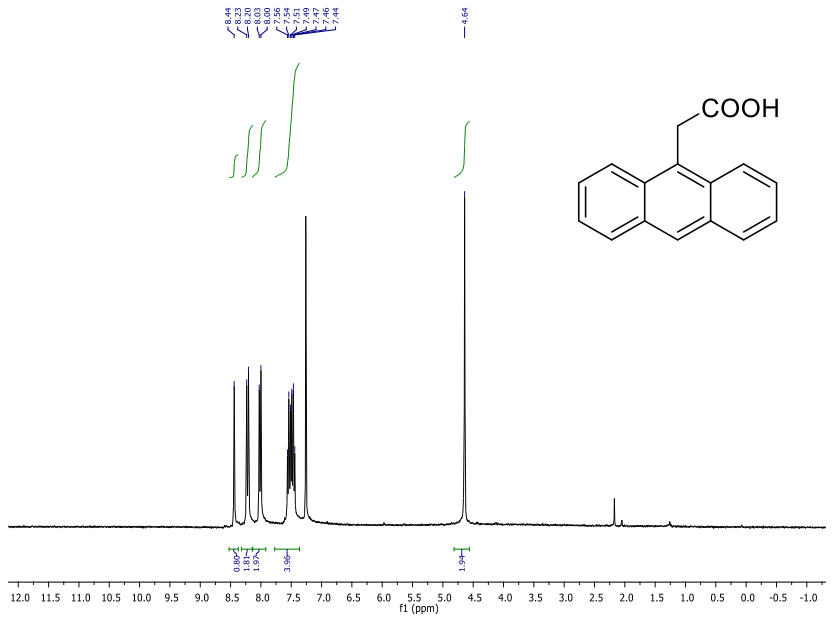

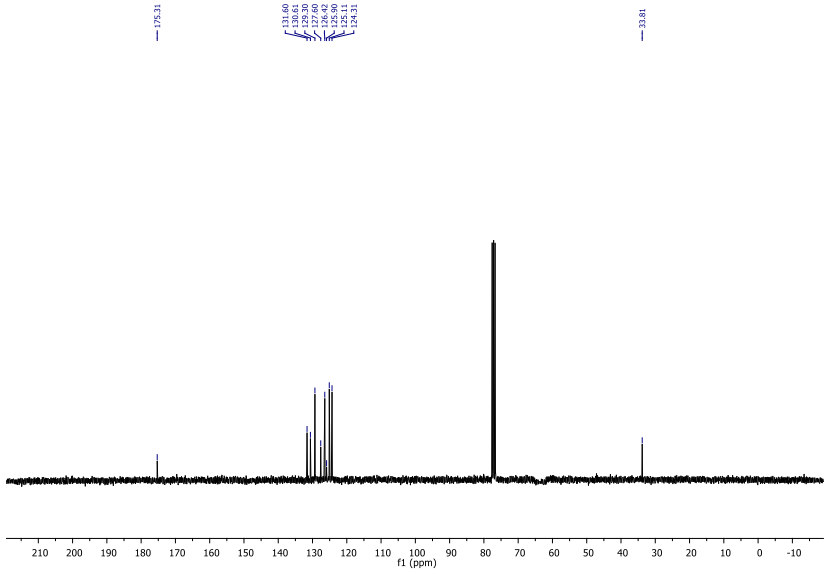

5.1.2.2. Synthesis of AAA-TEMPO.

2,2,6,6-Tetramethyl-4-(9-anthracenylacetoxy)-piperidine-1-oxyl (AAA-TEMPO). The profluorescent probe AAA-TEMPO was obtained by esterification of 2-(anthracen-9-yl)acetic acid with 4-hydroxy-TEMPO, adapting a methodology described by Scaiano *et al.*[17] Briefly, 2-(anthracen-9-yl)acetic acid (0.2 g, 8.5×10^{-4} mol),[16] dicyclohexylcarbodiimide (0.2 g, 9.3×10^{-4} mol), 4-hydroxy-TEMPO (0.16 g, 9.3×10^{-4} mol), and 4-DMAP (0.01 g, 8.5×10^{-5} mol) were diluted with 4 mL of CH_2Cl_2 at room temperature and stirred until the esterification was completed (6 h). The precipitated *N,N*-dicyclohexyl urea was filtered off, and the filtrate was washed with H_2O (3 × 30 mL), 5% acetic acid solution (3 × 5 mL), and once more with H_2O (3 × 50 mL), dried with $MgSO_4$, and evaporated to dryness. Purification was performed by flash column chromatography using hexane:ethyl acetate (4:1, v:v) as eluent to afford AAA-TEMPO as a coral-colored crystalline solid (0.256 g, 75%). The presence of the nitroxide prevented the characterization by NMR spectroscopy; thus, this compound was characterized by X-ray (CCDC 1444537).

Monocrystal X-RAY

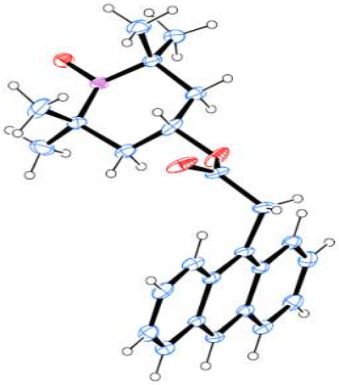

X-ray crystal structure of **AAA-TEMPO**, ellipsoids shown at 30% probability levels. CCDC 1444537 contains the supplementary crystallographic data for this paper. These data are provided free of charge by The Cambridge Crystallographic Data Centre. The **AAA-TEMPO** probe consists of a multicrystal containing two structures. The major structure is C2/c and the minor has a monoclinic P21 structure. There are two independent molecules in the asymetric unit of the primitive cell. One of them presents a disorder in the ester group zone, the refined final values of the two disordered positions are 73.8 (19)% and 26.2 (19)%.

6. References

[1] K. N. Carter and M. M. Greenberg, "Tandem lesions are the major products resulting from a pyrimidine nucleobase radical," *J. Am. Chem. Soc.*, **2003**, 125, 13376-13378.

[2] J. Maria, N. S. Pedro, and M. M. Greenberg, "5,6-Dihydropyrimidine peroxyl radical reactivity in DNA," *J. Am. Chem. Soc.*, **2014**, 136, 3928−3936.

[3] L. Weng, S. M. Horvat, C. H. Schiesser, and M. M. Greenberg, "Deconvoluting the reactivity of two intermediates formed from modified pyrimidines," *Org. Lett.*, **2013** 15, 3618–3621.

[4] S. H. In and M. M. Greenberg, "Mild generation of 5-(2'-deoxyuridinyl)methyl radical from a phenyl selenide precursor," *Org. Lett.*, **2004**, 6, 5011–5013.

[5] M. M. Greenberg, M.R. Barvian, G. P. Cook, B. K. Goodman, T. J. Matray, C. Tronche, and H. Venkatesan, "DNA damage induced via 5,6-dihydrothymid-5-yl in single-stranded oligonucleotides," *J. Am. Chem. Soc.*, **1997**, *119,* 1828-1839.

[6] J. M. N. San Pedro and M. M. Greenberg, "Photochemical generation and reactivity of the major hydroxyl radical adduct of thymidine," *Org. Lett.*, **2012,** 14, 2866–2869.

[7] A. Romieu, S. Bellon, D. Gasparutto, and J. Cadet, "Synthesis and UV photolysis of oligodeoxynucleotides that contain 5-(phenylthiomethyl)-2'-deoxyuridine: a specific photolabile precursor of 5-(2'-deoxyuridilyl)methyl radical," *Org. Lett.*, **2000,** 2, 1085–1088.

[8] M. R. Barvian and M. M. Greenberg, "Independent generation of 5,6-dihydro- thymid-5-yl in single-stranded polythymidylate. O_2 is necessary for strand scission," *J. Am. Chem. Soc.*, **1995,** 117, 8291-8292.

[9] M. J. E. Resendiz, V. Pottiboyina, M. D. Sevilla, and M. M. Greenberg, "Direct strand scission in double stranded RNA via a C5-pyrimidine radical," *J. Am. Chem. Soc.*, **2012,** 134, 3917–3924.

[10] J. P. Blinco, K. E. Fairfull-Smith, B. J. Morrow, and S. E. Bottle, "Profluorescent nitroxides as sensitive probes of oxidative change and free radical reactions," *Aust. J. Chem.*, **2011**, 64, 373–389.

[11] A. Aspée, O. García, L. Maretti, R. Sastre, and J. C. Scaiano, "Free radical reactions in poly(methyl methacrylate) films monitored using a prefluorescent quinoline-TEMPO sensor," *Macromolecules*, **2003**, 36, 3550-3556.

[12] C. Aliaga, J. M. Juárez-Ruiz, J. C. Scaiano, and A. Aspée, "Hydrogen-transfer reactions from phenols to TEMPO prefluorescent probes in micellar systems," *Org. Lett.*, **2008**, 10, 2147–2150.

[13] N. J. Turro, V. Ramamurthy and J. C. Scaiano, "Photochemistry of carbonyl compounds" In Modern Molecular Photochemistry of Organic Molecules, editor Jeannette Stiefel, University Science Book, **2010**.

[14] A. Capobianco, M. Carotenuto, T. Caruso, and A. Peluso, "The charge-transfer band of an oxidized Watson-Crick guanosine-cytidine complex," *Angew. Chem. Int. Ed.*, **2009**, 48, 9526–9528.

[15] G. M. Rodríguez-Muñiz, M. L. Marin, V. Lhiaubet-Vallet, and M. A. Miranda, "Reactivity of nucleosides with a hydroxyl radical in non-aqueous medium," *Chem. Eur. J.*, **2012,** 18, 8024–8027.

[16] J. R. Shah, P. D. Mosier, B. L. Roth, G. E. Kellogg, and R. B. Westkaemper, "Synthesis, structure-affinity relationships, and modeling of AMDA analogs at 5-HT2A and H1 receptors: Structural factors contributing to selectivity," *Bioorganic Med. Chem.*, **2009**, 17, 6496–6504.

[17] O. G. Ballesteros, L. Maretti, R. Sastre, and J. C. Scaiano, "Kinetics of cap separation in nitroxide-regulated 'living' free radical polymerization: Application of a novel methodology involving a prefluorescent nitroxide switch," *Macromolecules*, **2001**, 34, 6184–6187.

[18] T. Ito, H. Shinohara, H. Hatta, S. Nishimoto, and S. Fujita, "Radiation-induced and photosensitized splitting of C5−C5'-linked dihydrothymine dimers: product and laser flash photolysis studies on the oxidative splitting mechanism," *J. Phys. Chem. A*, **1999**, 103, 8413–8420.

[19] A. Wójcik, "Repair reactions of pyrimidine-derived radicals by aliphatic thiols," *J. Phys. Chem. B,* **2006**, *110,* 12738-12748.

[20] K. Andersson, P. Malmqvist, and O. Roos, "Second-order perturbation theory with a complete active space self-consistent field reference function," *J. Chem. Phys.*, **1992**, 96, 1218-1226.

[21] K. Andemson, P. Malmqvist, B. Roos, A. J. Sadlej, and K. Wolinskit, "Second-order perturbation theory with a CASSCF

reference function," *J. Phys. Chem.,* **1990**, *94,* 5483-5488.

[22] P. Widmark, P. Malmqvist, B. Roos, "Density matrix averaged atomic natural orbital (ANO) basis sets for correlated molecular wave functions," *Theor. Chim. Acta*, **1990**, 77, 291-306.

[23] F. Aquilante, "MOLCAS8 : New capabilities for multiconfigurational quantum chemical calculations across the periodic table," *J. Comput. Chem.*, **2016**, 37, 506–541.

Chapter 4:

5-Formyluracil as potential intrinsic DNA photosensitizer

1. Introduction

This chapter still addresses the issue of DNA damage photoinduced by an intrinsic agent. However, this time, the triggering entity is not a synthetic photolabile compound, as it was the case for *tert*-butyl ketone derivatives, but a previously generated DNA lesion.

The whole story is based on a previous hypothesis that claims that certain DNA damages could behave as endogenous photosensitizers inducing chemical changes in their nucleoside vicinity and generate multiple lesions known as cluster lesions. Interestingly, this hypothesis could be associated with scientific works [1], [2] where it has been demonstrated that the same irradiation dose but distributed in several sequences produces an increase in the number of double strand breaks. The authors proposed that continuous irradiation is less efficient due to the decomposition of a DNA-complexed photosensitizer, whereas the light/dark sequence allows its restoration during the dark phase. However, these results can also be interpreted in another way: the first photon flux could enable the generation of a DNA lesion that, during the second irradiation sequence, would participate as an intrinsic photosensitizer, *i.e.* absorbing photons and generating more damages in its neighborhood (Figure 1).

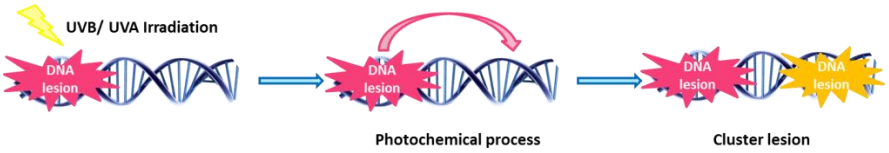

Figure 1. DNA lesions capable of behaving as endogenous photosensitiser to induce cluster lesions

This hypothesis has been strengthened by a recent example studied in our group that deals with the (6-4) photoproduct (6-4PP),

which is one of most common DNA damage formed by direct irradiation. Indeed, it has been demonstrated that 6-4PP acts as an intrinsic DNA photosensitizer and generates secondary photodamages in its vicinity.[3], [4] Photophysical and photobiological studies revealed that its 5-methyl-2-pyrimidone (Pyo) chromophore is the main responsible for the lesion photoreactivity. It induces a bathochromic shift of the absorption by respect with the initial thymine with the appearance of a band centered at 320 nm, which allows UVB/UVA irradiation. Moreover, efficient formation (ϕ_{ISC} *ca.* 0.86) of an energetic triplet excited state (E_T *ca.* 297 kJ mol^{-1}) has been evidenced by LFP and phosphorescence experiments. Furthermore, UVA irradiation of Pyo and 6-4PP in the presence supercoiled circular DNA has shown the ability of both compounds to generate DNA lesions, *ie.* oxidatively generated damage as well as cyclobutane pyrimidine dimers. [3], [4]

Here, the attention has been focused on 5-formyluracil (ForU), an oxidatively generated derivative of thymine. This damage is one of the most important lesions produced by γ-radiation, after those derived from guanine oxidation. [5], [6], [7]

This damage can be photochemically formed through a Type I mechanism. Product analysis reported in the literature using benzophenone (BP) or menadione as photosensitizers[8], [9], [10] have evidenced its formation by electron transfer, hydrogen abstraction mechanism and/or hydroxyl radical addition ($HO^{\bullet}$). This has been concluded from quantitation of 5-hydroxymethyldeoxyuridine (HMdUrd) 169 and 161 nmol, 5-formyldeoxyuridine (FordUrd) 470 and 372 nmol and 5,6-dihydroxy-5,6-dihydrodeoxythymidine (DOHdThd) 434 and 1250 nmol for BP and menadione photosensitized reaction respectively (Scheme 1). Indeed, the ratio [HMdUrd + FordUrd]/[DOHdThd] is a diagnostic value. These compounds could result from three different mechanisms (Scheme

1). [5], [6], [7] The first one is hydrogen abstraction from the methyl group of thymidine by the excited photosensitizer (^{3}Ph) yielding a neutral radical centered at the methyl group (Thd$^\bullet$) that reacts with molecular oxygen giving rise to HMdUrd and FordUrd as final products (pathway A). An electron transfer from thymidine to ^{3}Ph could also take place (pathway B). Subsequent deprotonation of the radical cation dThd$^{+\bullet}$ could lead to the neutral radical (Thd$^\bullet$) that ends in HMdUrd and FordUrd formation, whereas DOHdThd could arise from dThd$^{+\bullet}$ due to the hydration of the 5,6-π-bond. Finally, hydroxyl radical (HO$^\bullet$) addition to the C5-C6 double bond also leads to DOHdThd.[10] In the case of BP (or derived compounds), a mixed mechanism involving electron transfer and H-abstraction has been proposed on the basis of a high [HMdUrd + FordUrd]/[DOHdThd], whereas the lower value obtained for menadione points toward the predominance of the electron transfer. [9], [10]

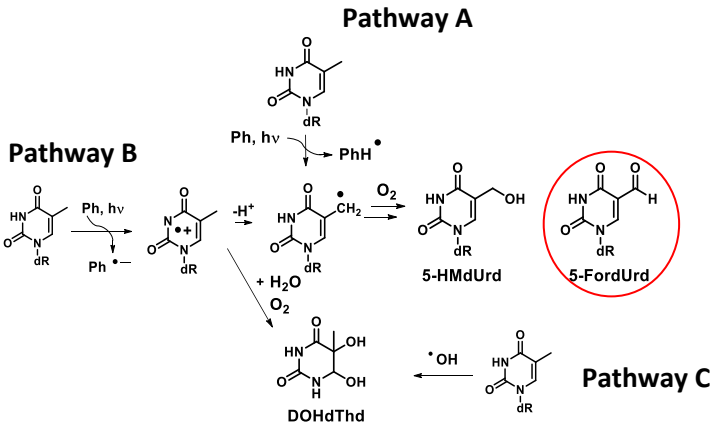

Scheme 1. Thymine photooxidation by Type I processes hydrogen and e-transfer on the top and from left to right side (pathway A and B) and hydration of Thd cation radical at the bottom (pathway C).

In addition of these Type I photosensitization mechanisms, ForU is also produced during endogenous metabolic processes as an intermediate of thymine oxidation catalyzed by thymine hydroxylase, an enzyme that belongs to the metabolic and catabolic dioxygenases.

This enzyme, which is capable of oxidizing the 5-methyl group of thymine, is found in a wide range of organisms including bacteria, yeast, plants, and humans.[11]

Moreover, from a photochemical point of view, the presence of formyl substituent at C5 might be of interest since it can affect the distribution and nature of the excited states if we compare them with those of thymine having the unaltered C5-methyl group. It should, this way, exhibit the UVB/UVA absorption, which is one of the basic requirements for a photosensitizing compound.

It is noteworthy that the presence of ForU in DNA can have harmful consequences on the organism because it induces mispairing during replication with a relatively high frequency.[12],[13] This is related to the electron withdrawing ability of the formyl substituent at C5 that increases the acidity of N3 proton and facilitates ionization; thereby it alters the base pairing specificity introducing a guanine and affects the Watson-Crick interactions.[14] Moreover, ForU is able to produce covalent cross-links with proteins through the reaction of the aldehyde functional group with amino- or thiol-containing amino acids leading to a Schiff base formation.[15]

Up to now, no photophysical or photobiological data were available in the literature. Thus, this chapter proposes to investigate the ability of 5-formyluracil to behave as an endogenous DNA photodamaging agent.

2. Objectives

The main objective of this chapter is to establish if the oxidatively generated lesion ForU could play the role of an intrinsic photosensitizer.

For this, it is necessary to pursue the following specific aims:

- To ensure that ForU fulfills the basic requirements to behave as an endogenous photosensitizer: i) it has to exhibit a red shifted absorption spectrum by respect to canonical DNA bases, which widens the DNA excitation to longer wavelength regions extending the active fraction of sunlight, likewise ii) it has to have the ability to populate its triplet excited state, which has to be sufficiently energetic.

- To evaluate if the triplet energy (E_T) of ForU is sufficiently energetic, to behave as an energy donor in a Triplet-Triplet Energy Transfer (TTET) to a pyrimidine nucleobase. Once excited, the ^{3}Pyr could react with a nearby counterpart in its ground state yielding to cyclobutane pyrimidine dimers (Pyr<>Pyr). For this purpose, two model dyads are designed, synthesized and their photoreactivity is evaluated.

- To extend the study to the whole DNA molecule quantifying ForU photosensitizing properties on a plasmid DNA.

3. Results and Discussion

3.1. Characterization of ForU photophysical properties.

In order to confirm that ForU could behave as an intrinsic photosensitizer, the first step was to perform a spectroscopic screening to characterize the photophysical properties of its excited states and the formation of other transient species such as radicals or reactive oxygen species (ROS).

First, UV-visible spectrophotometry allowed confirming that ForU exhibits an absorption in the UVB/UVA domain (Figure 2).

Indeed, in phosphate buffer at pH 7.4, it has a maximum at *ca.* 297 nm with a tail that reaches up to almost 350 nm. This result fulfills the first requirement needed for efficient photosensitizers providing a range for selective excitation in the UVB/UVA, and, therefore, extends the active fraction of sunlight.

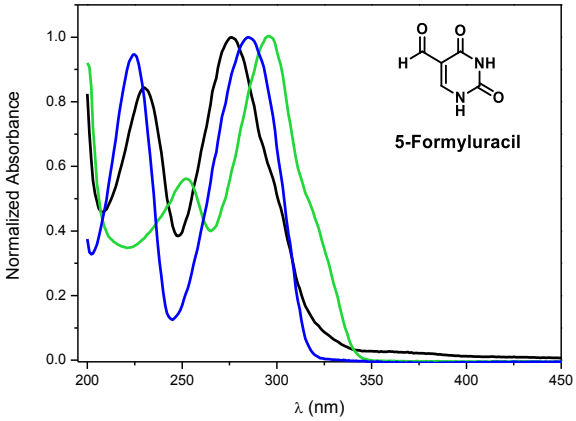

Figure 2. UV-Vis absorption spectra of ForU (0.077 mM) in milliQ H_2O (black line), PBS (green line) and acetonitrile (blue line).

Then, laser flash photolysis experiments (Nd:YAG, 266 nm) revealed a broad transient absorption from 320 to 560 nm with a maximum at *ca.* 460 nm for a N_2 flushed phosphate buffer solution of ForU (*ca.* 0.077 mM). The lifetime was 1.75 µs under N_2 and the transient species was efficiently quenched by oxygen, with a lifetime shortened to 0.56 µs under air and to 0.15 µs when O_2 was bubbled. The calculated bimolecular rate constant $k_q(O_2)$ determined from the Stern Volmer equation (eq. 1) was of *ca.* 4 x 10^9 M^{-1} s^{-1}. As a result, this transient was assigned to the triplet-triplet transition of ForU (Figure 3).

$$1/\tau = 1/\tau_0 + k_q \times [O_2] \qquad \text{eq. 1}$$

where τ is the lifetime after addition of an oxygen concentration $[O_2]$, τ_0 is the lifetime for ForU under N_2 conditions, for $[O_2]$ values of 2.9 x 10^{-4} M and 1.39 x 10^{-3} M were taken for air and oxygen atmosphere, respectively. [16]

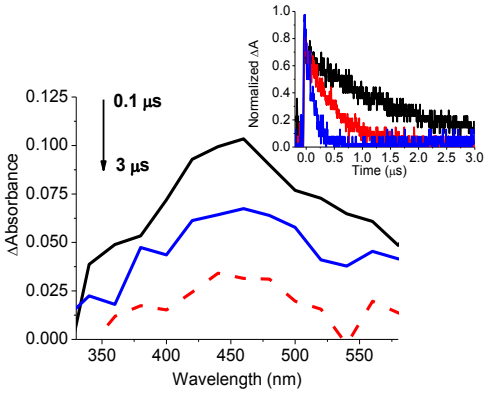

Figure 3. Transient absorption spectra of ForU in a PBS N_2-bubbled solution (0.077 mM) obtained at different times after 266 nm laser excitation. Inset: Decays monitored at 460 nm under N_2 (black), air (red) and O_2 (blue) atmosphere.

Moreover, the possibility of producing singlet oxygen ($^1O_2$) as a result of ^{3}ForU oxygen quenching was studied by means of EPR experiments, using TEMP (2,2,6,6-tetramethylpiperidine) as specific spin trap. The well-established triplet signal of TEMPO free radical (g=2.006, a_N= 17.3 G) was detected after irradiation of a ForU aqueous solution in the presence of TEMP (Figure 4).[17] Therefore, ForU can act as an DNA oxidative agent through generation of ROS, inducing formation of 8-oxo-7,8-dihydroguanine.

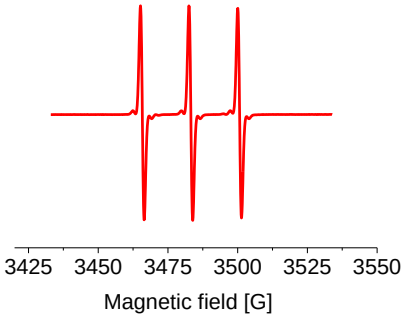

Figure 3. EPR signal obtained for an aqueous solution of ForU (0.35 mM) irradiated monochromatically at 290 nm for 80 min in the presence of TEMP (10 mM).

The next step was to get information about its triplet excited state energy by means of phosphorescence experiments performed in EtOH at 77 K (Figure 4). An E_T value of *ca.* 314 kJ mol^{-1} was obtained by using the equation 2.

$$E_T = N h c / \lambda_{0\text{-}0} \qquad \text{eq. 2}$$

where N is the Avogadro number (6.022×10^{23} mol^{-1}), h is the Planck constant (6.626×10^{-34} J s), c is the light velocity (3×10^{8} m s^{-1}), and $\lambda_{0\text{-}0}$ is the wavelength corresponding to the 20% of emission intensity (m).

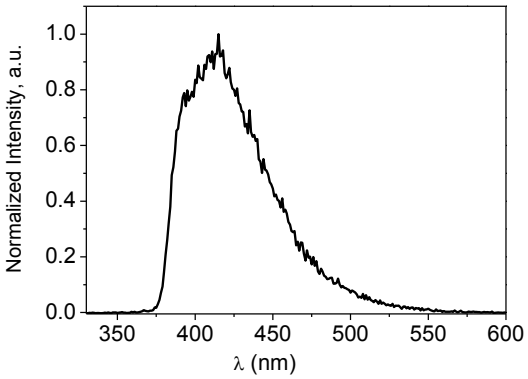

Figure 4. Phosphorescence emission spectrum of ForU (0.198 mM) in EtOH at 77 K.

Moreover, when ForU is complexed with DNA, a small hypsochromic shift was observed in the phosphorescence band (Figure 5). This is in concordance with the recently reported observations for other photosensitizers and it produces a slight increase of the triplet energy within DNA.[18] These E_T values are somewhat higher than that of isolated thymidine in bulk solution (E_T of *ca.* 310 kJ mol^{-1})[19]; however, it is more than 40 kJ mol^{-1} above that determined for thymine in DNA. [18],[20]

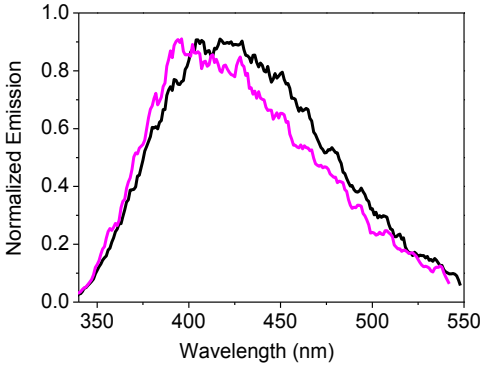

Figure 5. Phosphorescence emission spectra of ForU in PBS alone (black line) or in the presence of calf thymus DNA (1 mM in bases).

Hence, the high E_T value of ^{3}ForU makes it an appropriate energy donor for a TTET to a pyrimidine nucleobase. Once excited, the ^{3}Pyr can react with a nearby counterpart in its ground state and

lead to the well-known cyclobutane pyrimidine dimers (Pyr<>Pyr) (Scheme 2).

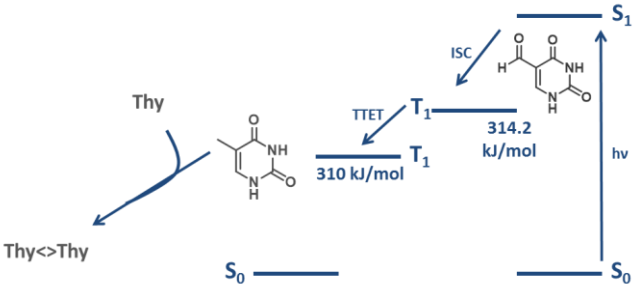

Scheme 2. Excitation of ForU and the feasible TTET process to pyrimidine, as for example thymine.

3.2. Study of pyrimidine cyclobutane dimer formation of model systems, the Thy-Thy and Cyt-Cyt dyads.

To continue with the study, two model dyads were prepared to confirm that TETT from ^{3}ForU leads to Pyr<>Pyr formation. The synthesis of the model dyad Thy-Thy was first carried out adapting the procedure described in the literature.[21], [22] A protection at N3 of thymine was performed in a three step procedure. First, treatment with acetic anhydride at a reflux temperature protected the N1 of thymine, this was followed by a treatment with sodium hydride and iodomethane for the N3 protection. Afterwards, N1 was deprotected with the addition of hydrochloric acid (0.012 M) to a solution CH_2Cl_2:MeOH, (98:2, v:v). Finally, the N3-protected thymine dyad was obtained by the introduction of a trimethylene chain using 1,3-dibromopropane and sodium hydride in acetonitrile at a reflux temperature (Scheme 3).

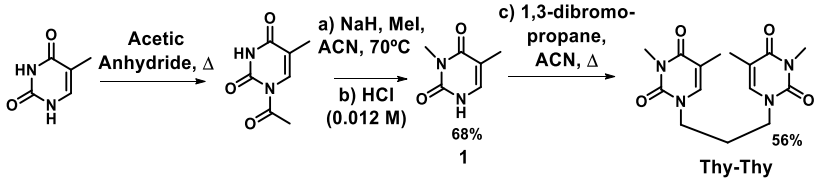

Scheme 3. Procedure for the synthesis of Thy-Thy model dyad.

The synthesis of cyclobutane thymine dimers was required to be used as a reference for HPLC analysis. Thus, Thy-Thy dyad was dissolved in acetone, which plays a dual role as solvent and photosensitizer, and irradiated for 15 minutes with a medium pressure mercury lamp (Scheme 4). The UV-visible spectrum of Thy<>Thy showed the disappearance of the Thy band at 270 nm reflecting the saturation of the thymine double bond due to the [2+2] photocycloaddition reaction (Figure 6). Both compounds, Thy-Thy dyad model and standard Thy<>Thy, were fully characterized by NMR measurements (see experimental section). The photoproduct was assigned to the *cis-syn* cyclobutane dimer by comparison with the literature data. [22]

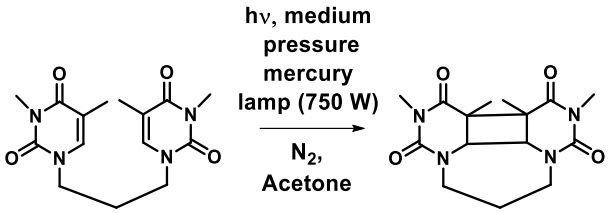

Scheme 4. Acetone photosensitized synthesis of standard Thy<>Thy (0.01 mM).

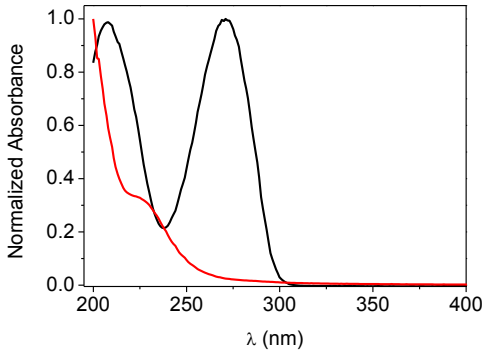

Figure 6. UV-Vis spectra of Thy-Thy dyad (black) and Thy<>Thy (red) in acetonitrile at 0.077 mM.

The Cyt-Cyt model dyad was also synthesized by a modification of the described procedure.[23] An excess of cytosine was

left to react with dibromopropane in the presence of tetrabutylammonium hydroxide at a reflux temperature (Scheme 5).

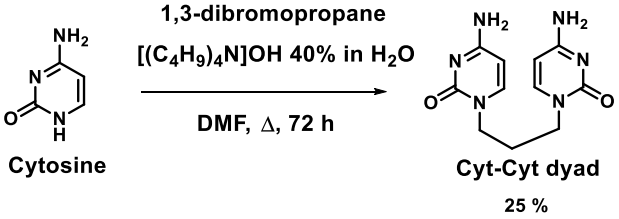

Scheme 5. Procedure for the synthesis of Cyt-Cyt model dyad.

3.3. Steady-state photolysis of Thy-Thy and Cyt-Cyt dyads in the presence of ForU.

The occurrence of the triplet-triplet energy transfer from ForU to pyrimidine nucleobase and the cyclobutane pyrimidine dimerization was first investigated for the Thy-Thy dyad by means of HPLC analysis and ^{1}H NMR.

As shown in Figure 7A and 7B, a selective excitation of ForU can be achieved in the region between 310 and 350 nm for the study of Thy-Thy and Cyt-Cyt dyad.

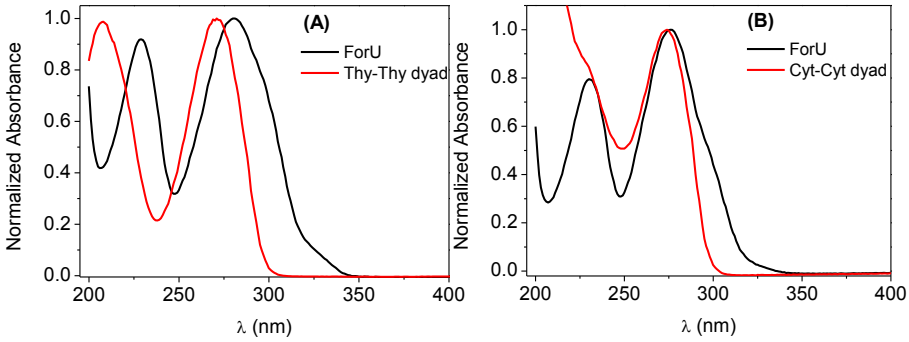

Figure 7. UV-Vis spectra of (A) ForU and Thy-Thy model dyad in acetonitrile at 0.077 mM and of (B) ForU and Cyt-Cyt model dyad in H_2O at 0.077 mM.

Thus, a monochromatic (λ_{irr}=320 nm, lamp 150 W) steady-state photolysis of a mixture of Thy-Thy dyad (8.7 mM) and ForU (5.3 mM) was carried out under anaerobic conditions using acetonitrile and milliQ H_2O (1:1, v:v) as solvents (Scheme 6).

The photoreaction was monitored by reversed phase HPLC. As shown in Figure 8A, the irradiation gives rise to a clean process where the peak of Thy-Thy eluting at 22 min decreased with irradiation time while only one product, eluting at 12 min, is formed. This new peak has been assigned to Thy<>Thy with the help of the reference compound synthesized photochemically.

Control experiments performed by irradiating Thy-Thy alone at the same wavelength showed a very slow degradation ruling out that Thy<>Thy observed in the presence of ForU results from direct excitation of the dyad (Figure 8B).

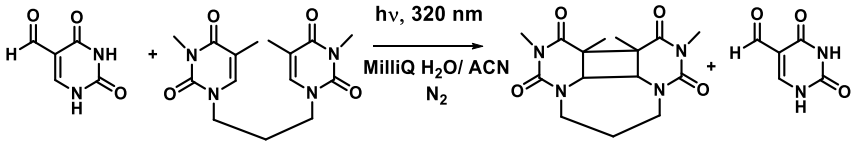

Scheme 6. Model system used to study cyclobutane thymine dimer formation.

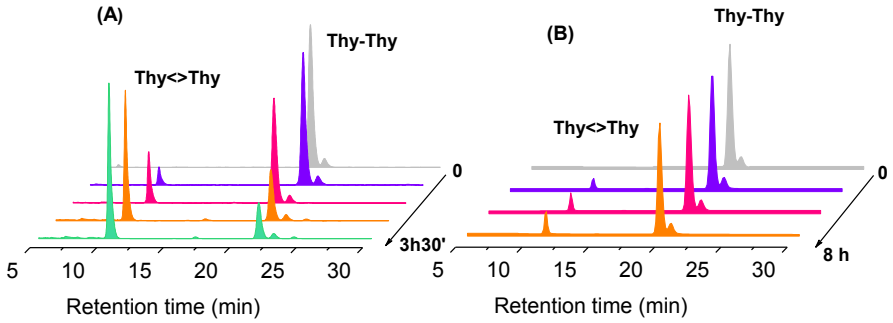

Figure 8. HPLC chromatograms of irradiations performed in H_2O:CH_3CN (1:1, v:v) from 0 to 3 h 30 min at 320 nm, (A) obtained for ForU:Thy-Thy (5.3:8.7 mM), (B) for Thy-Thy (7.7 mM) irradiated alone.

The cyclobutane pyrimidine dimerization was also analyzed by ^{1}H NMR spectroscopy. Measurements were performed through monochromatic irradiation (λ_{irr}=320 nm, lamp 75 W) but this time using a mixture of deuterated solvents CD_3CN:D_20 (1:1, v:v) to follow directly the progress of the reaction. Indeed, the [2+2] photocycloaddition produces a saturation of the C5-C6 double bond and provokes characteristic changes of the proton signals. In Figure 9A are shown the characteristic signals for the initial Thy-Thy dyad and the expected Thy<>Thy photoproduct. The Thy-Thy dyad presents a singlet in the allylic region, which is assigned to the H6 proton. The methyl group of C5 is in the aliphatic region around 2.30 ppm and the methyl group at the N3 is also a characteristic signal around 3.75 ppm. Regarding Thy<>Thy signals, the H6 singlet moves to the aliphatic region around 4.5 ppm, and the methyl groups at C5 and N3 are shifted to higher magnetic shielding region.

The ^{1}H NMR measurements of the steady state photolysis were performed at 4 and 7 h of irradiation (Fig. 9B and C) and the integral of the singlets corresponding to H6 and singlet of methyl group in C5 were used, as a double check, for kinetics monitoring. As well as for the HPLC analysis, a clean photocyclization was observed, reaching after 7 h of irradiation a chemical yield for Thy<>Thy formation of *ca.* 60 %.

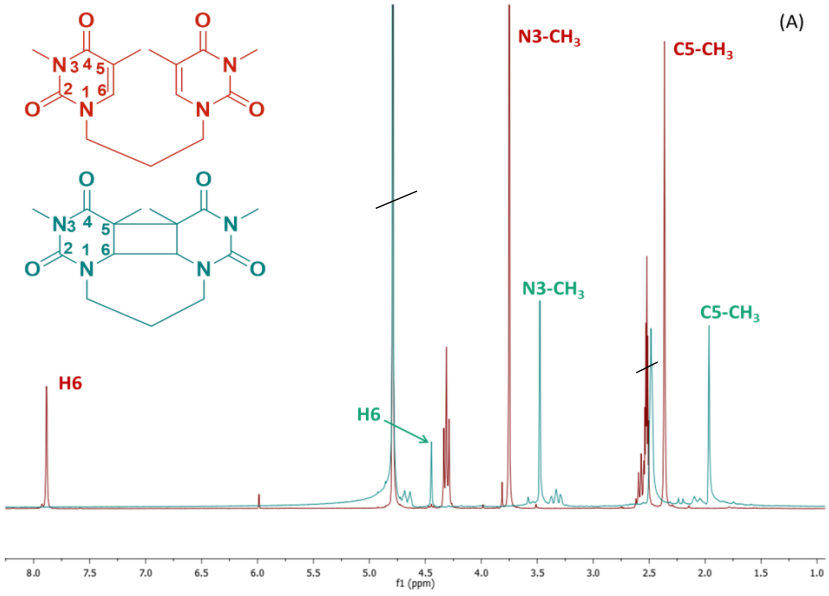
(A)
N3-CH3
C5-CH3
N3-CH3
C5-CH3
H6
H6
f1 (ppm)

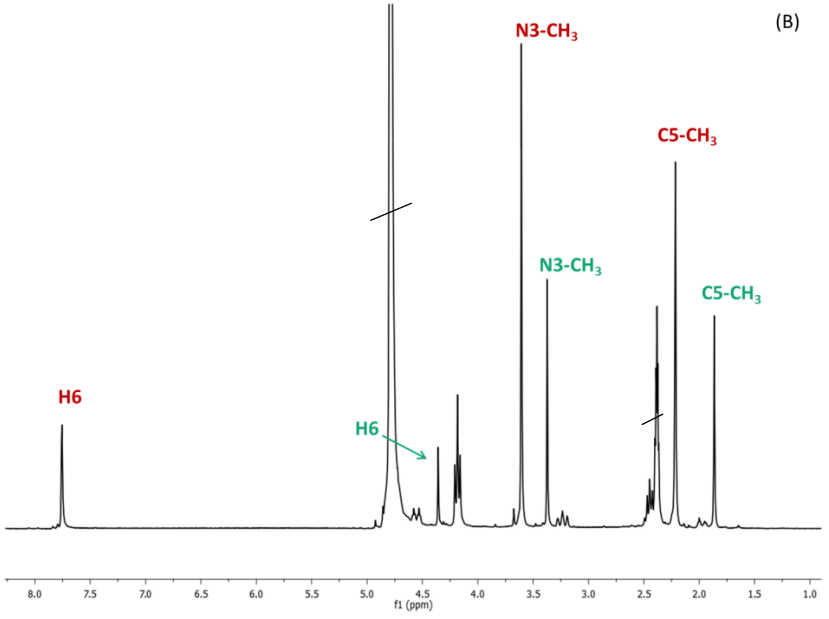
(B)
N3-CH3
C5-CH3
N3-CH3
C5-CH3
H6
H6
f1 (ppm)

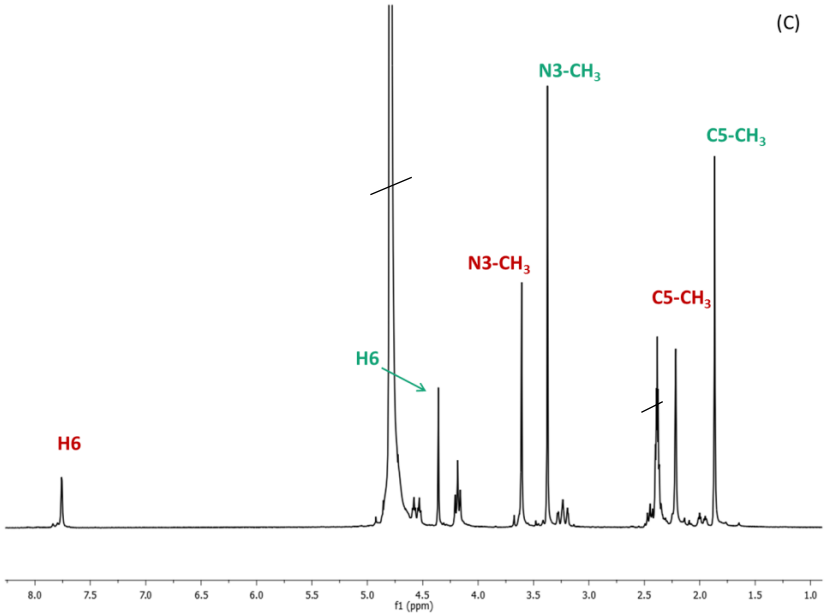

Figure 9. ^{1}H NMR spectra in D_20:CD_3CN (1:1, v:v) (A) pure Thy-Thy (red line) and Thy<>Thy (green line). Equimolar mixture of Thy-Thy and ForU (7 mM) irradiated 4h (B) or (C) 7 h.

In addition, the kinetics of the monochromatic photolysis at 320 nm of Cyt-Cyt model dyad in the presence of ForU in aqueous medium was followed by HPLC and UPLC-HMRS and it showed that Thy-Thy reacts much faster than Cyt-Cyt (Figure 10). The determined quantum yields are 0.10 and 0.01, respectively. These data are in agreement with the triplet excited state energy of the two bases, as ^{3}Cyt lies ca. 20 kJ mol^{-1} above ^{3}Thy.[24] It is noteworthy that cyclobutane cytosine dimers exhibit a particular behavior, as they are not stable and suffer a deamination process at C4, giving rise to the formation of cyclobutane uracil dimers.[25] These uracil homodimers were observed for the photolysis of Cyt-Cyt dyad in the presence of ForU (Figure 11A) through UPLC-HRMS experiments, which allowed detection of the exact mass *m/z* 265.0929 corresponding to the formula $C_{11}H_{13}N_4O_4$. A control experiment performed for Cyt-Cyt irradiated alone showed a low formation of Ura<>Ura (Figure 11B).

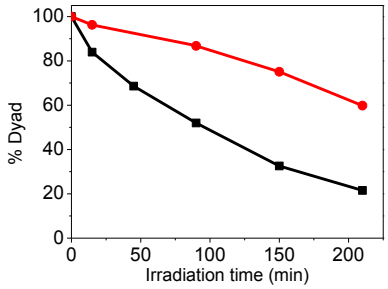

Figure 10. Time-dependent photodegradation of Thy-Thy (black) and Cyt-Cyt (red) in the presence of ForU (λ_{irr}=320 nm).

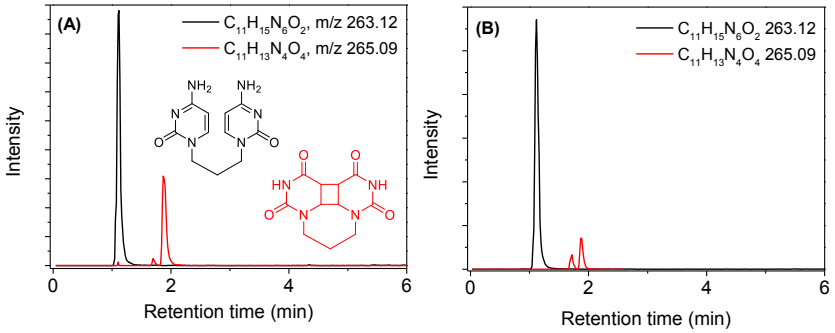

Figure 11. (A) Deaerated monochromatic irradiation (λ_{irr} = 320 nm) of ForU in the presence of Cyt-Cyt dyad. Selected ion monitoring at *m/z* 263.12 (black), corresponding to Cyt-Cyt dyad, and at *m/z* 265.09 (red), corresponding to cyclobutane uracil dimers. Exact mass (ESI^+) were determined for: $C_{11}H_{15}N_6O_2$ $[M+H]^+$: calculated 263.1256 found: 263.1253, and for: $C_{11}H_{13}N_4O_4$ $[M+H]^+$: calculated 265.0937 found: 265.0938. (B) Deaerated monochromatic irradiation (λ_{irr} = 320 nm) of Cyt-Cyt dyad in the absence of ForU. Selected ion monitoring at *m/z* 263.12 (black), corresponding to Cyt-Cyt dyad, and at *m/z* 265.09 (red), corresponding to cyclobutane uracil dimers.

3.4. Agarose gel electrophoresis experiments with plasmid DNA in the presence of ForU

From the results obtained with the model systems, it can be concluded that ForU is able to photosensitize the dimerization of pyrimidine in bulk solution. Therefore, the following step was to

confirm the occurrence of this process when the whole DNA molecule is the target. In this context, experiments on a plasmid DNA were performed using agarose gel electrophoresis technique. In this experiment, native supercoiled DNA, also known as form I, is converted into the circular form II after a single-strand break (SSB). The different electrophoretic mobility of both forms makes the agarose gel electrophoresis an appropriate technique to quantify the number of SSBs induced by densitometry.

The first step consisted on the estimation of SSB induced by UVA steady-state photolysis of plasmid DNA (pBR322, 38 μM in bp) in PBS in the absence and in the presence of ForU (25 or 50 μM). In Figure 12, an induced concentration and dose dependent formation of SSB is observed due to the presence of ForU, reaching after 15 min of irradiation values of 30 and 50 % for 25 and 50 μM, respectively. These DNA backbone breaks should result from sugar oxidation through formation of radicals derived from ForU excitation.

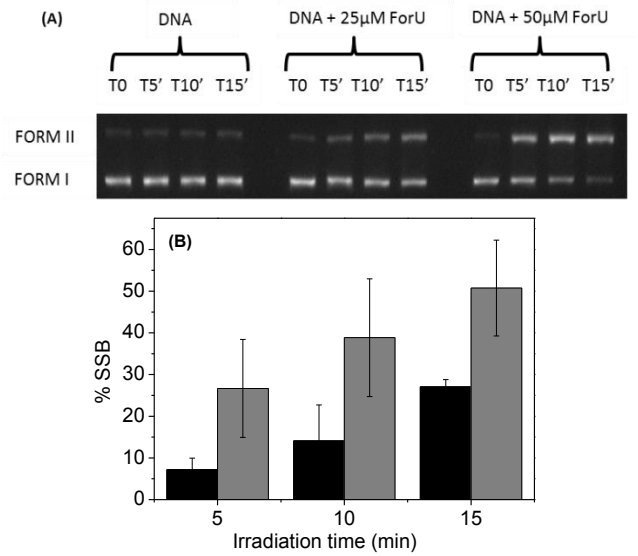

Figure 12. (A) Agarose gel electrophoresis for single strand break formation of UVA-irradiated samples of pBR322 (38 μM in bp) alone or in the presence of ForU (25 or 50 μM). (B) Quantitation of the photosensitized SSB (25 μM in black and 50 μM in grey).

However, with this technique Pyr<>Pyr cannot be directly observed as they do not end in SSB formation. Hence, a specific DNA repair enzyme must be added to selectively cleave the DNA backbone at Pyr<>Pyr site. In this context, T4 endonuclease V was used to selectively reveal the formation of the *cis-syn* isomer.

This combined experiment was carried out but using a ForU concentration of 40 μM, which provided a good balance between relevant Pyr<>Pyr formation and low SSB. Thus, solutions of DNA alone or in the presence of ForU were irradiated during different time (from 0 to 15 min), the solutions were then divided in two equivalent fractions. One was kept in the dark without further treatment (to quantify SSB), while the other one was incubated at 37 ºC for 1 hour with T4 endonuclease V (to quantify Pyr<>Pyr formation). The obtained results are shown in Figure 13. For samples treated T4 endonuclease V, a consistent increase of DNA form II with irradiation time was observed in the presence of ForU. The yield of photosensitized Pyr<>Pyr for 40 μM of ForU at 15 minutes of irradiation, determined from the subtraction between the total and the basal Pyr<>Pyr (without ForU), was of *ca.* 9 %. Therefore, the oxidatively generated product of thymine, ForU, can act as a triplet energy donor to generate Pyr<>Pyr in DNA.

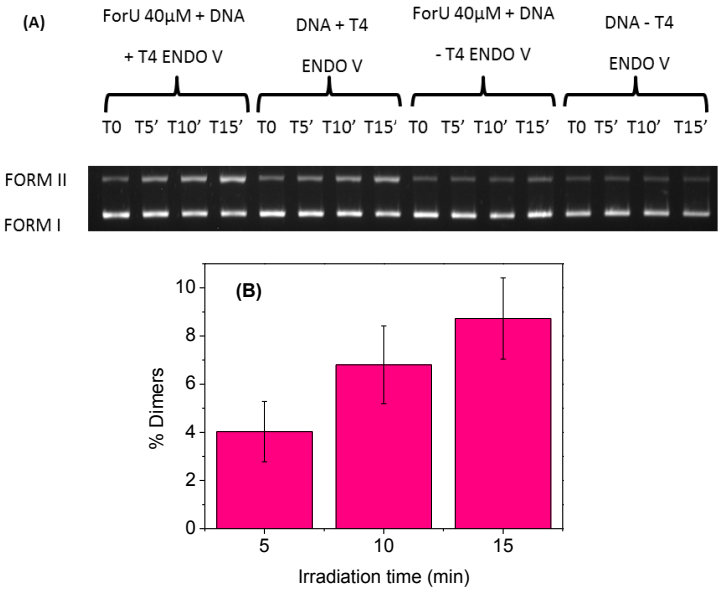

Figure 13. (A) Agarose gel electrophoresis for Pyr<>Pyr formation of UVA-irradiated samples of pBR322 (38 μM in bp) alone or in the presence of ForU (40 μM). (B) Quantitation of the cyclobutane pyrimidine dimers photoinduced by ForU (40 μM).

4. Conclusions

To sum up, the work presented in this chapter evidences that 5-formyluracil fulfills all the requirements to act as an efficient cyclobutane pyrimidine dimer photosensitizer. These requirements are the characterization of its photophysical properties, (*i*) an absorption band in the UVB-UVA region, (*ii*) a high triplet excited state energy E_T of 314.2 kJ mol^{-1} determined by low temperature phosphorescence emission, (ii) a triplet lifetime in the microsecond timescale (τ of *ca.* 1.75 μs) determined in solution at room temperature by laser flash photolysis.

This was corroborated by HPLC, UPLC-MS and ^{1}H NMR analyses run on the Thy-Thy and Cyt-Cyt model dyads. Finally, plasmid DNA studies support that ForU has also harmful effects on

the whole DNA biomolecule, as it contributes to increase the yield of Pyr<>Pyr formation of approximately 9%. Thus, after its formation as a result of a first sunlight exposure, the lesion can induce more damages, after absorption of more UVB/UVA photons, generating multiple lesions known as clusters.

This work is the first example proving that an oxidatively generated lesion is able to act as an endogenous photosensitizer, giving rise to pyrimidine dimerization and oxidative damage formation in DNA.

5. Experimental section

5.1. Synthesis procedure of Thy-Thy and Cyt-Cyt dyad model systems

5.1.1. Synthesis of 3,5-dimethylpyrimidine-2,4(1H,3H)-dione (1)

Thymine (1 g, 7.9 mmol) was dissolved with acetic anhydride under inert atmosphere and the mixture was stirred overnight at reflux temperature. The crude was evaporated under vacuum and a white crystalline solid was obtained. The acetylated derivative was added to a solution of sodium hydride in dry acetonitrile and it was stirred for 1 hour at room temperature. Afterwards, the iodomethane was dripped dropwise and it was stirred for 12 h at 70 °C. When reaction was completed, the crude was evaporated under vacuum, dissolved in CH_2Cl_2:MeOH (98:2, v:v) and stirred for 1 hour with HCl 37 % (0.012 M). Finally, it was purified by flash chromatography CH_2Cl_2:MeOH, (90:10, v:v) and, 0.753 g (5.37 mmol) of **1** was obtained as a white solid, yield 68 %.[21]

Characterization of 1.

^{1}H NMR (300 MHz, $CDCl_3$) δ ppm: 9.40 (bs, 1H, NH), 7.03 (d, J= 6Hz, 1H), 3.35 (s, 3H), 1.94 (s, 3H).

^{13}C NMR (75 MHz, $CDCl_3$) δ ppm: 164.5 (CO), 153.5 (CO), 134.6 (CH), 110.0 (C), 27.4 (CH_3), 13.0 (CH_3).

HMRS (ESI-TOF) m/z $[M- H]^-$ Calculated for $C_6H_7N_2O_2$: 139.0508 found: 139.0504.

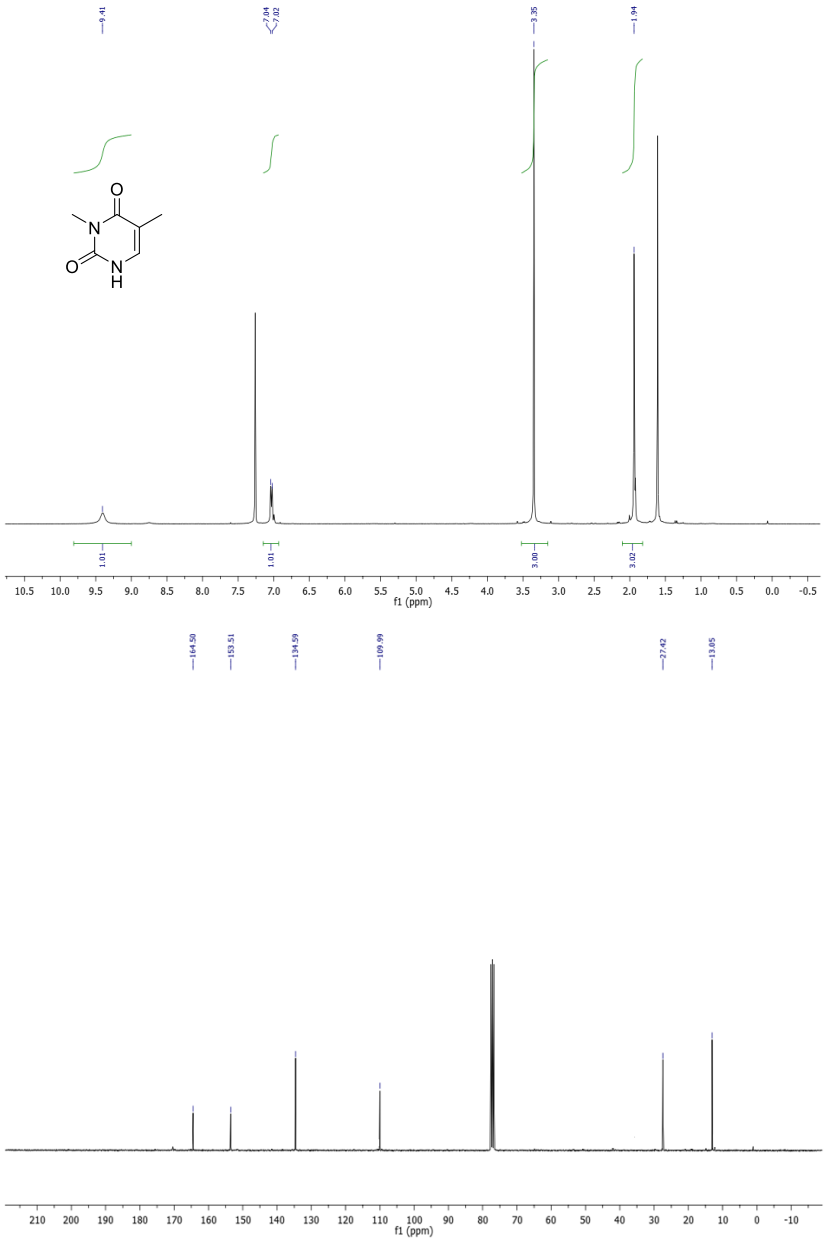

5.1.2. Synthesis of 1,1'-(propane-1,3-diyl)bis(3,5-dimethyl pyrimidine-2,4(1H,3H)-dione) (Thy-Thy).

The synthesis was performed as described in the literature.[22] Briefly, in a reflux system, NaH was suspended in dry acetonitrile, **1** (0.2 g, 1.4 mmol) was added and the solution was stirred for 1 hour at room temperature. Afterwards, 1,3-dibromopropane was added dropwise and heated to reflux temperature overnight. The crude was evaporated and purified by flash chromatography CH_2Cl_2:MeOH, (99:1, v:v) and Thy-Thy was obtained as a white crystalline solid (0.026 g, 0.08 mmol), yield 56 %.

Characterization of Thy-Thy.

^{1}H NMR (300 MHz, $CDCl_3$) δ ppm: 7.02 (s, 2H), 3.75 (t, *J* = 6Hz, 4H), 3.29 (s, 6H), 2.05 (m, 2H), 1.87 (s, 6H).

^{13}C NMR (75 MHz, $CDCl_3$) δ ppm: 163.8 (2CO), 151.7 (2CO), 138.0 (2CH), 110.2 (2C), 46.8 ($2CH_2$), 28.6 (CH_2), 28.0 ($2CH_3$), 13.0 ($2CH_3$).

HMRS (ESI-TOF) m/z $[M+H]^+$ Calculated for $C_{15}H_{21}N_4O_4$: 321.1563 found: 321.1559.

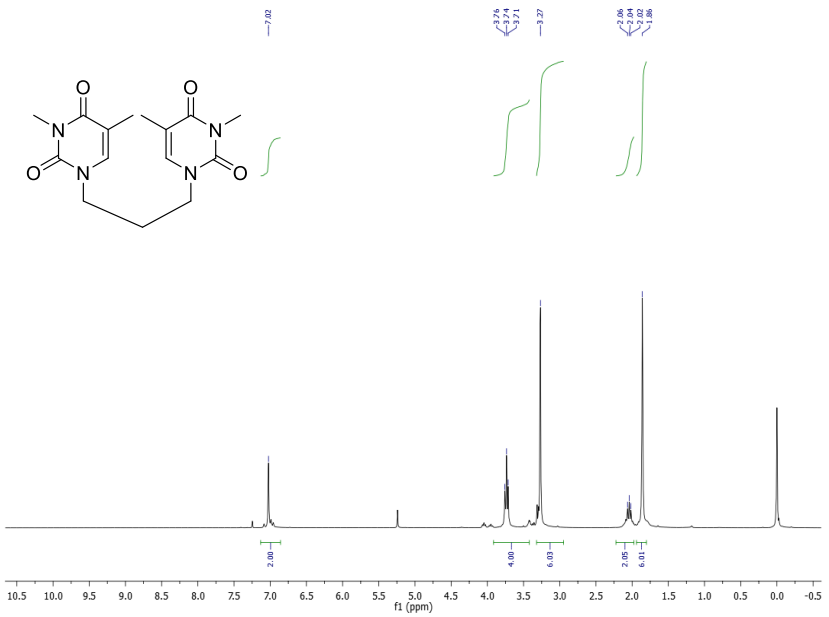

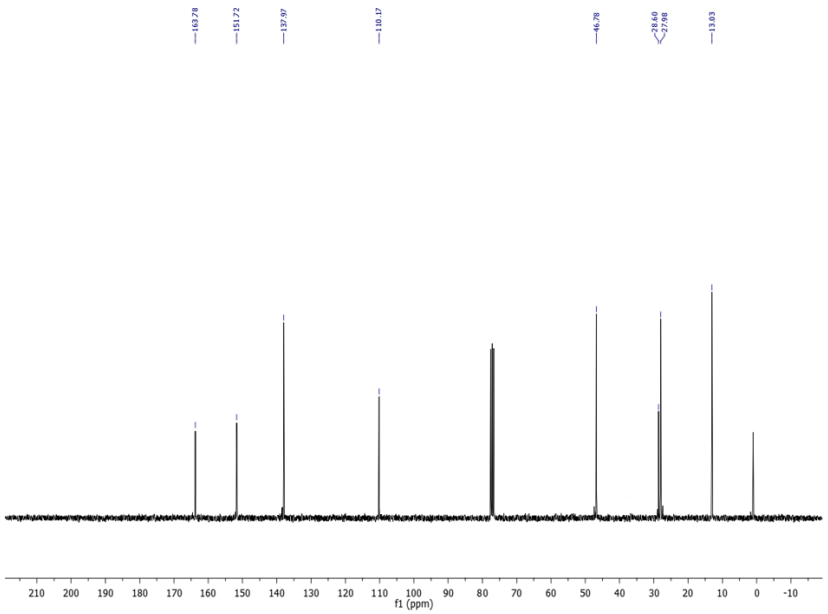

5.1.3. Synthesis of 1,1'-(propane-1,3-diyl)bis(4-aminopyrimidin-2(1H)-one) (Cyt-Cyt)

This compound was already reported and was synthesized by a modification of the described procedure.[23] Cytosine (0.5 g, 4.5 mmol) was suspended in DMF (2 mL) and subsequently 5 mL of tetrabutylammonium hydroxide 40% in H_2O was added. When cytosine was totally dissolved, 1,3-dibromopropane (0.23 mL, 2.25 mmol) was added dropwise and the reaction mixture was stirred at reflux temperature for 72 h. The solvent was evaporated under vacuum and a flash chromatography purification was performed (CH_2Cl_2:MeOH, 5:1, v:v) in order to obtain 0.150 g of Cyt-Cyt dyad (yield 25 %).

Characterization of Cyt-Cyt.

^{1}H NMR (300 MHz, D_2O) δ ppm: 7.53 (d, *J* = 6 Hz, 2H), 5.93 (d, *J* = 6 Hz, 2H), 3.85 (t, *J* = 6.9 Hz, 4H), 2.13 (m, 2H).

HMRS (ESI-TOF) *m/z* $[M+ H]^+$ Calculated for $C_{11}H_{15}N_6O_2$: 263.1256 found: 263.1251.

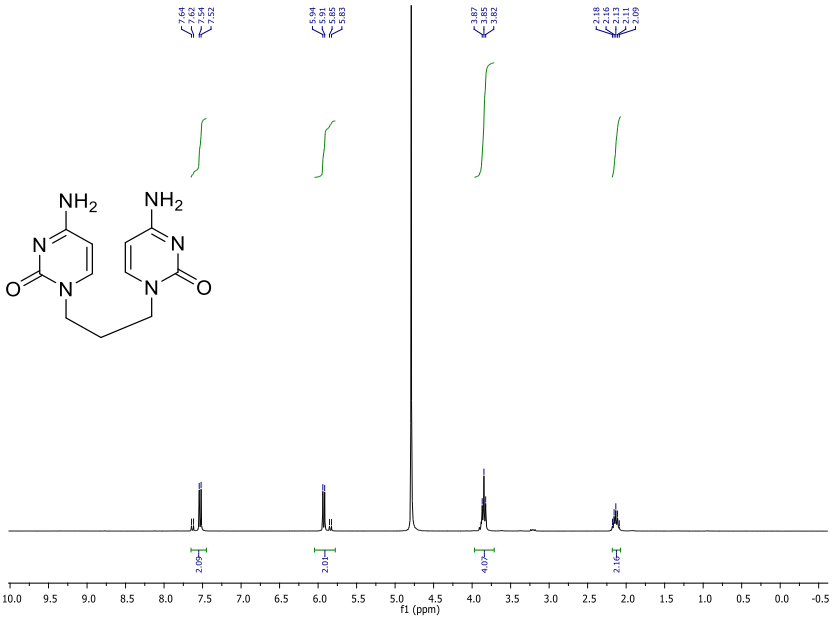

5.2. Synthesis of 5,6a,6b,8-Tetramethylhexahydro-1H-3a,5,8,9a-tetraazacyclohepta[def]biphenylene-4,6,7,9(5H,8H)-tetraone – Thy<>Thy reference

0.01 g (0.034 mmol) of the methylated thymine dyad Thy-Thy was dissolved in acetone (3.5 mL) in a pyrex tube (λ_{irr} > 290 nm) and was irradiated under inert N_2 atmosphere during 15 minutes with a medium pressure mercury lamp (750 W). The solvent was evaporated and the cyclobutane dimer Thy<>Thy was obtained as a white crystalline solid (0.01 g, yield > 98 %).

Characterization of Thy<>Thy.

^{1}H NMR (300 MHz, $CDCl_3$) δ ppm: 4.44 (m, 1H), 4.39 (m, 1H), 3.75 (s, 2H), 3.11 (s, 6H), 2.68 (m, 2H), 2.29 (m, 1H), 1.61 (m, 1H), 1.56 (s, 6H). ^{13}C NMR (75 MHz, $CDCl_3$) δ ppm: 169.0 (2CO), 151.5 (2CO), 60.0 (2CH), 49.1 ($2CH_2$), 46.0 (2C), 28.2 ($2CH_3$), 23.9 (CH_2), 21.3 ($2CH_3$). HMRS (ESI-TOF) m/z $[M+ H]^+$ Calculated for $C_{15}H_{21}N_4O_4$: 321.1563 found: 321.1562.

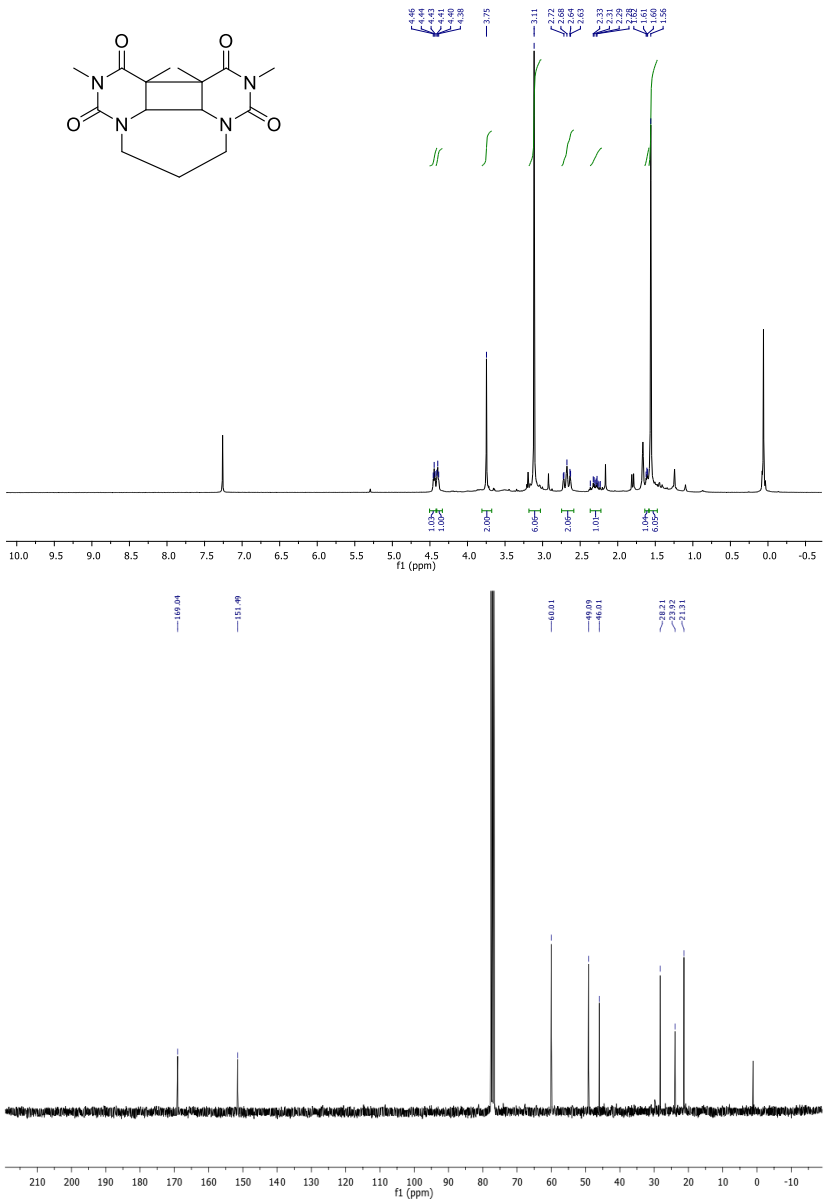
4.46
4.44
4.43
4.41
4.40
4.38
3.75
3.11
2.72
2.68
2.64
2.60
2.33
2.31
2.29
1.62
1.61
1.60
1.56
1.03
1.05
2.05
6.00
2.09
1.01
1.00
6.05
f1 (ppm)
169.04
151.49
60.01
49.09
46.01
28.21
23.92
21.31
f1 (ppm)

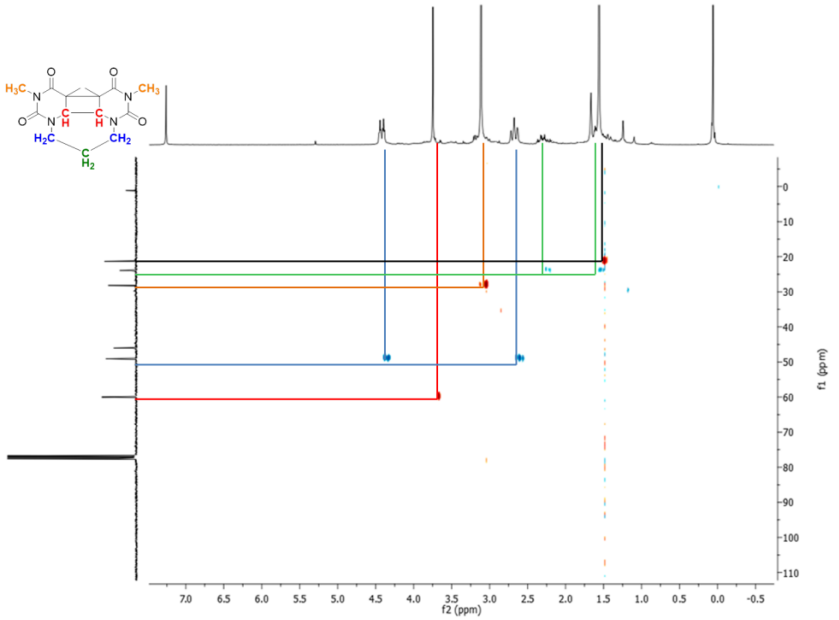

6. References

[1] R. Greinert, B. Volkmer, S. Henning, E. W. Breitbart, K. O. Greulich, M. C. Cardoso and A. Rapp, "UVA-induced DNA double-strand breaks result from the repair of clustered oxidative DNA damages," *Nucleic Acids Res.*, **2012**, 40, 10263–10273.

[2] S. Hoffmann-Dörr, R. Greinert, B. Volkmer, and B. Epe, "Visible light (>395 nm) causes micronuclei formation in mammalian cells without generation of cyclobutane pyrimidine dimers," *Mutat. Res.*, **2005**, 572, 142–149.

[3] V. Vendrell-Criado, G. M. Rodríguez-Muñiz, V. Lhiaubet-Vallet, M. C. Cuquerella and M. A. Miranda, "Photosensitization of DNA by 5-methyl-2-pyrimidone deoxyribonucleoside: (6-4) photoproduct as a possible Trojan horse," *Angew. Chem. Int.*

Ed., **2013**, 52, 6476 –6479.

[4] V. Vendrell-Criado, G. M. Rodríguez-Muñiz, V. Lhiaubet-Vallet, M. C. Cuquerella and M. A. Miranda, "The (6–4) dimeric lesion as a DNA photosensitizer," *Chem. Phys. Chem.*, **2016**, 17,1–5.

[5] T. Douki, "Formation and repair of UV-induced DNA damage," In *CRC Handbook of Organic Photochemistry and Photobiology*, *Third Ed.,* editors A. Griesbeck, M. Oelgemöller and F. Ghetti, **2012**, *2,* 1349–1392.

[6] J. Cadet, S. Mouret, J. Ravanat, and T. Douki, , "Photoinduced damage to cellular DNA: direct and photosensitized," *Photochem. Photobiol.*, **2012**, 88, 1048–1065.

[7] T. Douki, T. Delatour, F. Paganon, and J. Cadet "Measurement of oxidative damage at pyrimidine bases in γ -irradiated DNA," *Chem. Res. Toxicol.*, **1996**, 9, 1145-1151.

[8] M. C. Cuquerella, V. Lhiaubet-Vallet, J. Cadet, and M. A. Miranda, "Benzophenone photosensitized DNA damage," *Acc. Chem. Res.*, **2012**, 45, 1558–1570.

[9] T. Douki and J. Cadet, "Modification of DNA bases by photosensitized one-electron oxidation," *Int. J. Radiat. Biol.*, **1999**, 75, 571-581.

[10] T. Delatour, T. Douki, C. D'Ham, and J. Cadet, "Photosensitization of thymine nucleobase by benzophenone through energy transfer, hydrogen abstraction and one-electron oxidation," *J. Photochem. Photobiol. B, Biol.*, **1998**, 44, 191–198.

[11] J. W. Neidigh, A. Darwanto, A. A. Williams, N. R. Wall, and L. C. Sowers, "Cloning and characterization of Rhodotorula glutinis thymine hydroxylase," *Chem. Res. Toxicol.*, **2009**, 22, 885–893.

[12] D. K. Rogstad, J. Heo, N. Vaidehi, W. A. I. Goddard, A. Burdzy, and L. C. Sowers, "5-Formyluracil-induced perturbations of DNA function," *Biochemistry*, **2004**, 43, 5688–5697.

[13] H. Ånensen, F. Provan, A. T. Lian, H.S. Reinertsen, Y. Ueno, A. Matsuda, E. Seeberg and S. Bjelland, "Mutations induced by 5-formyl-2'-deoxyuridine in Escherichia coli include base substitutions that can arise from mispairs of 5-formyluracil

with guanine, cytosine and thymine," *Mutat. Res.*, **2001**, 476, 99–107.

[14] E. J. Privat and L. C. Sowers, "A proposed mechanism for the mutagenicity of 5-formyluracil," *Mutat. Res.*, **1996**, 354, 151-156.

[15] T. Sugiyama, A. Kittaka, H. Takayama, M. Tomioka, Y. Ida, and R. Kuroda, "Chemical cross-linking of peptides derived from RecA with single-stranded oligonucleotides containing 5-formyl-2'-deoxyuridine," *Nucleosides Nucleotides Nucleic Acids*, **2001**, 20, 1079–1083.

[16] J. Michl, "Photophysics of organic molecules in solution," In *Handbook of Photochemistry, Third Ed.*, editors M. Montalti, A. Credi, L. Prodi and M. T. Galdolfi, **2006**, 1, 1–47.

[17] Y. Lion, M. Delmelle and A. VanDeVorst, "New method of detecting singlet oxygen production," *Nature*, **1976**, 263, 442-443.

[18] M. C. Cuquerella, V. Lhiaubet-vallet, M. A. Miranda, and F. Bosca, "Drug–DNA complexation as the key factor in photosensitized thymine dimerization," *Phys. Chem. Chem. Phys*., **2017**, 19, 4951-4955.

[19] I. G. Gut, P. D. Wood, and R. W. Redmond, "Interaction of triplet photosensitizers with nucleotides and DNA in aqueous solution at room temperature," *J. Am. Chem. Soc.*, **1996**, 118, 2366-2373.

[20] V. Lhiaubet-Vallet, M. C. Cuquerella, J. V Castell, and M. A. Miranda, "The triplet energy of thymine in DNA," *J. Am. Chem. Soc.*, **2006**, 128 , 6318-6319.

[21] A. B. Fraga-Timiraos, V. Lhiaubet-Vallet, and M. A. Miranda, "Repair of a dimeric azetidine related to the thymine-cytosine (6-4) photoproduct by electron transfer photoreduction," *Angew. Chem. Int. Ed.*, **2016**, 55, 6037–6040.

[22] D. J. Fenick, H. S. Carr, and D. E. Falvey, "Synthesis and photochemical cleavage of *cis-syn* pyrimidine cyclobutane dimer analogs," *Photochem. Photobiol.*, **1996**, 30, 911–918.

[23] H. Stephan, I. Piantanida, S. Noll, M. Kralj, and S. Lidija,

"Synthesis of modified pyrimidine bases and positive impact of chemically reactive substituents on their *in vitro* antiproliferative activity," *Eur. J. Med. Chem.*, **2009**, 44, 1172–1179.

[24] M. C. Cuquerella, V. Lhiaubet-Vallet, F. Bosca, and M. A. Miranda, "Photosensitised pyrimidine dimerisation in DNA," *Chem. Sci.*, **2011**, 2, 1219-1232.

[25] Y. Tu, R. Dammann, and G. P. Pfeifer, "Sequence and time-dependent deamination of cytosine bases in UVB-induced cyclobutane pyrimidine dimers in vivo," *J. Mol. Biol.*,**1998**, 284, 297-311.

Chapter 5:

Photocages for protection and controlled release of bioactive compounds: (S)-Ketoprofen and Diclofenac

1. Introduction

This chapter centers the attention on the development of a new photoprotection strategy in order to counteract the photosensitizing effects of some drugs on biomolecules such as DNA.

In spite that nowadays the designed pharmaceutical drugs for diseases treatment are in general safe and efficient, side effects cannot be totally avoided. Among them, drug photosensitivity is becoming increasingly frequent. Indeed, under the same conditions of irradiation or at the same concentration, the drug or the solar exposure alone are not capable of producing these cutaneous side effects, which only appear when both components are combined.

Thereby, some chemical compounds (perfumes, sunscreen ingredients, therapeutic agents and their metabolites or photoproducts) become reactive under irradiation, most often in the UVA (320 - 400 nm), and they can trigger chemical modifications of biomolecules such as proteins or nucleic acids.

Clinically, drug photosensitivity consists on the appearance of cutaneous lesions such as exaggerated sunburn, blisters, rash, eczema, etc., in treated patients that have been exposed to solar light. It is generally divided in two phenomena: photoallergy and phototoxicity.[1],[2].

Photoallergy is an immunologically mediated reaction where the drug plays the role of a photohapten and undergoes covalent binding to proteins leading to a photoantigen, which is the molecule that triggers the immunological process. Thus, photoallergy requires a previous exposure to the photosensitizing agent and an induction period. After the sensitization step, reactions of cross-reactivity may be provoked by chemicals structurally related with the hapten.[3] Photoallergic contact dermatitis occurs not only on the areas exposed to sunlight but it may also be extended to other parts of the body.

By contrast, phototoxicity occurs only on exposed areas immediately after light exposure. It resembles an exaggerated sunburn with an early maximum intensity on the exposed areas,

followed by a decrescendo evolution within 24-72 hours. The response is dependent on the photosensitizer concentration and on the received light dose. Repeated phototoxic reactions might be at the origin of increasing the risk of skin cancer due to the formation of DNA damages such as nucleobase oxidation, pyrimidine cyclobutane dimers formation, etc. These lesions, not diagnosed with the naked eye, are of paramount importance as they can lead to mutation of the genome.

An important number of photoactive drugs has now been reported. Non steroidal anti-inflammatory drugs (NSAIDs), especially those derived from the aryl propionic acid family (*ie.* ketoprofen, carprofen, tiaprofenic acid), represent an important class of photosensitizing compounds (Figure 1); [4],[5] but others can also be mentioned such as antibiotics (fluoroquinolones[6],[7], tetracyclines and sulfamides), antihistaminics (promethazine), neuroleptics (phenotiazine), hypolipidemiants (fibrates), anxiolytics (benzodiazepines), acne treatment (isotretinoin), psoriasis treatment (psolarens), [6] etc.

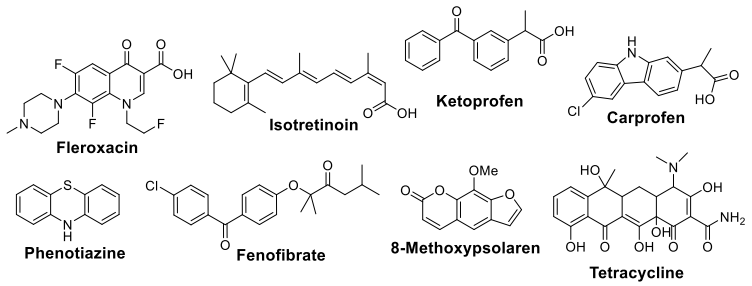

Figure 1. Examples of photosensitizing drugs.

The topical form of the drugs generally exhibits a better safety profile than the systemic one since the diffusion of the drug in the organism is reduced, thus, avoiding the appearance of the most common side effects. In this context, topical formulations containing (*S*)-ketoprofen (KP) or diclofenac (DF) as pharmacologically active agent are among the NSAIDs most commonly employed because they

are available in many countries without medical prescription. However, preparations that contain ketoprofen have gained notoriety as it has been reported to cause severe skin dermatitis such as pruritic and papulovesicular, bullous, and edematous lesions.[1] Photoallergic contact dermatitis has been reported for diclofenac as topical pain reliever[8], but also when it is the active component in the treatment of actinic keratosis.[9] The risk / benefit ratio of topical forms is being reevaluated and it is advised to avoid sun exposure for example by covering skin areas with clothes or using sun protection.

In order to understand the processes involved in drug photosensitization of biomolecules, it is necessary to draw a complete map of the drug photophysical properties. [1]

Thus, (*S*)-ketoprofen, which is the pharmacologically active enantiomer (eutomer) of the drug, has its absorption maximum at 260 nm with an extended spectrum reaching the UVA region up to 350 nm. This long wavelength absorption is a key parameter in the photosensitizing effect of chemicals as UVA is not significantly filtered by the atmosphere and thus represents the most important UV range reaching the earth surface. Fortunately, it is hardly absorbed by DNA or other biological components; but, it is able to ''activate'' chemicals inducing phototoxic and photoallergic effects. In fact, it has been shown that the *in vivo* photosensitizing properties of KP are linked to its reactivity in the UVA region of sunlight. [5]

The KP photochemistry in neutral aqueous media is dominated by an efficient photodecarboxylation (ϕ=0.75) triggered by intramolecular electron transfer from the carboxylate group to the excited carbonyl (Scheme 1). Therefore, its steady-state photolysis gives rise to a variety of photoproducts, the major one being 3-ethylbenzophenone. [1], [5]

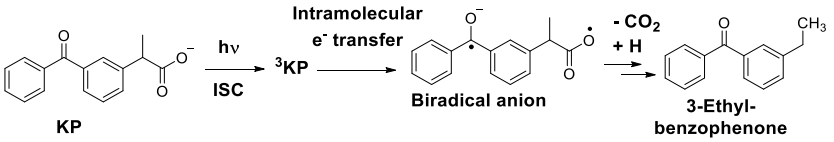

Scheme 1. Mechanism of KP photodecomposition resulting in formation of the major photoproduct, 3-ethylbenzophenone.

From the photophysical point of view, KP has an intersystem crossing quantum yield of unity, excitation induces thus a quantitative population of its triplet state. Phosphorescence experiments showed a $n\pi^*$ nature of the triplet excited state with an energy of 69.3 kcal/mol (289.7 kJ/mol). Picosecond laser flash photolysis of KP in phosphate buffer (pH *ca.* 7) allows the detection of a transient species with $\lambda_{max} \sim 525$ nm and a lifetime of 250 ps, which has been assigned to the triplet excited state of the drug ^{3}KP. [5], [10]

The high photolability of KP renders it a poor candidate for ROS generation. The detected ROS might be related to the formation and photoreactivity of its main photoproduct, 3-ethylbenzophenone, which for example exhibits a singlet oxygen quantum yield of 0.29. [1],[5]

In line, the strong photosensitizing properties of KP have been attributed to its benzophenone chromophore. In DNA, the main process is a Type I mechanism (e^- transfer) that affects mainly the guanine nucleobase oxidizing it to 8-oxo-7,8-dihydro-2'-deoxyguanosine (8-OxodGuo) and 2,6-diamino-4-hydroxy-5 formamido-pyrimidine (FapyGua). Nonetheless, other nucleobases such as thymine are also oxidized producing 5-hydroxymethyluracil, 5-formyluracil, thymine glycol and 5-hydroxymethyl hydantoin. [11], [12] Moreover, formation of cyclobutane pyrimidine dimers has also been evidenced. This lesion is formed by a triplet-triplet energy transfer where the triplet excited state (E_T of *ca*. 289.7 kJ/mol) of KP lies 21 kJ/mol higher than that of thymine in DNA (E_T of *ca.* 267.5 kJ/mol). [6],[11]

Diclofenac is another NSAID, which belongs to the acetic acid drug family. Its potential phototoxicity has been ascribed to a biologically active photoproduct able to generate radicals upon photolysis in a more efficient way that the parent drug. [4],[13]

Mechanistic studies indicate that the photochemistry of diclofenac involves an electrocyclization to a monohalogenated carbazole (Scheme 2). Indeed, 2-chlorocarbazole and carbazole, which are the primary and secondary photoproducts, can be considered as the active chromophores of diclofenac photosensitization.[4] The 2-chlorocarbazole photoreactivity is especially relevant to understand the photobiological properties of diclofenac because of the formation of radical species during its photodehalogenation.

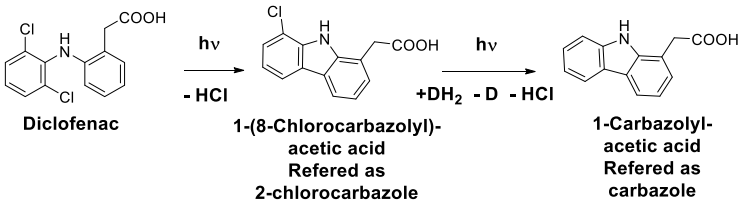

Scheme 2. Formation of DF carbazole derived photoproducts (DH_2 represents a H donor compound).

Indeed, comparison of the photobiological studies of diclofenac with that of 2,6-dichloro and 2-chlorocarbazole revealed that this latter is the most damaging agent during membrane oxidation acting through a radical-mediated mechanism.[4],[14] By contrast with the non emissive diclofenac, 2-chlorocarbazole showed two fluorescence bands with maxima around 367 and 352 nm in ethanol. A transient absorption band at λ_{max} *ca.* 430 nm with a lifetime of 270 ns was observed by laser flash photolysis and assigned to the triplet-triplet transition. The carbazolyl radical ($R_2N^{\cdot}$) was also detected as a long-lived signal at 640 nm.[4]

Formation of carbazole derived photoproducts is not innocuous as they exhibit a higher UVA absorption than diphenylamine derivatives, being thus more prone to be excited by sunlight radiation, and reaching this way their photoreactive states.[13] Moreover, other chlorocarbazoles, such as the NSAID carprofen, have been described in the literature for their photoactive role in H abstraction from lipids producing lipid peroxidation and cell hemolysis.[15] In the DNA field, chlorocarbazole derivatives have been shown to photoinduce nucleobase oxidation as well as the formation of cyclobutane thymidine dimers through a triplet-triplet energy transfer. [16],[17]

Therefore, efficient skin photoprotection is required to neutralize all these negative aspects of sunlight exposure. This can be accomplished by the application of broad-spectrum (UVA/UVB) sunscreens or by the use of protective clothes.

As above mentioned, photosensitizing effects are mainly due to drug (or its photoproducts) absorption in the UVA region. It is thus important to combine the (topical) drug treatment with application of a UVA filter.

In this context, avobenzone (AB, 4-*tert*-butyl-4'-methoxydibenzoylmethane) is a 1,3-dicarbonyl compound that exhibits a large absorbance at 350 nm (Figure 2) due to its ''chelated'' keto-enol tautomer largely favored in the ground state (Scheme 3). After UV light absorption, extensive photoisomerization to the β-diketone occurs (band absorption at 260 - 280 nm); in the dark, the enol form is slowly recovered. [18]

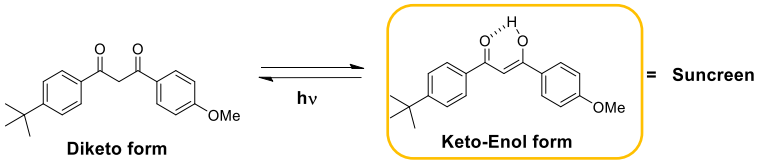

Scheme 3. Structure of the two tautomers of AB.

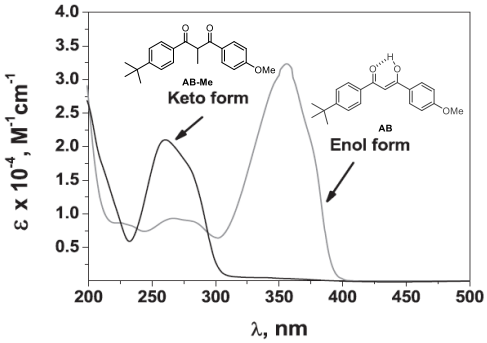

Figure 2. UV-Vis absorption spectra of the two AB tautomers, enol form, grey line and diketo (obtained from AB-Me model compound) form black line.

In this context, the development of sunscreen-based photocages (equivalent to covalently linked pro-drug/pro-filter systems) could be considered a clever solution. This concept makes use of light-sensitive chemical moieties previously introduced in Chapter 3 (known as photoremovable protecting groups, PPGs) to allow controlled and simultaneous release of the masked drug and the solar filter upon irradiation. This would bring advantages over the mere mixture because it would allow a controlled release of the two components.[19] Photocages have become very popular because they provide spatial and temporal control over the activation of molecules triggered by light [20],[21],[22],[23] and have previously been employed for biological applications,[20],[22],[23],[24],[25] such as photocaged nucleotides,[26],[27] proteins, neurotransmitters, pharmaceuticals, [28],[29],[30],[31] fluorescent dyes, or small molecules.

More concretely, during the last two decades the use of phenacyl chromophores as PPGs has been a subject of interest in order to improve the persistence of the bioactive molecules.[20] α-Substituted esters of the phenacyl chromophores are typical PPG frameworks for the release of carboxylic acids. The release process involves hydrogen abstraction, generally from H donating solvents, by the excited carbonyl group (photoreduction) of the phenacyl

ester, leading to the formation of a ketyl radical intermediate. Finally, the carboxylic acid is released from the chromophore moiety.[32] (Scheme 4).

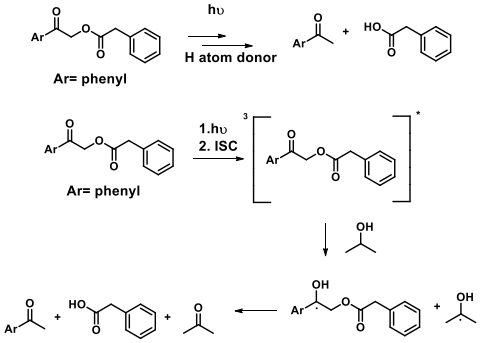

Scheme 4. Photolysis of phenacyl carboxylate in the presence of propan-2-ol.

Interestingly, avobenzone in its diketo form is composed of two phenacyl chromophores, and the photosensitizing drugs KP and DF contain carboxylic acid funcional group. Therefore, a photoactivatable dyad incorporating one of the drugs and the solar filter can be conceived (Figure 3). The designed compounds should result in a remarkable combination capable of providing a phototriggered slow delivery of the drug together with that of its UVA protective shield. Thus, KP and DF photoreactivity should be inhibited and the risk of adverse skin reactions minimized, since the AB absorption at *ca.* 350 nm is more than 200 and 600 times higher than that of KP and DF, respectively.

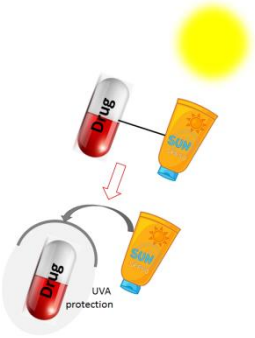

Figure 3. Design of photoactivable dyad containing a drug and a solar filter

2. Objectives

The main objective is to develop a new photoprotection strategy in order to counteract the harmful effects of photosensitizing drugs (especially for NSAIDs). This has been achieved by the design of photoactivable dyads that allowed the controlled release of photosensitive pharmaceutical active principles under the photoprotective action of a solar filter effect. In this context, (*S*)-ketoprofen and diclofenac are the selected drugs and avobenzone the UVA filter. This should allow prevention from the very beginning of the drug associated DNA photosensitizing side effects and should propose a safer way of use.

For this purpose, the following specific objectives have been defined:

- To synthesize the dyads containing (*S*)-ketoprofen or diclofenac and the UVA filter, avobenzone.

- To evaluate the viability of the concept by preliminary steady-state photolysis of the dyads in different solvents and conditions.

- To quantify the different released ingredients.

- To characterize the photophysical properties of AB-KP and AB-DF dyads in order to get more insights into the photoactive excited states involved in the photorelease process.

3. Results.

3.1. Synthesis procedure of AB-KP and AB-DF dyads.

The synthesis of these photoactivatable dyads (AB–KP and AB-DF, Scheme 5 and 6) was performed applying the method described by I. Pravst and coworkers[33] by bromination at the α position of the carbonyl groups by using *N*-bromosuccinimide under solvent free conditions. The resulting intermediate was reacted with the cesium salt of the drug to afford the desired dyad as a diastereoisomeric or enantiomeric mixture for AB-KP or AB-DF, respectively. The obtained compounds contained mainly the diketo tautomer of the AB moiety, as shown in the NMR spectra with the shift of the proton of the enol form at 6.75 ppm to 6.79 and 6.94 ppm for AB-KP and AB-DF, respectively.

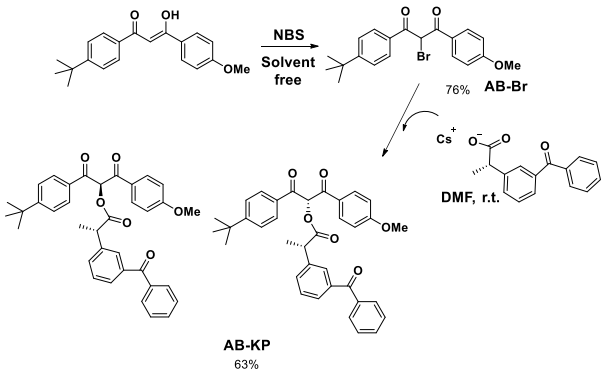

Scheme 5. Synthetic procedure for AB-KP dyad.

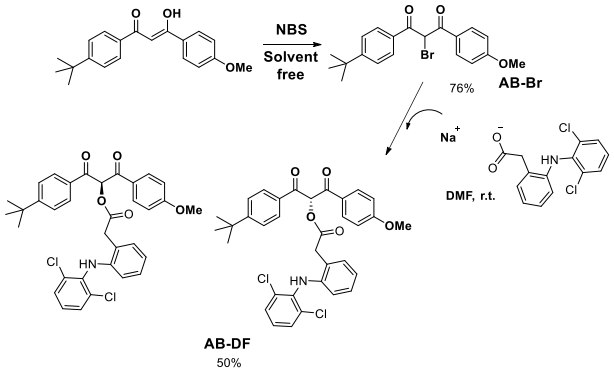

Scheme 6. Synthetic procedure for AB-DF dyad.

Moreover, as shown in Figure 4, the UV-Vis absorption spectra of both dyads have a main band in the same range as the α-methyl derivative of AB (AB-Me, Figure 2 inset), used as a model compound for AB in its diketo form. The AB-KP dyad presents a maximum band absorption at 260 nm, whereas AB-DF dyad band is peaking at 270 nm. Both dyads exhibit a little shoulder, less pronounced for AB-DF, at 290 nm and an extended band reaching the UVA region up to 350 nm (Figure 4). This long wavelength absorption allows a sunlight triggered release of the active latent ingredients *ie.* AB, KP and DF.

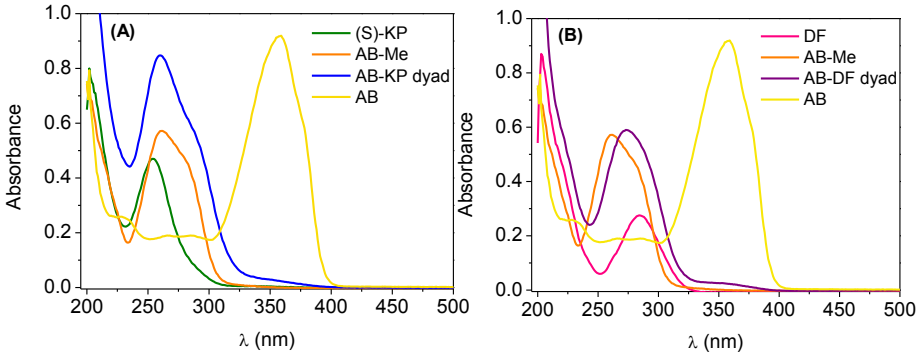

Figure 4. UV-Vis spectra of all of the ingredients performed in EtOH at a concentration *ca.* 2 x 10^{-5} M. (A) (S)-KP (green line), AB-enol (yellow line), AB-Me (orange line), AB-KP (blue line) and (B) DF (pink line), AB-DF (purple line).

3.2. Preliminary steady-state photolysis studies of the dyads.

First, steady state photolysis of the dyads was performed in different solvents and atmosphere conditions in order to check the pro-drug/pro-filter concept. The release can be easily followed by UV-Vis absorption spectrometry, monitoring the formation of AB at 355 nm.

Thus, the AB-KP dyad was irradiated with a multilamp photoreactor (equipped with UVA lamps with a maximal output *ca.* 355 nm) under anaerobic conditions. For H donor solvents (ethanol and isopropanol), the AB-KP band at 260 nm decreased with the irradiation time concomitantly with the appearance of the keto-enol AB band centered at 355 nm. By contrast, in the case of acetonitrile, a solvent that lacks H donating properties, no band at 355 nm appeared. This points towards the viability of the photorelease uniquely under H donating conditions (Figure 5).

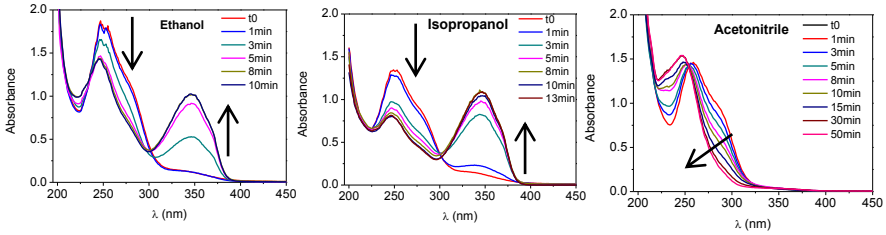

Figure 5. Steady-state photolysis of AB-KP dyad under anaerobic conditions in different solvents: left ethanol (0.25 mM), middle isopropanol (0.178 mM) and right acetonitrile (0.21 mM).

Then, a nitrogen flushed solution of AB-KP (9 x 10^{-5} M) in ethanol, selected on the basis of the previous experiment, was irradiated with simulated sunlight (SSL) provided by the filtered emission of a Xenon arc lamp. The reactivity was similar to that observed for UVA irradiation. When the experiment was run under aerobic conditions no band appeared at 355 nm. This is in line with the described photorelease of phenacyl-like PPG that takes place through a triplet excited state mediated process. Under air

conditions, triplet excited states are quenched by oxygen, opening the way towards other photoprocesses (Figure 6).

Similar results were observed for AB-DF dyad (4.3 x 10^{-5} M) irradiated with SSL in ethanol under aerobic or anaerobic conditions (Figure 7).

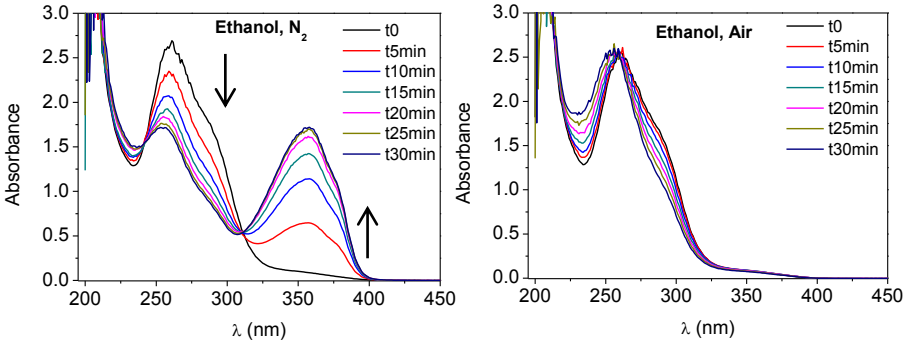

Figure 6. Steady-state photolysis of AB-KP dyad (9 x 10^{-5} M) by means of simulated sunlight (SSL) in N_2 (left) and air (right) atmosphere.

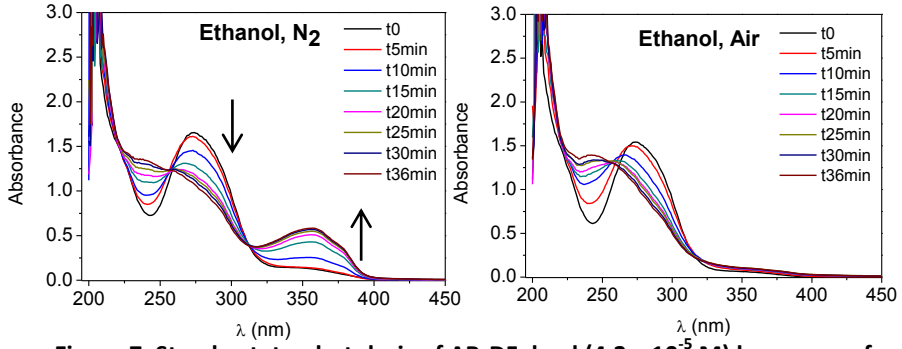

Figure 7. Steady-state photolysis of AB-DF dyad (4.3 x 10^{-5} M) by means of simulated sunlight (SSL) in N_2 (left) and air (right) atmosphere.

In a more realistic approach and to simulate the more viscous composition of topical creams, the photorelease was performed in air using propylene glycol as matrix for AB-KP (9 x 10^{-5} M) and diethylene glycol for AB-DF (6.6 x 10^{-5} M). This way, the medium still presents hydrogen donor capability, but its lower diffusion-controlled rate constant should disfavor the deactivation of excited states by oxygen. This hypothesis was confirmed for both dyads as shown in

Figure 8, where the AB absorption band appeared as a function of SSL irradiation time.

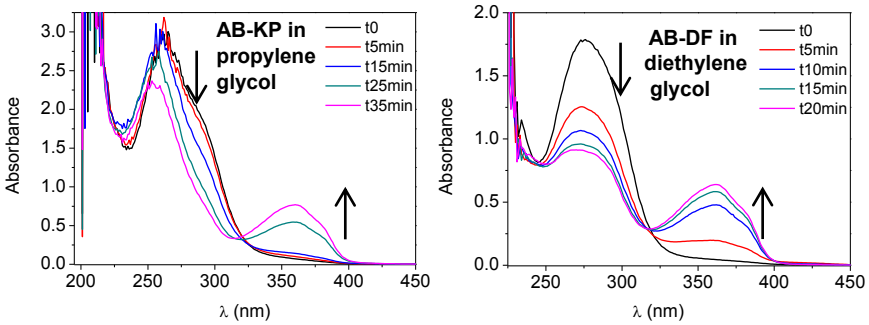

Figure 8. Steady-state photolysis of AB-KP (9 x 10^{-5} M, right) and AB-DF (6.6 x 10^{-5} M, left) by means of simulated sunlight (SSL) using propylene glycol and diethylene glycol, respectively, under aerobic atmosphere.

3.3. HPLC analysis of the active ingredients photorelease.

Due to the close absorption maxima between KP and AB-KP and between DF and AB-DF and the comparatively low molar absorption coefficient of KP and DF at these wavelengths, an accurate determination of the released drugs required HPLC analysis. This was accomplished at a higher concentration in a deaerated ethanol solution for AB-KP (1.1 x 10^{-3} M) and AB-DF (*ca.* 1.1 x 10^{-3} M). For aerated propylene glycol and diethylene glycol solutions, concentrations of 7.2 x 10^{-4} M and 9.3 x 10^{-4} M were used for AB-KP and for AB-DF, respectively. Quantitation of the photoproducts was done by means of calibration curves by comparing with authentic samples of KP, DF and AB. The HPLC traces revealed that the starting dyad peak (AB-KP or AB-DF) disappeared over time giving rise to formation of the drug (KP or DF) and of the solar filter, AB (see Figure 9 and 10).

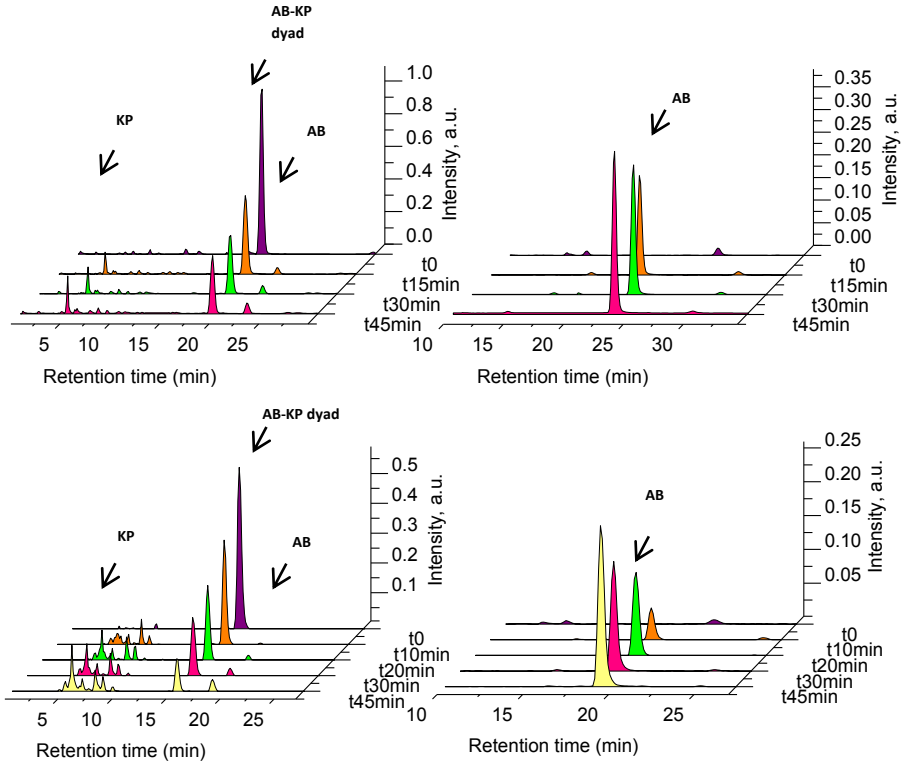

Figure 9. Top, SSL irradiation in deaerated ethanol. Bottom, SSL irradiation in aerated propylene glycol. Chromatogram at 260 nm (left, AB-KP dyad maximum band absorption) and chromatogram at 357 nm (right, AB maximum band absorption).

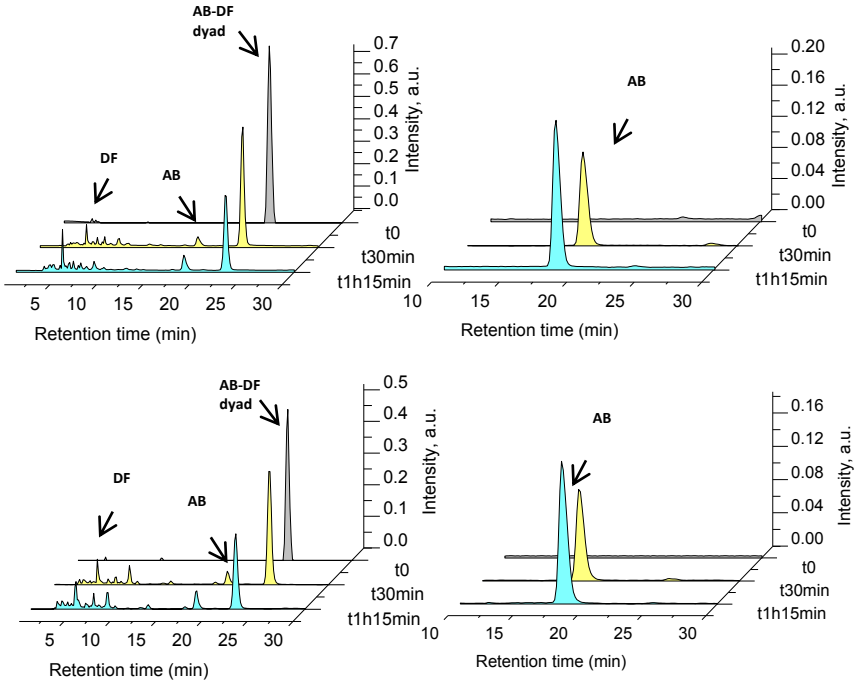

Figure 10. Top, SSL irradiation in deaerated ethanol. Bottom, SSL irradiation in aerated diethylene glycol. Chromatogram at 274 nm (left, AB-DF dyad maximum band absorption) and chromatogram at 357 nm (right, AB maximum band absorption).

After 15 min, 30% of the initial AB–KP had reacted, while after 2 h AB–KP was almost totally consumed. Regarding AB-DF after 15 min of irradiation, 23% of the starting dyad had been consumed and after 75 min 60% had reacted (Figure 11 and 12, respectively). As explained above, irradiation of the corresponding AB-KP and AB-DF aerated ethanol solutions under the same experimental conditions did not lead to the formation of AB in agreement with the involvement of a triplet excited state as an intermediate of the photoreaction.

Interestingly, under the same experimental conditions, *ie.* in deaerated ethanol or aerated propylene glycol, KP was completely

photolyzed in less than 30 min, clearly demonstrating the protecting role of the released AB filter (Figure 11C and D). However, in the case of DF, its degradation is slower in deaerated ethanol than in aerated diethylene glycol, where decomposition is similar to that of KP (Figure 12C and D).

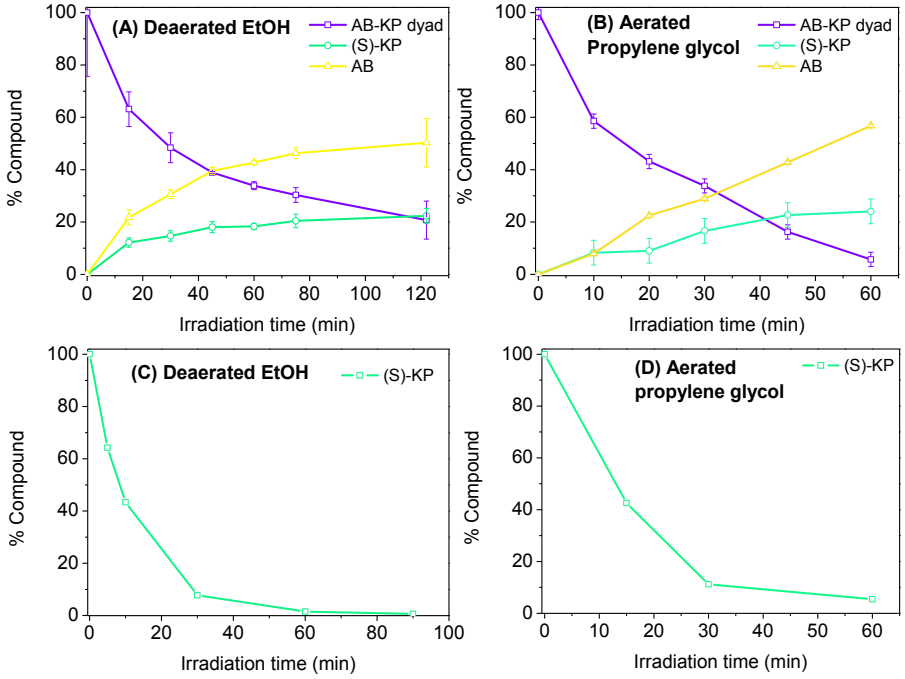

Figure 11. Photorelease process of AB and KP from AB-KP dyad in deaerated ethanol (A) and aerated propylene glycol (B). SSL photolysis of (*S*)-KP in deaerated EtOH (C) and aerated propylene glycol (D).

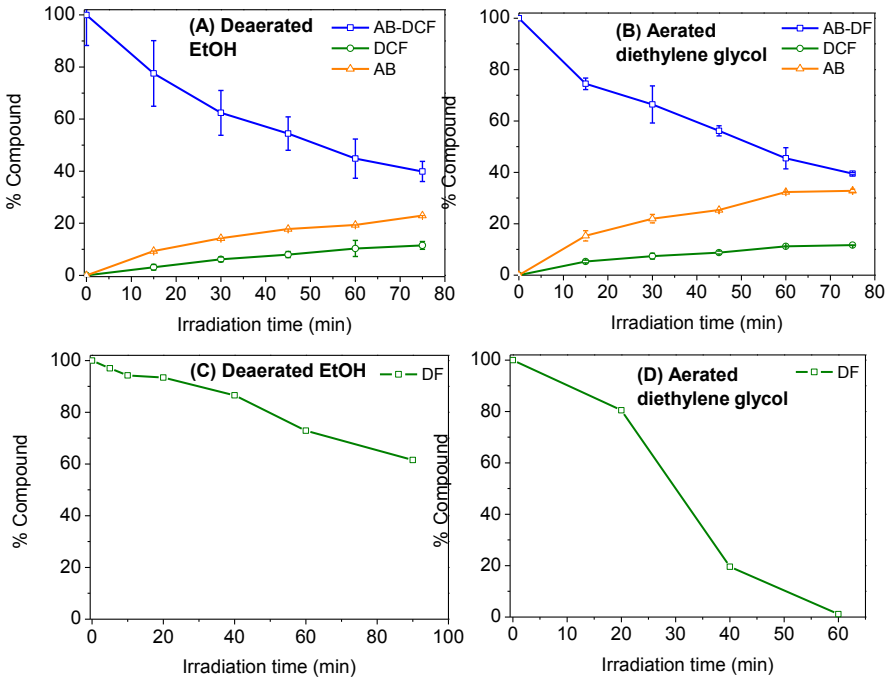

Figure 12. Photorelease process of AB and DF from AB-DF dyad in deaerated ethanol (A) and aerated diethylene glycol (B). SSL photolysis of DF in deaerated EtOH (C) and aerated diethylene glycol (D).

3.4. Phosphorescence experiments: Triplet energy characterization.

As above mentioned, the triplet excited state is a key intermediate in the release process for phenacyl-derived PPGs. Thus, in order to study if these dyads were able to experience an intersystem crossing relaxation pathway, the presence of triplet states was examined by phosphorescence experiments in ethanol solutions at 77 K.

Concerning AB-KP dyad, it presented a structured emission spectrum with a first maximum peak at *ca.* 400 nm. The spectrum is similar to that of (S)-KP and somewhat different in shape from that of

AB-Me. For AB-DF a narrow band was observed with maximum *ca.* at 430 nm. Interestingly, as stated in the introduction, no phosphorescence was found for diclofenac so this moiety does not contribute to the obtained spectrum of AB-DF. This emission is somewhat red-shifted by respect with that of the described AB-Me phosphorescence, used as reference to illustrate AB in its diketo form. [34] However, this is consistent with a change in the α-substitution *ie*. alkyl chain versus ester moiety.

The triplet energies for AB-Me, AB-KP dyad, AB-DF dyad and (*S*)-KP are found in Table 1. They were calculated from the $\lambda_{0\text{-}0}$ (first emission peak) band of their phosphorescence emission (Figure 13) applying the following equation 1:

$$E_T = \text{Ŋ}hc / \lambda_{0\text{-}0} \qquad \text{Eq. 1}$$

Where Ŋ is the Avogadro number (6.022×10^{23} mol^{-1}), **h** the Planck constant (6.626×10^{-34} J s), **c** the light velocity (3×10^{8} m s^{-1}), and $\lambda_{0\text{-}0}$ the wavelength at the emission first peak (m) for AB-KP but for AB-DF $\lambda_{0\text{-}0}$ was approximated from the wavelength corresponding to the 20 % of the emission intensity.

In the literature, triplet energies of (*S*)-KP and AB-Me are given at 289.7 kJ/mol[5] and 295.5 kJ/mol[35], respectively.

Molecule	Experimental E_T data	Literature E_T data
AB-Me	302.3 kJ/mol	295.5 kJ/mol
(S)-KP	299.3 kJ/mol	289.7 kJ/mol
AB-KP	297.8 kJ/mol	-
DF	No phosphorescence	No phosphorescence
AB-DF	297.0 kJ/mol	-

Table 1. Comparison of literature E_T data with experimental E_T data of AB-Me (8.8 mM), (S)-KP (9.24 mM), AB-KP (0.82 mM), DF (0.058 mM) and AB-DF (0.027 mM) in ethanol solutions at 77 K.

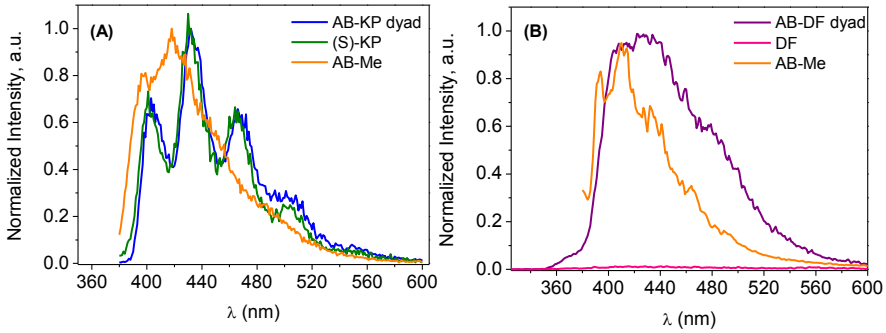

Figure 13. Phosphorescence emission spectra: (A) AB-KP dyad, (S)-KP and AB-Me (λ_{exc} of *ca.* 310 nm) and (B) AB-DF dyad, DF and AB-Me (λ_{exc} of *ca.* 284 nm) at the concentrations indicated above.

3.5. Fluorescence experiments on AB-DF dyad.

As explained in the introduction, the phototoxic properties of diclofenac are due to the formation of its 2-chlorocarbazole photoproduct and its subsequent photodehalogenation to carbazole. Formation of these photoproducts can be easily followed by emission spectroscopy as, by contrast with the parent drug, they exhibit a fluorescence band with λ_{em} at *ca.* 350 and 360 nm.[13]

Three solutions (sodium diclofenac salt, equimolar mixture of AB and DF, and AB-DF dyad) were irradiated in parallel with SSL in aerated diethylene glycol solution at *ca.* 1.7 x 10^{-5} M. In the UV-Vis absorption spectra, a change was observed for irradiation of the diclofenac sample; the band at 270 nm decreased concomitantly with the increase of red-shifted bands with λ_{max} at *ca.* 294, 325 and 336 nm corresponding to the typical spectrum of carbazole. Concerning the fluorescence emission measurements, two bands with maxima at 362 and 347 nm were increasing (Figure 14A and A'). These two observations are in agreement with formation of the carbazole-derived photoproducts as described in the literature.[13],[15] For the equimolar mixture DF+AB or for the dyad, the UVA absorption band of the keto-enol form of AB overlaps with those of the photoproducts (Figure 14B and 14C), avoiding to follow their kinetics of formation by

means of UV-Vis absorption photospectrometry. This difficulty was anticipated, as AB was expected to provide photoprotection to the photoproducts. Fortunately, the non-fluorescent AB did not interfere in emission measurements, allowing us to monitor the photoproducts formation.

As shown in Figure 14A´, 14B´ and 14C´, the increased emission intensity due to carbazole derivatives was lower for the equimolar DF+AB mixture as well as for the dyad AB-DF. This is clearly illustrated in Figure 15 by plotting of the fluorescence intensity (at λ_{em} *ca.* 367 nm) as a function of the irradiation time.

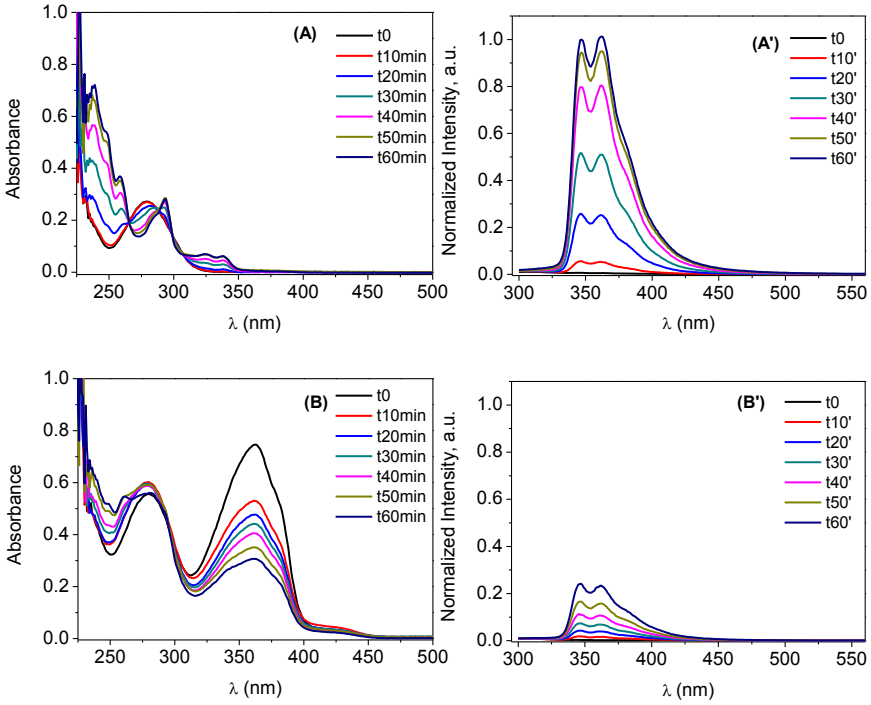

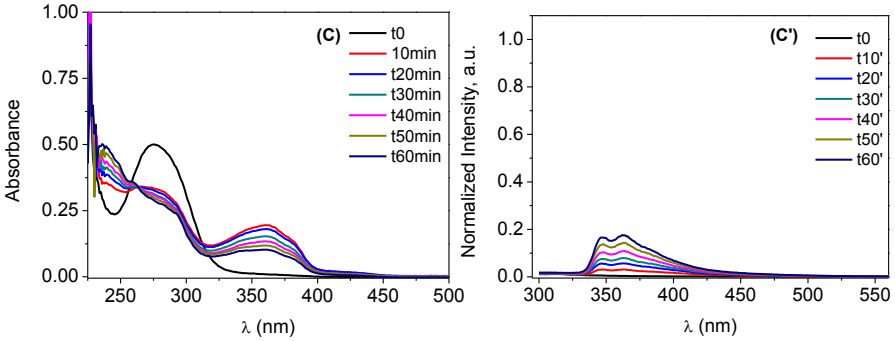

Figure 14. UV-Vis spectra (left, (A), (B), and (C)) and fluorescence emission spectra (right, (A'), (B') and (C')) of sodium diclofenac salt ((A) and (A')), AB and diclofenac mixture ((B) and (B')), and AB-DF dyad ((C) and (C')).

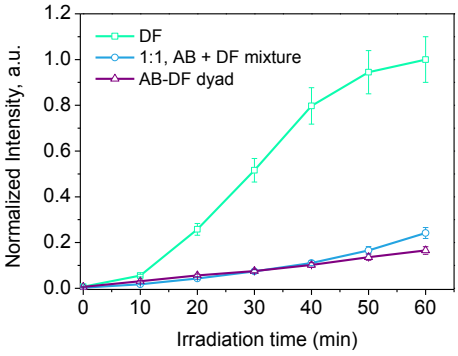

Figure 15. Normalized fluorescence emission intensity at 347 nm emission peak for DF, AB+DF mixture and AB-DF dyad in diethylene glycol (1.7 x 10^{-5} M).

Thus, fluorescence monitoring of the irradiation experiments reveals that, although formation of carbazole-derived photoproducts is not completely prevented in the equimolar DF+AB mixture and in the AB-DF dyad, partial protection is provided by the preexisting or nascent keto-enol form of the filter.

3.6. Laser Flash Photolysis experiments: Transient species characterization.

Finally, transient absorption spectroscopy was carried out to obtain direct information on the excited states involved in the

photochemical process. Laser flash photolysis experiments in the nanosecond timescale (Nd:YAG, 355 nm) were performed on a nitrogen bubbled ethanol solution of AB–KP (6.4 x 10^{-4} M). A transient absorption band centered at 400 nm appeared immediately after the pulse (Figure 16A) and decayed with a short lifetime of 0.2 µs without leading to further detectable species. Regarding AB-DF dyad, laser flash photolysis of ethanolic solutions (6.4 x 10^{-4} M) also gives rise to the formation of a transient with a maximum at 420 nm and a short lifetime 0.4 µs (Figure 16B). The detected transients were quenched in the presence of oxygen.

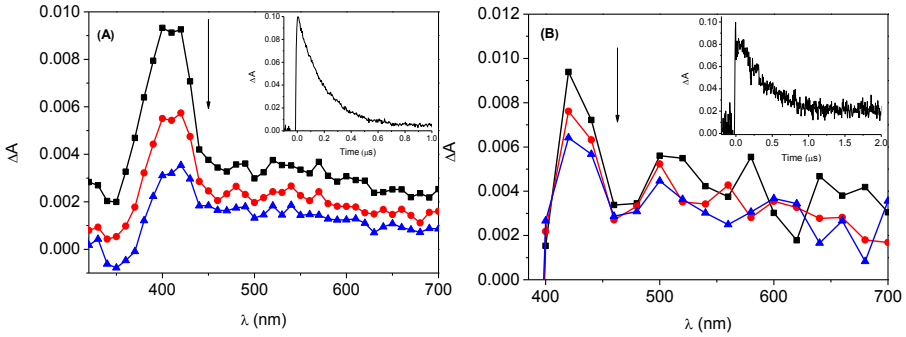

Figure 16. Transient absorption spectra of (A) AB–KP in ethanol under N_2, from 0.05 to 0.3 µs after the 355 nm laser pulse. Inset: Corresponding decay monitored at 400 nm. (B) AB-DF dyad in ethanol under N_2, from 0.02 to 0.34 µs after the 355 nm laser pulse. Inset: Corresponding decay monitored at 420 nm.

According to the literature data[34], these bands are similar to that of the triplet-triplet transition of AB-Me, used as a model to mimic the diketo form of AB. Thus, the observed transient absorption bands at 400-420 nm were assigned to the triplet-triplet transition of the dyad. Furthermore, at this time window the signal of the KP-like triplet excited state at *ca.* 525 nm [13],[36] was not observed. This could mean that it is not formed during the process or that it is indeed formed, but it disappears at a shorter timescale. Thereby, ultrafast transient absorption spectroscopy was used to analyze the sub-nanosecond processes. For an ethanolic solution of KP alone, the characteristic singlet–singlet transition at 580 nm was observed; after

a few picoseconds an intersystem crossing process with the formation of the triplet excited state absorbing at 525 nm was also noticed (Figure 17).[37] By contrast, the 525 nm species was hardly detected in the case of AB–KP (Figure 17, inset). This is in agreement with the accepted mechanism involved in the uncaging of compounds using phenacyl as PPG.[32] After light absorption, the triplet excited state of the phenacyl chromophore of the dyad abstracts hydrogen from the solvent, and subsequently releases KP or DF. Once released, KP and DF are protected by the AB enolic and AB diketo form, respectively, which absorb much more efficiently UVA and UVB light, thus avoiding excitation of the drug.

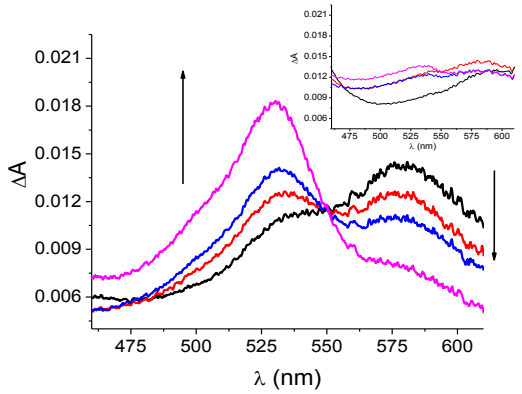

Figure 17. Transient absorption spectra in the femtosecond time scale of KP and AB–KP (inset) from 3.1 to 15.8 ps after pump excitation.

4. Conclusions

To conclude, the work presented in this chapter has demonstrated that it is possible to develop photocages for protection and controlled release of the photosensitive pharmaceutical active principles upon light exposure. The concept has been proven using sunscreen-based photocages for topical drugs ((*S*)-ketoprofen and diclofenac). Since both ingredients are registered compounds already

in use, the pro-drug/pro-filter concept could be eventually brought to practical application in a time- and cost-efficient way.

5. Experimental Section

5.1. Synthesis and Characterization

5.1.1. General Procedures for Synthesis of AB-KP dyad

5.1.1.1. Synthesis of 2-bromo-1-(4-(*tert*-butyl)phenyl)-3-(methoxyphenyl)-propane-1,3-dione (AB-Br).

Two solids, avobenzone (AB, 1 g, 3.2 mmol) and *N*-bromosuccinimide (0.57 g, 3.2 mmol) were mashed under solvent free conditions in a mortar for 10 minutes. The mixture was left stand for 2 hours and then, crushed each 15 minutes during 2 h. Then, water was added and the solution was filtered under vacuum. The solid was left overnight to dry up. Purification was performed by flash chromatography using hexane:ethyl acetate as eluent (6:1, v:v). Colorless crystals of AB-Br were obtained (0.94 g) in a 76% yield.

Characterization AB-Br:

^{1}H NMR (300 MHz, D_2O) δ: 7.99 (d, 2H, J=9Hz), 7.93 (d, 2H, J=9Hz), 7.46 (d, J=6Hz, 2H), 6.92 (d, *J* = 6Hz, 2H), 6.47 (s, 1H), 3.86 (s, 3H), 1.32 ppm (s, 9H).

^{13}C NMR (75 MHz, D_2O) δ: 188.7 (CO), 187.7 (CO), 164.4 (C), 158.2 (C), 131.9 (CH), 131.3 (C), 129.3 (CH), 126.8 (C), 126.1 (CH), 114.3 (CH), 55.7 (CH_3), 53.3 (CH), 35.3 (C), 31.0 ppm (CH_3).

HMRS (ESI-TOF): *m/z*, $[M+H]^+$ Calculated for $C_{20}H_{22}O_3Br$: 389.0752 found: 389.0753.

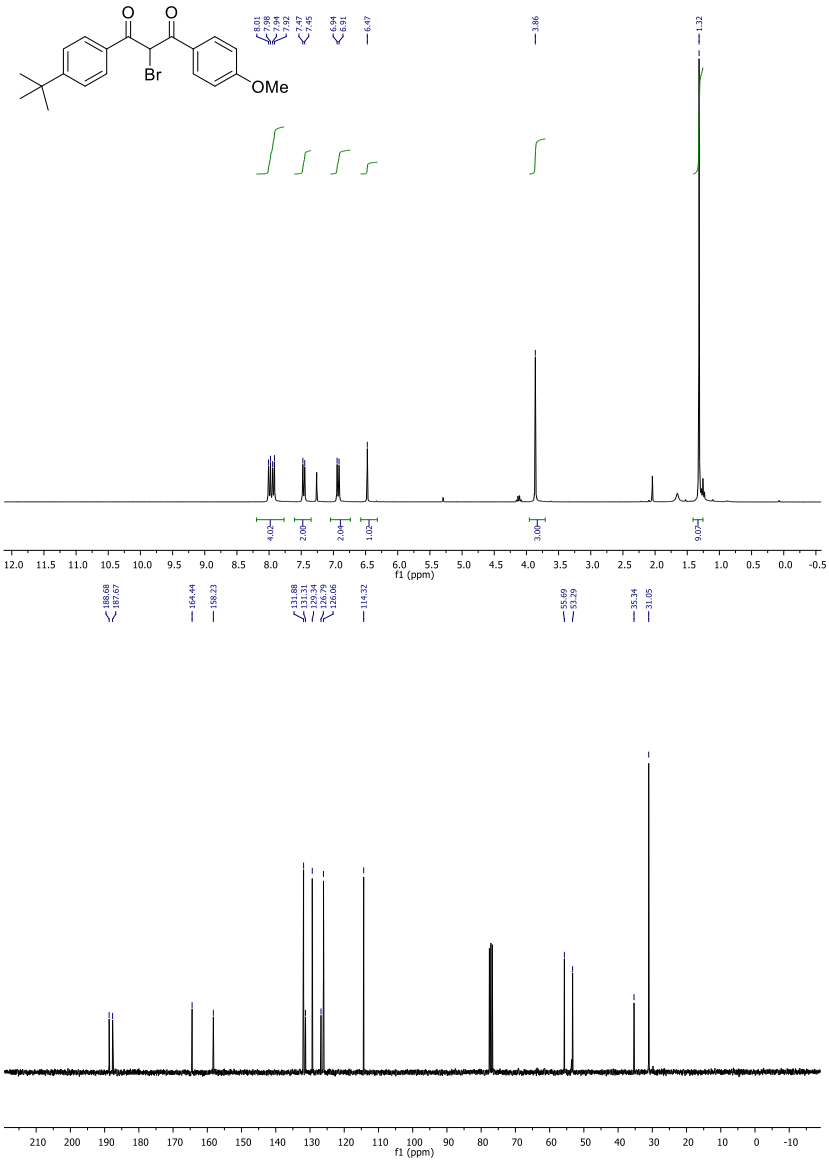

5.1.1.2. Synthesis of 1-(4-(*tert*-butyl)phenyl)-3-(4-methoxy- phenyl)-1,3-dioxoprop-2-yl (2S)-2-(3-benzoylphenyl)propanoate (AB-KP).

First, cesium (*S*)-ketoprofen salt was formed by titration of a (*S*)-ketoprofen water solution (8 mM) against a cesium carbonate water solution (4 mM) until pH stabilized at 7. Then, this salt (0.498 g,

1.29 mmol) dissolved in 5 mL of dimethylformamide was added to a flask containing AB-Br (0.2 g, 0.52 mmol). After 17 hours of stirring, the reaction turned orange. The solvent was directly evaporated and the reaction was purified by flash chromatography, hexane:ethyl acetate, (7:1, v:v). The product, a yellowish solid, was obtained as a diastereoisomeric mixture in a 63% yield (0.18 g).

Characterization of AB-KP:

^{1}H NMR (300 MHz, D_2O) δ: 7.94-6.79 (m, 18H), 4.00 (q+q, J=7.1 Hz, 1H), 3.81 (s+s, 3H), 1.61 (d+d, *J* = 7.1 Hz, 3H), 1.28 ppm (s, 9H).

^{13}C NMR (75 MHz, D_2O) δ: 196.4 (CO), 196.3 (CO), 190.4 (CO), 190.3 (CO), 189.0 (CO), 172.4 (CO), 172.3 (CO), 164.3 (C), 158.1 (C), 158,0 (C), 139.8 (C), 138.0 (C), 137.9 (C), 137.4 (C), 132.5 (CH), 132.1 (CH), 132.0 (CH), 131.8 (CH), 131.7 (CH), 131.6 (C), 131.5 (C), 130.1 (CH), 129.6 (CH), 129.5 (CH), 129.1 (CH), 128.7 (CH), 128.3 (CH), 127.2 (C), 127.1 (C), 125.6 (CH), 113.9 (CH), 81.2 (CH), 81.1 (CH), 55.5 (CH_3), 45.2 (CH), 45.1 (CH), 35.2 (C), 30.9 (CH_3), 18.1 (CH_3).

HMRS (ESI-TOF): *m/z*, $[M+Na]^+$ Calculated for $C_{36}H_{34}O_6Na$: 585.2253, found: 585.2256.

The presence of two diastereoisomers was confirmed by HPLC using a chiral column Kromasil 5-AmyCoat (4.6 x 250 mm, 5µ). The mobile phase was an isocratic mixture of hexane:isopropanol (80:20, v:v) at a flow rate of 0.7 mL/min; the detection wavelength was fixed at 260 nm. The AB-KP isomers (*R,S*) and (*S,S*) were present in 1:1 proportion (see chromatogram below).

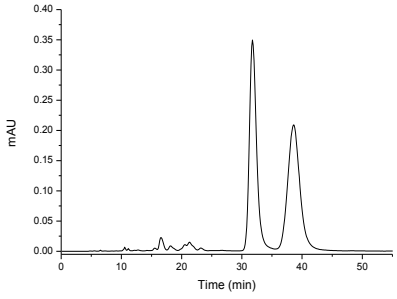

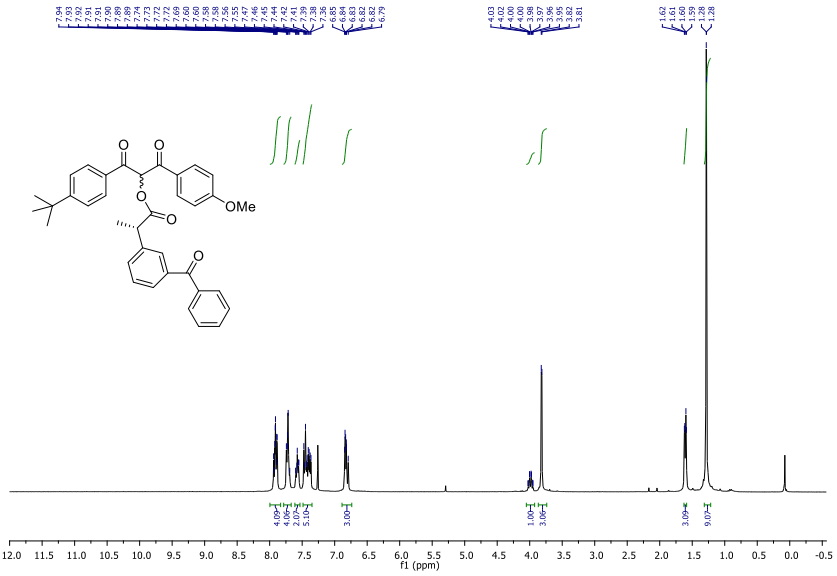

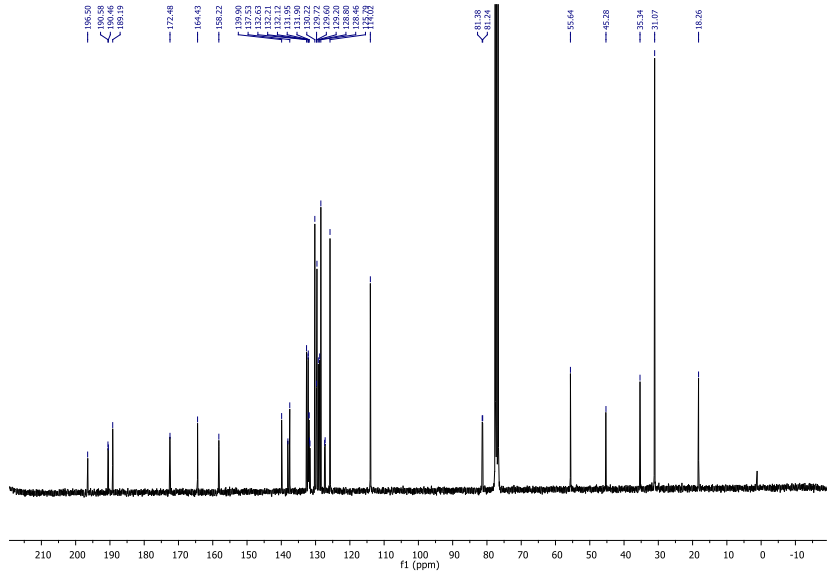

5.1.2. General Procedures for Synthesis of AB-DF dyad

5.1.2.1. 1-(4-(*tert*-butyl)phenyl)-3-(4-methoxyphenyl)-1,3-dioxopropan-2-yl 2-(2-((2,6 dichlorophenyl)-amino)phenyl)acetate (AB-DF)

To a solution of AB-Br (0.18 g, 0.515mmol) in DMF under inert atmosphere, commercial sodium diclofenac salt was added

(0.18 g, 0.567 mmol) and it was stirred at r.t. for 22 hours. The DMF was evaporated under vaccum and the dyad was purified by column flash chromatography using hexane:ethyl acetate (9:1, v:v) as eluent. The enantiomeric mixture of AB-DF was obtained in 50% yield as a yellowish solid.

Characterization of AB-DF:

^{1}H NMR (300 MHz, $CDCl_3$) δ: 8.01 (d, *J* = 9Hz, 2H), 7.96 (d, J = 6Hz, 2H), 7.42 (d, *J* = 9Hz, 2H), 7.31 (d, *J* = 9Hz, 2H), 7.24 (dd, J = 6Hz, J = 1Hz, 1H), 7.13 (m, 1H), 6.98 (d, J = 9Hz, 2H), 6.94 (s, 1H), 6.86 (d, *J* = 9Hz, 2H), 6.54 (dd, J = 9Hz, J = 1Hz, 1H), 6.46 (bs, 1H), 4.03 (s, 2H), 3.83 (s, 3H), 1.30 (s, 9H).

^{13}C NMR (75 MHz, $CDCl_3$) δ: 190.5 (CO), 189.2 (CO), 170.7 (COO), 164.4 (C), 158.2 (C), 143.0 (C), 138.2 (C), 132.2 (2CH), 131.8 (C), 131.2 (CH), 129.7 (2 C), 129.6 (2 CH), 128.9 (2 CH), 128.3 (CH), 127.4 (C), 125.8 (2 CH), 124.4 (C), 124.1 (CH), 122.6 (CH), 119.1 (CH), 114.1 (2 CH), 81.2 (CH, diketonic), 55.6 (CH3, -OMe), 38.2 (CH_2), 35.3 (C), 31.1 (3 CH_3).

HMRS (ESI-TOF): *m/z*, $[M+H]^+$ Calculated for $C_{34}H_{31}Cl_2NO_5$: 604.1658 found: 604.1660.

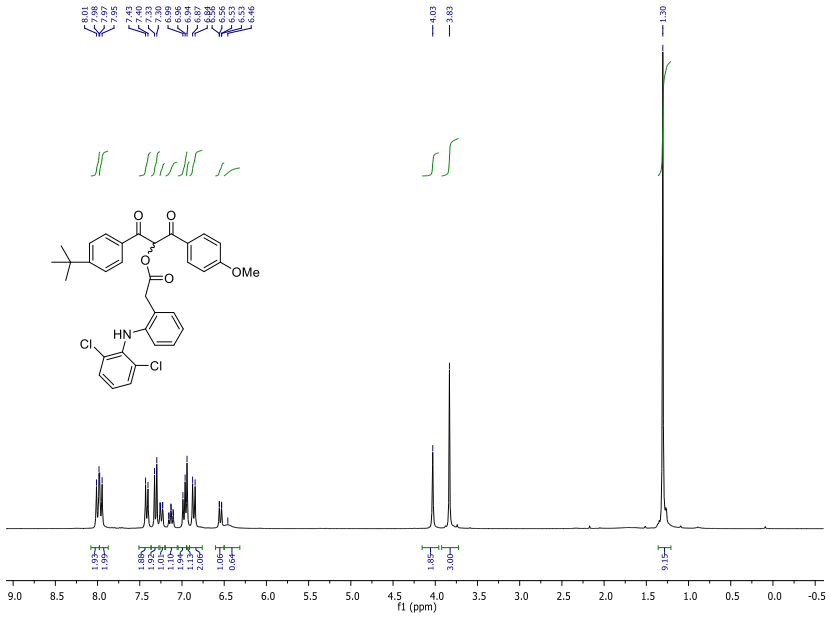

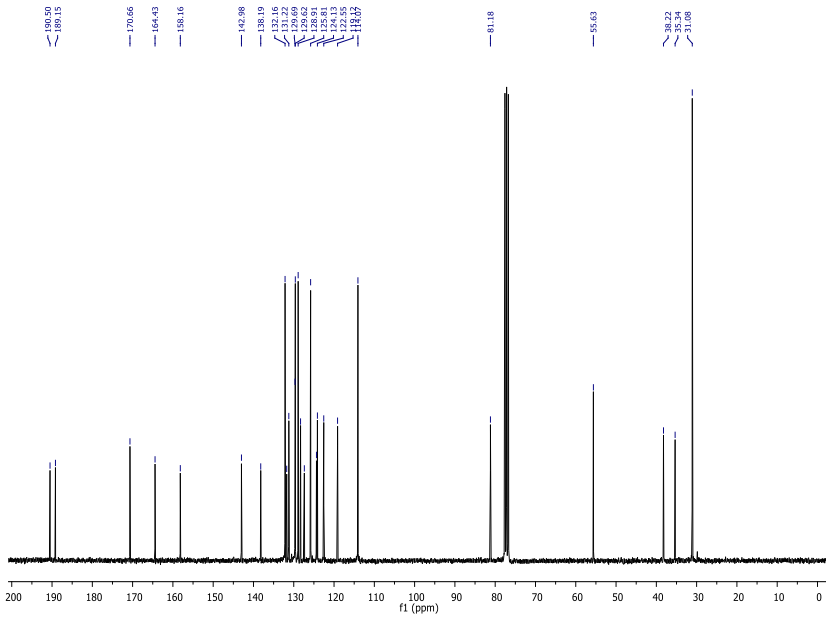

6. References

[1] V. Lhiaubet-Vallet, M. A. Miranda, "Phototoxicity of drugs", In *CRC Handbook of Organic Photochemistry and Photobiology*, *Third Ed. - Two Vol. Set*, Editors: A. Griesbeck, M. Oelgemöller, F. Ghetti, **2012**, 66, 1541-1556.

[2] M. A. Miranda, "Química de la fotosensibilización por fármacos," *An. R. Soc. Esp. Quím.*, **2005**, 43–48.

[3] A. Lahoz, D. Hernández, M. A. Miranda, J. Pérez-Prieto, I. M. Morera, and J. V. Castell, "Antibodies directed to drug epitopes to investigate the structure of drug-protein photoadducts. Recognition of a common photobound substructure in tiaprofenic acid/ketoprofen cross-photoreactivity," *Chem. Res. Toxicol.*, **2001**, 14, 1486–1491.

[4] S. Encinas, F. Bosca, and M. A. Miranda, "Phototoxicity associated with diclofenac: a photophysical, photochemical, and photobiological study on the drug and its photoproducts,"

Chem. Res. Toxicol., **1998**, 11, 946–952.

[5] F. Bosca, M. L. Marín, and M. A. Miranda, "Photoreactivity of the nonsteroidal anti-inflammatory 2-arylpropionic acids with photosensitizing side effects," *Photochem. Photobiol.,* **2001**, 74, 637–655.

[6] M. C. Cuquerella, V. Lhiaubet-Vallet, F. Bosca, and M. A. Miranda, "Photosensitised pyrimidine dimerisation in DNA," *Chem. Sci.*, **2011**, 2, 1219-1232.

[7] V. Lhiaubet-Vallet, F. Bosca, and M. A. Miranda, "Photosensitized DNA damage: the case of fluoroquinolones," *Photochem. Photobiol.*, **2009**, 85, 861–868.

[8] J. Montoro, M. Rodríguez, M. Díaz and F. Bertomeu, "Photoallergic contact dermatitis due to diclofenac," *Contact Derm.*, **2003**, 46, 115–119.

[9] L. Kowalzick and H. Ziegler, "Photoallergic contact dermatitis from topical diclofenac in Solaraze gel, " *Contact Derm.,* **2006**, 54, 348–349 .

[10] L. J. Martínez and J. C. Scaiano, "Transient intermediates in the laser flash photolysis of ketoprofen in aqueous solutions : unusual photochemistry for the benzophenone chromophore," *J. Am. Chem. Soc.*, **1997**, 119, 11066–11070.

[11] M. C. Cuquerella, V. Lhiaubet-Vallet, J. Cadet, and M. A. Miranda, "Benzophenone photosensitized DNA damage," *Acc. Chem. Res.*, **2012**, 45, 1558–1570.

[12] T. Douki, "Formation and repair of UV-induced DNA damage," In *CRC Handbook Organic Photochemistry and Photobioliogy, Third Ed. - Two Vol. Set*, Editors: A. Griesbeck, M. Oelgemöller, F. Ghetti **2012**, 1349–1392.

[13] S. Encinas, F. Bosca, and M. A. Miranda, "Photochemistry of 2,6-dichlorodiphenylamine and 1-chlorocarbazole, the photoactive chromophores of diclofenac, meclofenamic acid and their major photoproducts," *Photochem. Photobiol.*, **1998**, 68, 640–645.

[14] H. Görner, "Photocyclization of 2,6-dichlorodiphenylamines in solution," *J. Photochem. Photobiol. A, Chem.*, **2010**, 211, 1–6.

[15] F. Bosca, S. Encinas, P. F. Heelis, and M. A. Miranda, "Photophysical and photochemical characterization of a photosensitizing drug : a combined steady state photolysis and laser flash photolysis study on carprofen," *Chem. Res. Toxicol.* **1997**, 10, 820-827.

[16] J. Trzcionka, V. Lhiaubet-Vallet, C. Paris, N. Belmadoui, M. J. Climent, and M. A. Miranda, "Model studies on a carprofen derivative as dual photosensitizer for thymine dimerization and (6-4) photoproduct repair," *ChemBioChem*, **2007**, 8, 402–407.

[17] V. Lhiaubet-Vallet, Z. Sarabia, D. Hernández, J. V. Castell, and M. A. Miranda, "In vitro studies on DNA-photosensitization by different drug stereoisomers," *Toxicol. in Vitro*, **2003**, 17, 651–656.

[18] W. Schwack and T. Rudolph, "Photochemistry of dibenzoyl methane UVA filters Part 1," *J. Photochem. Photobiol. B, Biol.*, **1995**, 28, 229-234.

[19] K. Atarashi, M. Takano, S. Kato, H. Kuma, M. Nakanishi, and Y. Tokura, "Addition of UVA-absorber butyl methoxy dibenzoylmethane to topical ketoprofen formulation reduces ketoprofen-photoallergic reaction," *J. Photochem. Photobiol. B, Biol.*, **2012**, 113, 56–62.

[20] P. Klán, T. Šolomek, C. G. Bochet, A. Blanc, R. Givens, M. Rubina, V. Popik, A. Kostikov, and J. Wirz, "Photoremovable protecting groups in chemistry and biology: reaction mechanisms and efficacy," *Chem. Rev.*, **2013**, 113, 119−191.

[21] T. Šolomek, J. Wirz, and P. Klán, "Searching for improved photoreleasing abilities of organic molecules," *Acc. Chem. Res.*, **2015**, 48, 3064−3072.

[22] D. D. Young and A. Deiters, "Photochemical control of biological processes," *Org. Biomol. Chem*., **2007**, 5, 999–1005.

[23] H. Yu, J. Li, D. Wu, Z. Qiu, and Y. Zhang, "Chemistry and biological applications of photo-labile organic molecules," *Chem. Soc. Rev.*, **2010**, 39, 464–473.

[24] A. Herrmann, "Using photolabile protecting groups for the

controlled release of bioactive volatiles," *Photochem. Photobiol. Sci.*, **2012**, 11, 446–459.

[25] C. Bao, L. Zhu, Q. Lin, and H. Tian, "Building biomedical materials using photochemical bond cleavage," *Adv. Mater.*, **2015**, 27, 1647–1662.

[26] M. C. Pirrung, "Spatially addressable combinatorial libraries," *Chem. Rev.*, **1997**, 97, 473–488.

[27] S. Panja, R. Paul, M. M. Greenberg, and S. A. Woodson, "Light-triggered RNA annealing by an RNA chaperone," *Angew. Chem. Int. Ed*., **2015**, 54, 7281–7284.

[28] R. Horbert, B. Pinchuk, P. Davies, D. Alessi, and C. Peifer, "Photoactivatable prodrugs of antimelanoma agent vemurafenib," *ACS Chem. Biol.*, **2015**, 10, 2099−2107.

[29] M. Lukeman and J. C. Scaiano, "Carbanion-mediated photocages : rapid and efficient photorelease with aqueous compatibility," *J. Am. Chem. Soc.*, **2005**, 127 , 7698-7699.

[30] G. Cosa, M. Lukeman, and J. C. Scaiano, "How drug photodegradation studies led to the promise of new therapies and some fundamental carbanion reaction dynamics along the way," *Acc. Chem. Res.*, **2009**, 42, 599-607.

[31] A. Jana, K. T. Nguyen, X. Li, P. Zhu, N. S. Tan, H. Agren, and Y, Zhao, "Organic nanoparticles with tunable emission : efficient anticancer drug carriers with real-time monitoring of drug release," *ACS Nano*, **2014**, 8, 5939–5952.

[32] J. Literák, A. Dostálová, and P. Klán, "Chain mechanism in the photocleavage of phenacyl and pyridacyl esters in the presence of hydrogen donors," *J. Org. Chem.*, **2006**, 71, 713–723.

[33] I. Pravst, M. Zupan, and S. Stavber, "Solvent-free bromination of 1,3-diketones and β-keto esters with NBS," *Green Chem.*, **2006**, 8, 1001–1005.

[34] C. Paris, V. Lhiaubet-Vallet, O. Jiménez, C. Trullas, and M. A. Miranda, "A blocked diketo form of avobenzone: Photostability, photosensitizing properties and triplet quenching by a triazine-derived UVB-filter," *Photochem.*

Photobiol., **2009**, 85, 178–184.

[35] M. Yamaji, C. Paris, and M. A. Miranda, "Steady-state and laser flash photolysis studies on photochemical formation of 4-tert-butyl-4′-methoxydibenzoylmethane from its derivative via the Norrish Type II reaction in solution," *J. Photochem. Photobiol. A, Chem.*, **2010**, 209, 153–157.

[36] V. Lhiaubet-Vallet, N. Belmadoui, M. J. Climent, and M. A. Miranda, "The long-lived triplet excited state of an elongated ketoprofen derivative and its interactions with amino acids and nucleosides," *J. Phys. Chem. B*, **2007**, 111, 8277-8282.

[37] T. Suzuki, T. Okita, Y. Osanai, and T. Ichimura, "Reaction dynamics of excited 2-(3-benzoylphenyl) propionic acid (ketoprofen) with histidine," *J. Phys. Chem. B*, **2008**, 112, 15212–15216.

Chapter 6:

Photosafety assessment by photosensitizing studies on AB-KP dyad

1. Introduction

The interaction between sunlight and living organisms may lead to both beneficial and damaging effects. On the one hand, solar energy is needed for the normal development of life or can even be used for therapeutic purposes, but, on the other hand, it is responsible for undesired photosensitization processes. In this context, the increasing incidence of skin cancer has been associated with excessive sun exposure that might produce chemical changes on the DNA molecules, the so-called photogenotoxicity. [1], [2]

Indeed, new chemicals with therapeutic or cosmetic applications that are systemically or topically applied need to undergo a photosafety test in order to assess their photosensitizing potential. Since 2000 *in vivo* testing experiments in animals are no longer permitted. Therefore, efforts have been conducted to develop new strategies as an alternative to animal test methods. These alternatives are *in vitro* and *in chemico* tests as well as *in vivo assays* on human volunteers. The *in chemico* tests consist in the evaluation of the potential generation of ROS by the chemical compounds and their subsequent ability of inducing DNA strand breaks by using DNA plasmids. [3], [4]

In Chapter 5, a new strategy has been developed to take advantage of sunlight for slow release of photosensitizing topical NSAIDs together with their protective shield.[5],[6] Thus, the next step is to evaluate the photosafety of this new pro-drug/pro-filter compound by studying its photosensitizing potential on key biomolecules such a fatty acid, as model of membrane components, or DNA by *in chemico* and *in vitro* tests, respectively.

In this context, peroxidation of polyunsaturated fatty acids plays a crucial role in many oxidative processes in humans [7],[8],[9] and is considered as the basis of alterations of the membrane structure.[10] The key step of lipid peroxidation through a type I

mechanism is exemplified by hydrogen abstraction of the allylic H atoms of linoleic acid that leads to the four conjugated dienic hydroperoxides 13-hydroxyperoxide-*cis*-9, *trans*-11-octadecadienoic acid (LA1), 9-hydroxyperoxide-*trans*-10, *cis*-12-octadecadienoic acid (LA2), 9 hydroxyperoxide-*trans*-10, *trans*-12-octadecadienoic acid (LA3), 13-hydroxyperoxide-*trans*-9, *trans*-11-octadecadienoic acid (LA4) (Scheme 1). By contrast, Type II processes involve cycloaddition and "ene" reaction, which finally give rise to the *cis,trans* isomers LA1 and LA2 together with two non conjugated dienic hydroperoxides LA5 and LA6 (Scheme 2).[11],[12] The photoperoxidation of LA is easily followed by means of UV-vis absorption by monitoring the band with maximum centered at 233 nm, which corresponds to the conjugated dienic hydroperoxides absorption.

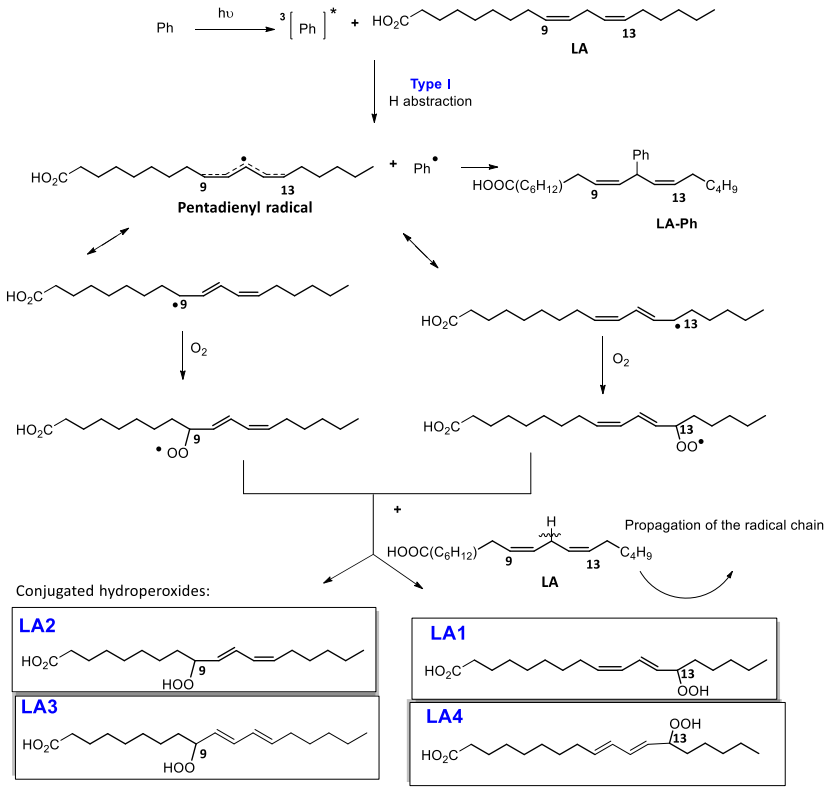

Scheme 1. Type I mechanism for photoperoxidation of linoleic acid.

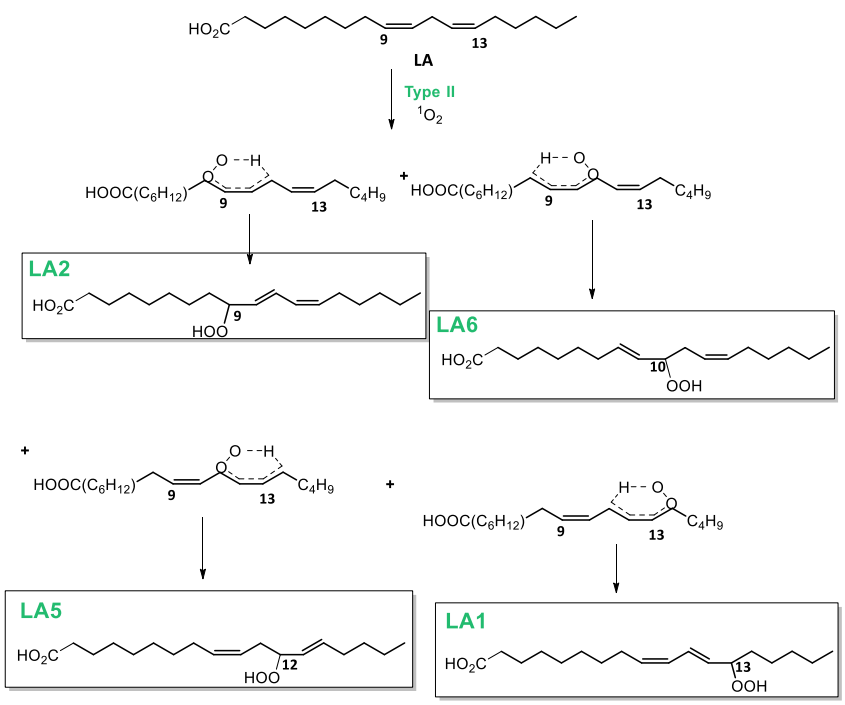

Scheme 2. Type II mechanism for photoperoxidation of linoleic acid.

After taking into account the damage photogenerated onto membrane components, the attention has been centered on the photogenotoxic potential of AB-KP on cellular DNA. Over the years, the comet assay, also known as single cell gel electrophoresis (SCGE) has become one of the standard methods for assessing DNA damage. The assay is attractive for its simplicity, sensitivity, versatility, speed and economy. The first approach was performed by Ostling and Johanson in 1984, who took advantage of the methodology of cell lysis described by Cook and colleagues.[13]

Indeed, comet assay involves lysis after embedded the cell in agarose gel, allowing this way to immobilize the DNA for its subsequent electrophoresis. The increased DNA break frequency increases the tail intensity, while undamaged molecules stay in the head of the comet (Figure 1). Over the years a protocol has been established which is described in Annex I.

Although the assay can be performed under neutral conditions, the alkaline procedure at pH > 10 is the most commonly adopted, and allows the detection of alkali-labile lesions as well as single and double strand breaks.

The agarose gel electrophoresis technique relies on the different migration of the different size and form of embedded DNA. Indeed, when an electric field is applied, the negatively charged DNA molecules migrate toward the anode. The original DNA moves slower than the broken fragments, thus under neutral conditions only double strand breaks are detected. However, alkaline conditions denature the helix allowing single strand breaks quantitation. The information can be completed by the use of endonuclease to reveal specific lesions. Oxidized purines are for example revealed using formamido pyrimidine DNA glycosylase (Fpg), oxidized pyrimidine are recognized by endonuclease III or cyclobutane pyrimidine dimers evidenced by using the T4 endonuclease V.

Thus, the comet head contains the high-molecular-weight DNA and the comet tail contains the fragments ends, which migrate more efficiently. More concretely, the more genotoxic a chemical is, the more DNA is denaturized and broken, hence, more free DNA fragment ends are able to migrate, and therefore a larger fraction of the DNA moves away from the comet head.

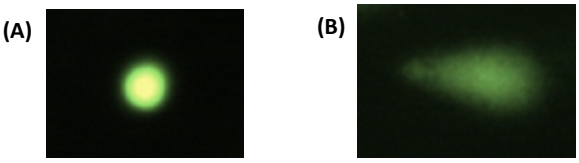

Figure 1. (A) Intact FSK cell Comet. (B) Damaged FSK cell Comet.

Hence, a photosensitizing assessment in the safety evaluation of new chemical compounds is essential. In this chapter, the photosensitizing assessment of AB-KP dyad and other related compounds is addressed on key biomolecules such as fatty acids using *in chemico* test, and DNA by *in vitro* test, by means of the Comet assay.

2. Aims

The main objective of this chapter is to assess the photosafety of the new pro-drug/pro-filter compound, AB-KP, by studying its photosensitizing potential on key biomolecules such a fatty acid, as model of membrane components, or DNA by *in chemico* and *in vitro* tests, respectively.

For this, it is necessary to pursue the following specific aims:

- To study the AB-KP photophysical properties in a non-polar solvent with H-donating properties to approach the lipophilic media that can be found in biological environment.

- To synthesize the methyl ester of KP in order to mimic the coupling in the dyad between KP and AB, blocking the well-described photodecarboxylation that the KP free acid suffers.

- To evaluate the ability of the dyad AB-KP to damage linoleic acid, as a mimic of cellular membrane, by *in chemico* test and cellular DNA by *in vitro* test, namely the comet assay.

3. Results

3.1. AB-KP photophysical properties in non-polar solvent with H-donating properties

In the previous chapter, polar solvents with H-donating properties such as ethanol or propylene glycol were used to study the photophysics of AB-KP and the photorelease of its active ingredients.[5] In this chapter, interesting results were obtained using the non polar solvent cyclohexane. First, the absorption spectra of AB-KP exhibited a weak bathochromic shift of the maximum when changing the solvent from ethanol to cyclohexane as expected for $\pi\pi^*$ transitions (Figure 2). By contrast, the shoulder, observed at

longer wavelengths, was displaced to the blue, and it was more defined when cyclohexane was used as solvent (Figure 2, inset). These results are in agreement with the nπ* nature of the UVA transition.

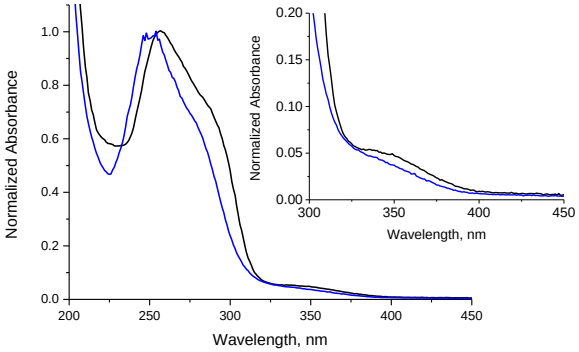

Figure 2. Normalized UV-Vis absorption spectra of AB-KP in cyclohexane (black) and ethanol (blue). Inset: zoom of the absorption in the 300-450 nm range.

Then, laser flash photolysis experiments were performed by means of a nanosecond pulsed laser (Nd:YAG) using 355 nm as excitation wavelength. Interestingly, different transient spectra were monitored for deaerated solutions of AB-KP prepared in ethanol or cyclohexane (Figure 3). In EtOH, a transient species with a maximum at 400 nm was observed and assigned to the triplet-triplet transition of the avobenzone-like moiety in its diketo form. These bands decreased in a sub μs timescale without giving rise to the appearance of new species. In cyclohexane, AB-KP exhibited another photobehavior. An important negative band was present at ca. 350 nm together with weak positive band at *ca.* 520 nm. This band was similar to the well-established T-T transition of KP. A weak transient absorption is also present at *ca.* 400 nm as expected for the triplet excited state of AB in its diketo form.

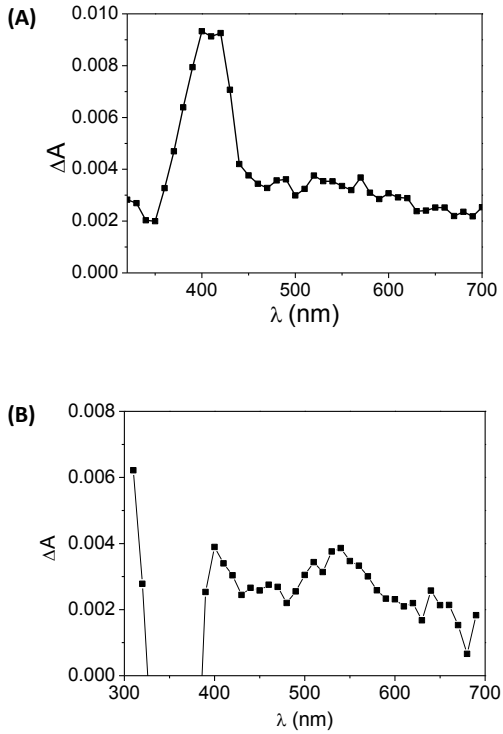

Figure 3. Transient absorption spectra of AB-KP in EtOH (A), and cyclohexane (B) obtained 0.08 μs after the 355 nm laser pulse.

The photorelease was proposed to take place from the triplet excited state of the phenacyl-like moiety of the dyad, *ie.* the AB in its diketo form. Thus, detection of both triplet excited state might questioned the efficiency of the photoreaction in this solvent. However, the UVA irradiation of AB-KP in cyclohexane showed that the photorelease is effective as the characteristic UVA band of AB is increasing as a function of irradiation time (Figure 4A). This photobehavior is very close to that observed for EtOH (Figure 4B). This interesting result supports that the presence of these triplet excited states with very close energies does not avoid the photorelease to occur.

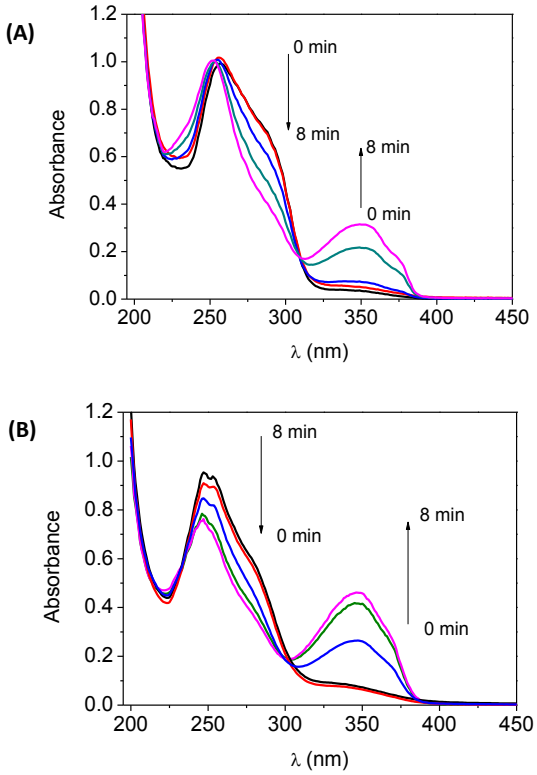

Figure 4. UV absorption changes for AB–KP in deaerated cyclohexane (A) or ethanol (B) under UVA irradiation (from 0 to 8 min).

Moreover, the nature of the triplet excited state is of paramount importance in photosensitization processes.[14],[15],[16] On the one hand, it is now well-established that benzophenone-like compounds, such as KP, are able to damage biomolecules by triplet excited state mediated Type I and Type II mechanisms.[14],[16] In addition, the potential of the diketo AB to react with biological components has also been reported.[17] On the other hand, the proposed photorelease process involves H abstraction from the solvent by the excited phenacyl-like moiety.[5],[18],[19],[20] Thus, biological substrates can also play the role of the H donor, leading to the subsequent formation of oxidation products.

3.2. Evaluation of the photosensitizing properties of AB-KP dyad

Taking into account these data, the photoinduced oxidation of cellular membrane was evaluated. In this context, linoleic acid (LA) has been largely used as a model polyunsaturated fatty acid because its oxidation to conjugated hydroperoxides is easily followed by UV-vis absorption. Thus, solutions of AB-KP, KP and KPMe (10^{-5} M) were UVA-irradiated in the presence of LA (10^{-3} M) for 2, 5, 10, 15 and 20 min. As shown in Figure 5A for KP, under irradiation the characteristic band of the conjugated hydroperoxide of LA, centered at λ=233 nm, increased as a function of irradiation time. Similar behavior was observed for AB-KP and KPMe (see experimental section). The relative intensity changes of this 233 nm band are represented in Figure 5B, this demonstrated that the three compounds are able to photooxidize LA in a similar way.

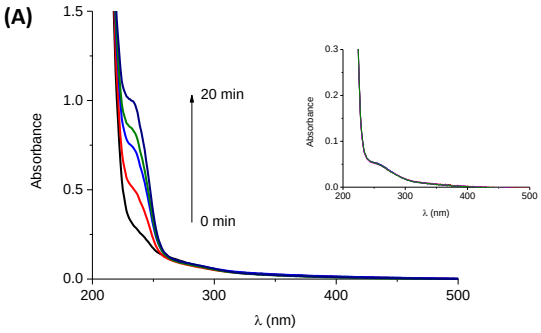

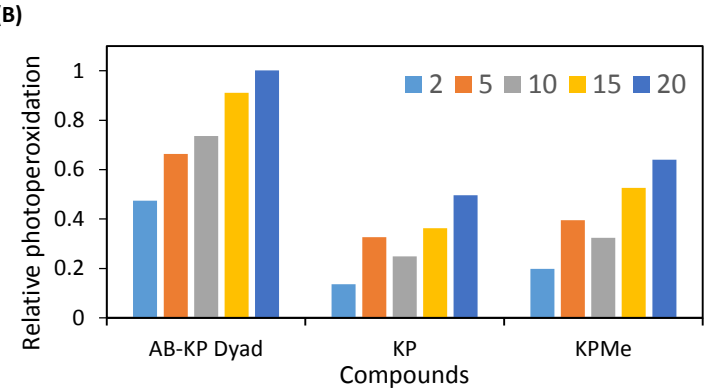

Figure 5. Photodynamic lipid peroxidation by the dyad AB-KP, KP and KPMe. (A) Absorption changes observed for a solution of LA (10^{-3}M) and KP (10^{-5} M) in PBS/SDS (10^{-2}M) irradiated in the UVA and diluted 4 times. Inset: KP irradiated alone. (B) Relative absorbance changes at 233 nm used as diagnostic for lipid photoperoxidation for AB-KP, KP and KPMe. For each compound, the values of the control of the compound alone together with that of LA irradiated alone were subtracted from the values of the irradiated mixture LA+compound.

Then, the ability of the dyad AB-KP to damage cellular DNA was evaluated and compared to that of KP and KPMe. Thus, the alkaline comet assay was performed in order to analyze the photogenotoxicity of the compounds at the level of the individual cell. Briefly, the principle is based on the imaging of the DNA migration in an agarose matrix under electrophoretic conditions. The resulting image resembles a “comet” with a distinct head and tail. In the alkaline version, the head is composed of intact DNA, while the tail consists of the DNA damage resulting from single- and double strand breaks as well as alkali-labile sites. The extent of DNA present in the tail is diagnostic to the amount of DNA damage.

Thus, fibroblast cells (FSK) were seeded in 12-well plates, incubated with the different compounds (50 µM) and irradiated for 5 minutes (2.27 J cm^{-2}) with UVA light. Then, the cells were embedded in agarose gel and drop off on slides, which were treated overnight with a lysis solution. An alkaline electrophoresis was performed and

the comets were revealed using SYBR GOLD as fluorescent DNA intercalant dye.[21] The results were interpreted following visual scoring, using a scale ranging from 0 (non damaged cell) to 6 (highly damaged cell).[22] The obtained images are shown in Figure 6. All the unirradiated samples kept a round shape, which thus discard dark genotoxicity of the studied compounds. In this experiment, FSK cells without any chemical were used as negative control, no changes were detected for samples exposed or not to the UVA radiation; thus, no directly photoinduced damages are generated under the used conditions (Figure 6 and 7). By contrast, comets with an important tail and almost no head and corresponding to form 4 and 5 in the visual scale analysis) were observed for samples irradiated in the presence of (*S*)-KP (Figure 6 and 7), which was used as the positive control due to its previously described photoactivity.[23] The methyl ester derivative of this drug presented a somewhat lower damaging potential than the free acid (Figure 6 and 7), scoring of 2 and 3 in the visual scale analysis). By contrast, a very low yield of DNA damage was detected for the AB-KP dyad, which exhibits a weak tail migration.

The total comet scores determined from the formula given in Materials and Methods section are summarized in Figure 7. The observed photogenotoxicity can be classified as follows: (S)-KP > KPMe > AB-KP.

In the case of KPMe, the lower DNA damage by respect with free carboxylate form could be attributed to a higher lipophilicity of the ester derivative, preventing its diffusion until the nuclear DNA.

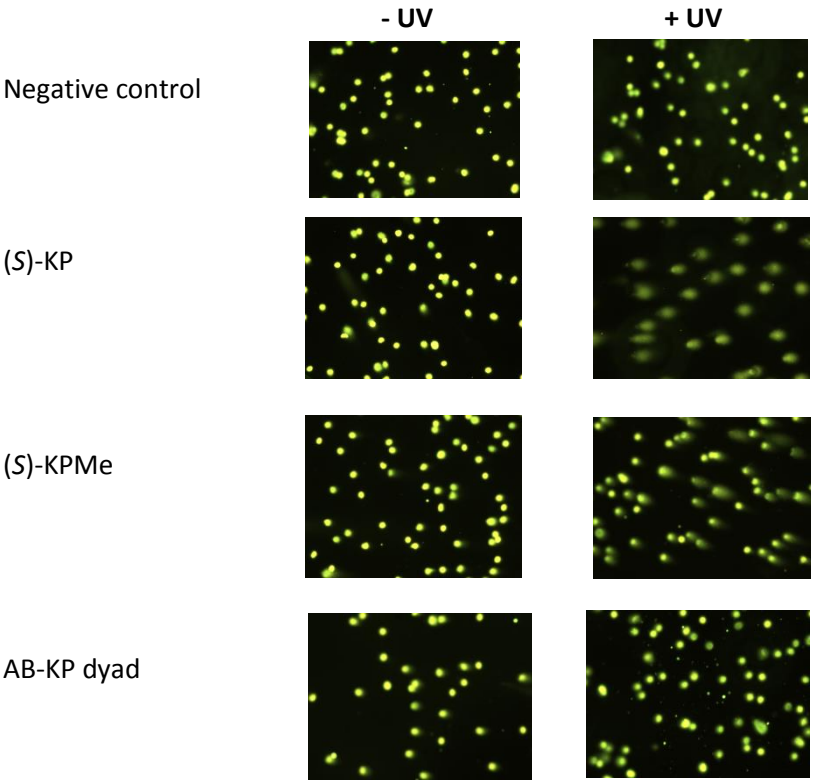

Figure 6. UV-induced direct stand breaks in nuclei of fibroblast detected by comet assay technique. Photomicrographs of typical DNA migration patterns for unexposed cells and UVA-exposed cells (2.27 J/cm^2) with the different compounds.

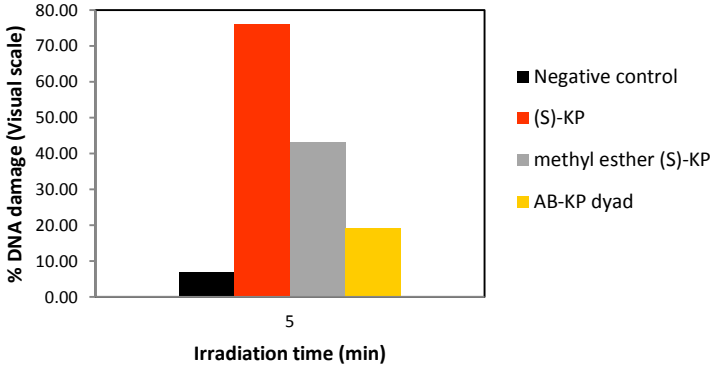

Figure 7. DNA damage quantitation by visual scale analysis of fibroblast exposed to UVA irradiation of different experimental conditions (DNA control in black, (*S*)-KP in red, (*S*)-KPMe in grey, AB-KP dyad in yellow).

4. Conclusions

A photosafety assessment of the photoactivatable dyad AB-KP has been accomplished in this chapter in order to guarantee its harmlessness towards the DNA.

The photophysical study performed by laser flash photolysis of KP-AB dyad revealed a transient absorption spectrum showing a band *ca.* 530 nm in cyclohexane which has been assigned to the triplet excited state of KP and not that of the AB in its diketo form. By contrast, the transient absorption spectrum in ethanol shows a band at 400 nm that corresponds to AB in its diketo form.

Moreover, the impact on the cellular membrane has been addressed by UVA irradiation of linoleic acid solutions in the presence of the dyad. The phototoxic potential of the AB-KP dyad has been confirmed by UV-Vis spectrophotometry through the formation of the conjugated dienic hydroperoxides derived from linoleic acid.

Finally, the comet assay experiments demonstrate that AB-KP dyad does not exhibit a photogenotoxic potential towards cellular DNA since the non-damaged round shape of the cell is still observed after UVA irradiation, if compared to that of KP.

5. Experimental section

5.1. Synthesis of methyl ester (S)-ketoprofen

(*S*)-Ketoprofen (0.2 g) was dissolved in methanol (0.491 M, 1.61 mL) and a catalytic amount of sulfuric acid was added (0.79 mmol, 43 µL).[24] It was stirred overnight for 20 hours at a reflux temperature. Work up: the reaction mixture was evaporated in vaccum and the crude was purified by column flash chromatography CH_2Cl_2:MeOH (98:2, v:v). The methyl ester of (*S*)-ketoprofen (KPMe) was obtained as transparent oil in a 92 % yield (0.1931 g).

Characterization of methyl ester (S)-KP.

^{1}H NMR (300 MHz, $CDCl_3$) δ: 7.78 (m, 3H), 7.67 (m, 1H), 7.56 (m, 2H), 7.45 (m, 3H), 3.80 (q, *J* = 9 Hz, 1H), 3.66 (s, 3H), 1.53 (d, *J* = 9 Hz, 3H).

^{13}C NMR (75 MHz, $CDCl_3$) δ: 196.45 (CO), 174.54 (COO), 140.92 (C), 138.00 (C), 137.58 (C), 132.55 (CH), 131.55 (CH), 130.11 (2CH), 129.26 (CH), 129.05 (CH), 128.61 (CH), 128.35 (2CH), 52.17 (CH), 45.33 (CH_3), 18.56 (CH_3).

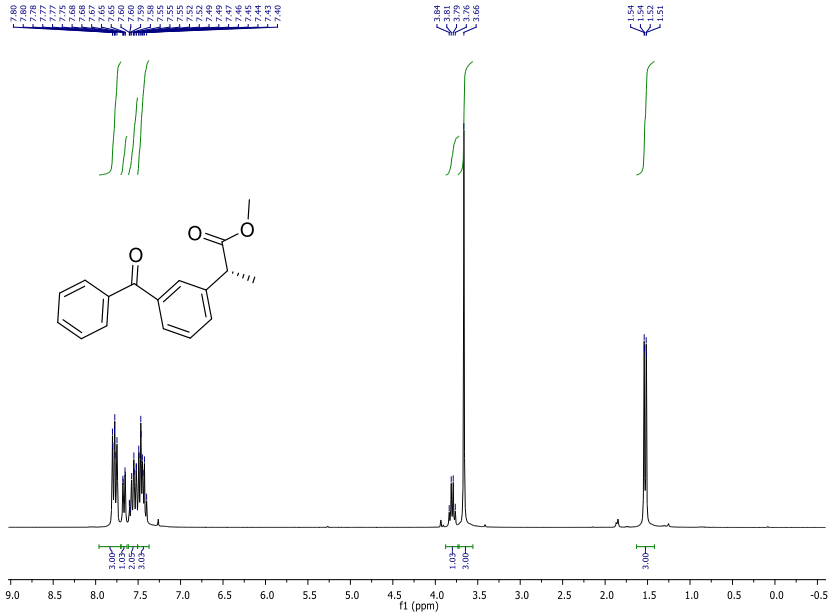

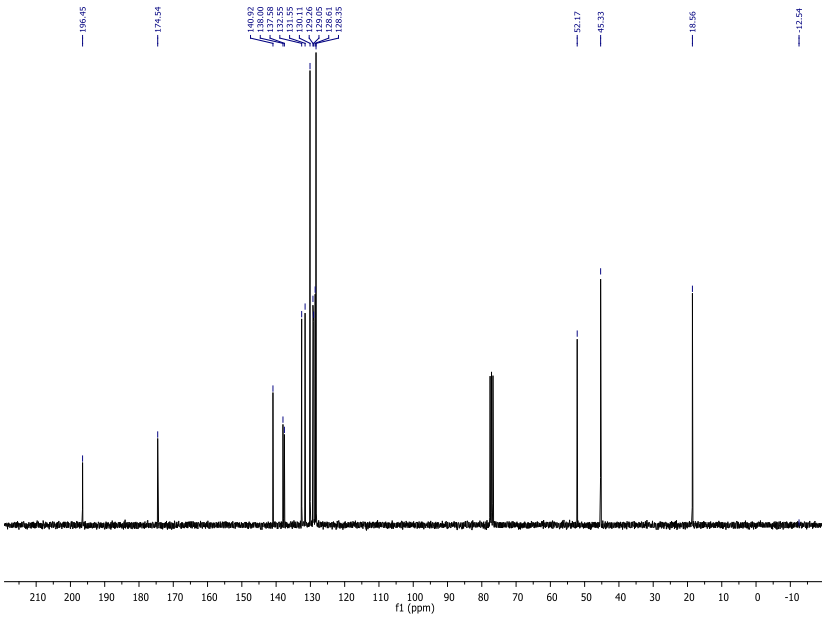

5.2. Lipid peroxidation experiment

Solutions of linoleic acid (10^{-3}M) with the photosensitizer (10^{-5}M) were prepared was in PBS with SDS (10^{-2}M). A UVA irradiation at 355 nm was carried out, and each solution was incubated 30 min in the dark. Then, solutions were diluted 4 times and their absorption was determined @233 nm to follow the lipid peroxidation process. Control solutions, which contain the different compounds without linoleic acid as well as solutions of linoleic acid alone, were irradiated under identical conditions.

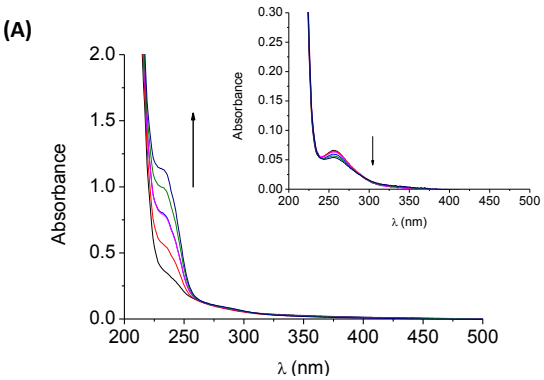

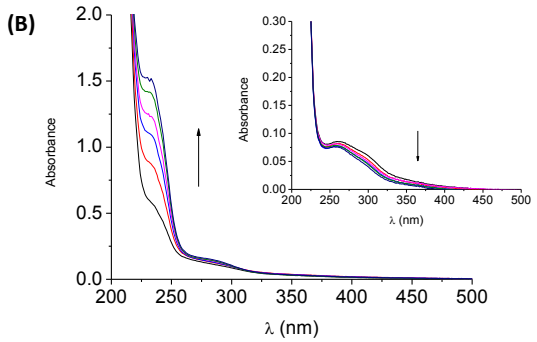

Figure 8. (A) Absorption changes observed for a solution of LA (10^{-3}M) and KPMe (10^{-5} M) in PBS/SDS (10^{-2}M) irradiated in the UVA and diluted 4 times. Inset: KPMe irradiated alone. (B) Absorption changes observed for a solution of LA (10^{-3}M) and AB-KP (10^{-5} M) in PBS/SDS (10^{-2}M) irradiated in the UVA and diluted 4 times. Inset: AB-KP irradiated alone.

6. References

[1] Skin cancer trends. https://www.cdc.gov/cancer/skin/statistics/trends.htm (accessed 22/02/2018).

[2] R. L. Siegel, K. D. Miller, and A. Jemal, "Cancer statistics, 2018," *CA. Cancer J. Clin.*, **2018**, 68, 7–30.

[3] L. R. Gaspar, J. Tharmann, P. M. B. G. Maia Campos, and M. Liebsch, "Skin phototoxicity of cosmetic formulations containing photounstable and photostable UV-filters and vitamin A palmitate," *Toxicol. in Vitro*, **2013**, 418–425.

[4] K. Kim, H. Park, and K. M. Lim, "Phototoxicity: its mechanism and animal alternative test methods," *Toxicol. Res.*, **2015**, 31, 97–104.

[5] I. Aparici-Espert, M. C. Cuquerella, C. Paris, V. Lhiaubet-Vallet, and M. A. Miranda, "Photocages for protection and controlled

release of bioactive compounds," *Chem. Commun.*, **2016**, 52, 14215–14218.

[6] I. Aparici-Espert, M. A. Miranda, and V. Lhiaubet-vallet, "Sunscreen-based photocages for topical drugs: A photophysical and photochemical study of a diclofenac-avobenzone dyad," *Molecules*, **2018**, 23, 673.

[7] F. Shahidi and Y. Zhong, "Lipid oxidation and improving the oxidative stability," *Chem. Soc. Rev.*, **2010**, 39, 4067-4079.

[8] T. J. Montine, M. D. Neely, J. F. Quinn, M. F. Beal, W. R. Markesbery, L. J. Roberts, and J. D. Morrow, "Causes and consequences of oxidative stress in alzheimer' s disease," *Free Radic. Biol. Med.*, **2002**, 32, 1050–1060.

[9] A. Sevanian, and F. Ursini, "Lipid peroxidation in membranes and low-density lipoproteins: similarities and differences," *Free Radic. Biol. Med.*, **2000**, *29*, 306-311.

[10] A. W. Girotti, "Photosensitized oxidation of membrane lipids: Reaction pathways, cytotoxic effects, and cytoprotective mechanisms," *J. Photochem. Photobiol. B, Biol.*, **2001**, 63, 103–113.

[11] E. N. Frankel, W. E. Neff, and D. Weisleder, "Determination of methyl linoleate hydroperoxides by ^{13}C nuclear magnetic resonance spectroscopy," *Methods Enzymol.,* **1990***, 186*, 380-387.

[12] A. Samadi, L. A. Martínez, M. A. Miranda, and I. M. Morera, "Mechanism of lipid peroxidation photosensitized by tiaprofenic acid: product studies using linoleic acid and 1,4-cyclohexadienes as model substrates," *Photochem. Photobiol.*, **2001**, 73, 359–365.

[13] P. R. Cook, , I. A. Brazell, and E. Jost, "Characterization of nuclear structures containing superhelical DNA," *J. Cell Sci.*, **1976**, *22*, 303-324.

[14] F. Boscá and M. A. Miranda, "Photosensitizing drugs containing the benzophenone chromophore," *J. Photochem. Photobiol. B, Biol.*, **1998**, 43, 1–26.

[15] M. Yamaji, C. Paris, and M. Á. Miranda, "Steady-state and

laser flash photolysis studies on photochemical formation of 4-tert-butyl-4'-methoxydibenzoylmethane from its derivative via the Norrish Type II reaction in solution," *J. Photochem. Photobiol. A, Chem.*, **2010**, 209, 153–157.

[16] Lhiaubet-Vallet, V. and Miranda, M. A., "Phototoxicity of drugs," In *CRC Handbook of Organic Photochemistry and Photobiology, 3rd Ed*, CRC Press: Boca Raton, **2012**; 2, 1541-1555.

[17] C. Paris, V. Lhiaubet-Vallet, O. Jiménez, C. Trullas, and M. Á. Miranda, "A blocked diketo form of avobenzone: Photostability, photosensitizing properties and triplet quenching by a triazine-derived UVB-filter," *Photochem. Photobiol.*, **2009**, 85, 178–184.

[18] P. Klán, T. Šolomek, C. G. Bochet, A. Blanc, R. Givens, M. Rubina, V. Popik, A. Kostikov, and J. Wirz, "Photoremovable protecting groups in chemistry and biology: Reaction mechanisms and efficacy," *Chem. Rev.*, **2013**, 113, 119–191.

[19] J. Wirz and P. Klán, "Searching for improved photoreleasing abilities of organic molecules," *Acc. Chem. Res.*, **2015**, *48*, 3064-3072.

[20] D. D. Young, and A. Deiters, "Photochemical control of biological processes," *Org. Biomol. Chem.*, **2007**, *5*, 999-1005.

[21] F. Palumbo, G. Garcia-Lainez, D. Limones-Herrero, M. D. Coloma, J. Escobar, M. C. Jiménez, M. A. Miranda, and I. Andreu, "Enhanced photo(geno)toxicity of demethylated chlorpromazine metabolites," *Toxicol. Appl. Pharmacol.*, **2016**, 313, 131–137.

[22] P. Møller, "Assessment of reference values for DNA damage detected by the comet assay in human blood cell DNA," *Mutat. Res. - Rev. Mutat. Res.*, **2006**, 612, 84–104.

[23] A. L. Vinette, J. P. McNamee, P. V. Bellier, J. R. N. McLean, and J. C. Scaiano, "Prompt and delayed nonsteroidal anti-inflammatory drug–photoinduced DNA damage in peripheral blood mononuclear cells measured with the comet assay," *Photochem. Photobiol.*, **2003**, 77, 390-396.

[24] P. Miro, M. L. Marin, and M. A. Miranda, “Radical-mediated dehydrogenation of bile acids by means of hydrogen atom transfer to triplet carbonyls,” *Org. Biomol. Chem.*, **2016**, 14, 2679–2683.

Chapter 7:

Instrumentation

1. Absorption measurements

All UV-Vis absorption spectra were registered with a simple beam spectrophotometer (Varian Cary 50) with a quartz cell of 1 cm optical path length.

2. Emission measurements

Fluorescence: The steady-state fluorescence measurements were performed using a spectrofluorimeter Photon Technology International (PTI), LPS-220B model, equipped with a Xenon lamp of 75 W and a monochromator that covers a range from 200 to 700 nm. Measurements were registered after having adjusted the compound absorbance between 0.03 and 0.1 at the excitation wavelength. The time-resolved fluorescence experiments were carried out with a spectrometer Easy Life V equipped with a pulsed LED (λ excitation 340 nm, chapter 3) as an excitation source; the residual excitation signal was filtered in emission by using a cut off filter (50% transmission at 365 nm).

Phosphorescence: the phosphorescence spectra were registered with a spectrophosphorimeter Photon Technology International (PTI, TimeMaster TM/2003) equipped with a pulsed Xenon lamp. The equipment worked in time-resolved mode with a delay time of 500 μs. Compounds were dissolved in ethanol, adjusting their absorbance at ca. 0.8 at the excitation wavelength (with a cuvette of 1 cm optical pathway), then measurements were performed in a quartz tube (0.5 mm diameter) at 77 K.

3. Laser Flash Photolysis (LFP)

For the LFP experiments, two different laser systems were used to achieve excitation at 308 nm, 266 or 355 nm:

- Pulsed excimer Xe/HCl laser (LEXTRA 50 Lambda Physic Laser Technik) with a pulse duration of 10 ns for excitation λ at 308 nm.
- Pulsed laser Nd:YAG (L52137V LOTIS TII) with a pulse duration of 6-8 ns for excitation λ at 355 and 266 nm, using the 3rd and 4th harmonic, respectively.

The full LFP system consists in a pulsed laser, a Xenon lamp (Lo 255 Oriel), a monochromator (Oriel 77200), a photomultiplier (Oriel 70705) and an oscilloscope (TDS-640A Tektronic). The output signal from the oscilloscope was transferred to a personal computer. All experiments were performed in a quartz cell of 1 cm optical path length. All components concentration was adjusted in order to have an absorbance of ~0.3 in the excitation wavelength.

4. Steady-state photolysis:

Irradiations of the samples were run using four different systems:

- A Xenon lamp (150 W or 75 W) equipped with a monochromator from Photon Technology International (PTI) for monochromatic irradiations
- A medium pressure mercury lamp (750 W).
- A Luzchem photoreactor (model LZC-4V) with 14 lamps with a maximum output at 350 nm for UVA irradiations.
- A Thermo Oriel Newport (A91192A) solar simulator equipped with a 1000 W Xenon arc for simulated sunlight irradiations (SSL). The output was adequately filtered to produce a spectrum approximating natural sunlight (1.5 G air mass filter). The spectral output was measured as ca. 1000 mW/cm^2.

Irradiations were performed under anaerobic or aerobic conditions in quartz cells of 1 cm optical path or pyrex tubes, see the experimental details in the corresponding chapter for more information.

5. Femtosecond transient absorption spectroscopy.

The transient absorption spectra were recorded using a typical pump−probe system. The femtosecond pulses were generated with a compact regenerative amplifier that produces pulses centered at 800 nm (~100 fs, 1 mJ/pulse). The output of the laser was split into two parts to generate the pump and the probe beams. Thus,

tunable femtosecond pump pulses were obtained by directing the 800 nm light into an optical parametric amplifier. In the present case, the pump was set at 355 nm and passed through a chopper prior to focus onto a rotating cell containing the solutions under study. The white light used as probe was produced after part of the 800 nm light from the amplifier travelled through a computer controlled 8 ns variable optical delay line and impinge on a CaF_2 rotating crystal. This white light is in turn, split in two identical portions to generate reference and probe beams that then are focused on the rotating cell containing the sample. The pump and the probe are made to coincide to interrogate the sample. A computer controlled imaging spectrometer is placed after this path to measure the probe and the reference pulses and obtain the transient absorption decays/spectra.

6. Nuclear Magnetic Resonance (NMR)

The ^{1}H and ^{13}C NMR spectra were measured by a 300 MHz instrument, and $CDCl_3$ and D_2O were used as solvent for the spectra. The solvent signal was taken as the reference using a chemical shift (δ of ca. 7.26 ppm and 4.79 ppm, 77.16 ppm, for ^{1}H NMR and ^{13}C NMR, respectively. Coupling constants (*J*) are given in Hz.

7. Electronic paramagnetic resonance (EPR) experiments using spin trap

Samples were monochromatically irradiated in a quartz cell of 1 cm path length and then introduced in a flat cell (50 mm of path length, volume 150 µl). The spectrophotometer was a EPR Bruker EMX 10/12 using the following parameters: microwave power 20 mW, amplitude modulation 1 G and modulation frequency 100 kHz.

8. UPLC-HRMS analyses

Exact mass values were determined by using a QTof spectrometer coupled with a liquid chromatography system with a conditioned autosampler at 10 °C. The separation was carried out on an UPLC with a BEH C18 column (50 mm × 2.1 mm i.d., 1.7 µm) or

HSS T3 column (150 mm × 2.1 mm, 1.8 µm). The ESI source was operated in positive or negative ionization mode with the capillary voltage at 1.9 kV or 2.4 kV, respectively. The temperature of the source and desolvation was set at 80 and 400 °C, respectively. The cone and desolvation gas flows were 20 and 800 L h^{-1}, respectively. All data were collected in centroid mode. Leucine-enkephalin was used as the lock mass generating an $[M + H]^+$ ion (*m/z* 556.2771) or $[M - H]^-$ ion (*m/z* 554.2615) at a concentration of 250 pg/mL and flow rate of 50 µL/min to ensure accuracy during the MS analysis.

9. HPLC analyses

The irradiation mixtures were analyzed by reverse phase HPLC using a Varian ProStar instrument equipped with a diode array detector covering a detection range from 200 to 400 nm. Two columns were used: 1) a Mediterranean Sea C18 column 5 µm (250 mm × 4.6 mm). In chapter 5 isocratic mixture of H_2O TFA:acetonitrile (20:80, v:v) with a flow rate of 0.7 mL/min was used, and an isocratic mixture of H_20:acetonitrile (80:20, v:v) with a flow rate of 1 mL/min in chapter 4. 2) LC column 150 x 4.6 mm (Synergi 4 µm Polar-RP 80 Å) in chapter 4 with an isocratic mixture of ammonium acetate (20 mM) in H_20 pH 4.5: acetonitrile (98:2, v:v) and a flow rate 1 mL/min,). All injections were performed by removing a sample from the cuvette at different irradiation times, the injection volume was of 10 µL.

A third column, a chiral column Kromasil 5-AmyCoat (4.6 x 250 mm, 5µ), was used in order to confirm the presence of two diastereoisomers in the dyad AB-KP (isocratic mixture of hexane:isopropanol (80:20, v:v) at a flow rate of 0.7 mL/min, Chapter 5).

Chapter 8:

Annex I

1. Profluorescent probes for radical trapping

In chapter 3, paramagnetic profluorescent probes have been used to investigate the generation of C-centered radicals. These probes consist of a paramagnetic moiety (ie. TEMPO, NR) together with a covalently attached fluorophore (FL) (Figure 2). This way the fluorescence of FL is quenched due to electronic interactions between the two linked species that enhance the intersystem crossing rate and thus, non-radiative deactivation.[1] Indeed, interactions between the unpaired spin of nitroxide radical with the electrons in the conjugated system of the fluorophore induce a change in the multiplicity of the electronic states (Figure 1). The singlet ground state (S_0) and the lowest singlet excited state (S_1) become doublet states (D_0 and D*n* respectively) due to the antiparallel spin of the nitroxide radical.

Furthermore, the triplet excited state (T_1) becomes the lowest excited doublet state (D_1). The consequence of this change in multiplicity means that forbidden transitions, such as the S_1 to T_1 transition (ISC) and subsequent T_1 to S_0 energy loss, become spin-allowed processes between doublet states of different energies.

This way, the relative number of molecules that produce fluorescence from the first excited singlet state is reduced producing, a decrease in the fluorescence signal due to the increase of non-radiative deactivation processes (ie. ISC).

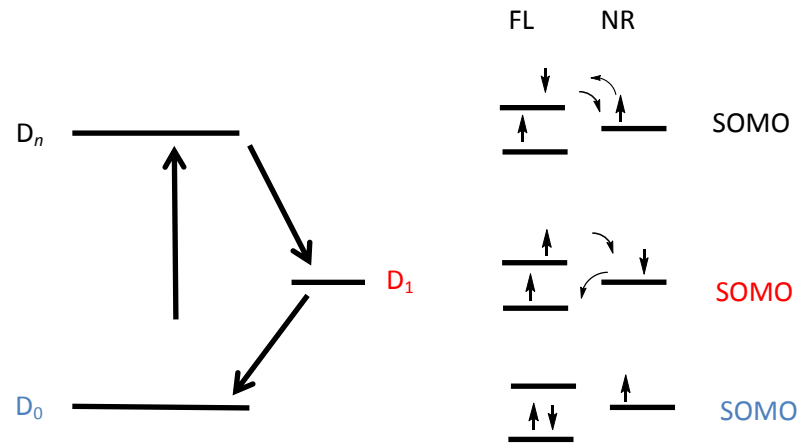

FL = electronic configuration of fluorophore moiety
NR= electronic configuration of nitroxide moiety

Figure 1. The electron exchange mechanism between nitroxide and fluorophore moieties for the D*n* - D_1 and D_1 - D_0 transitions. SOMO, singly occupied molecular orbital.

The covalent binding of the nitroxide and the fluorophore via a spacer unit induces that the two moieties can be considered to be in a constant 'encounter complex', and hence such molecules exist in a 'profluorescent' state with a very low emission yield. The fluorescence is completely restored by removal of the radical character from the molecule after either radical trapping or redox processes.

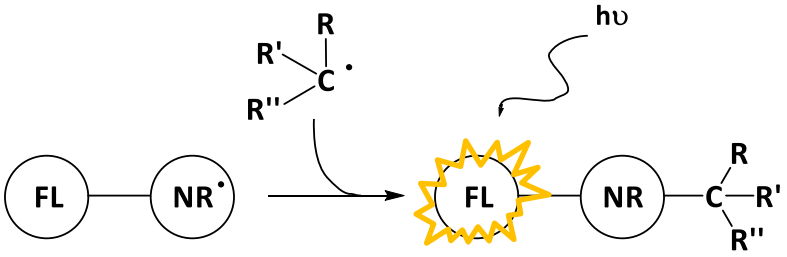

Figure 2. Profluorescent probe composed by a paramagnetic specie (NR) which is covalently attached to a fluorophore (FL).

2. Comet assay, a three day procedure

Comet assay, also known as single cell gel electrophoresis, has been used in Chapter 6 to assess the photogenotoxic potential of the new AB-KP dyad. The step by step procedure is described below.

First day: Irradiation and preparation of the slides

1) Detach FSK (fibroblast skin) cells grown in confluence from the bottom of two 75 cm^2 flask with 2 mL of trypsin/ flask (each flask contains a total of 2.000.000 cells approximately).

2) Centrifuge the cells at 1500 rpm during 5 minutes and suspend the cellular pellet with 5 mL of PBS (free from calcium and magnesium).

3) Count the number of cells with the Neubauer chamber and adjust it in order to have 200.000 cells/ mL of PBS in a 15 mL tube.

4) Incubate cells in ice or at 4°C during 2 hours in order to get repaired from the basal damage that could happen during the trypsin treatment.

5) Suspend cells that could have been sedimented and seed them, *ca.* 500 µL in 12-well plate (100.000 cells per well).

6) Add the compounds to the seeded cells at the desired concentrations and incubate the plates at 4°C during 1 hour. (*S*)-KP is used as the photogenotoxic positive control.

7) Irradiate the plates during 5 minutes with UVA light (2.27 J / cm^2) in the Luzchem photoreactor.

8) Collect the cells in eppendorf tubes, mix 100 µL of cells with 100µL of agarose (1%) (previously heated at the microwave); and place 1 drop for each experimental condition in slides.

9) Let that the drops jellify in the slides and add the lysis solution until covering the slides and incubate overnight at 4°C in the dark. The lysis solution provokes the cellular lysis and allows the DNA extraction.

Second day: Electrophoresis and staining

1) Prepare of the alkaline solution for electrophoresis: 200 mM NaOH and 1mM EDTA in deionized water and keep at 4°C.

2) Transfer the slides to the electrophoresis cuvette, add the electrophoresis alkaline solution until covering the slides, and perform the electrophoresis is performed during 30 minutes at a constant voltage of 21 V.

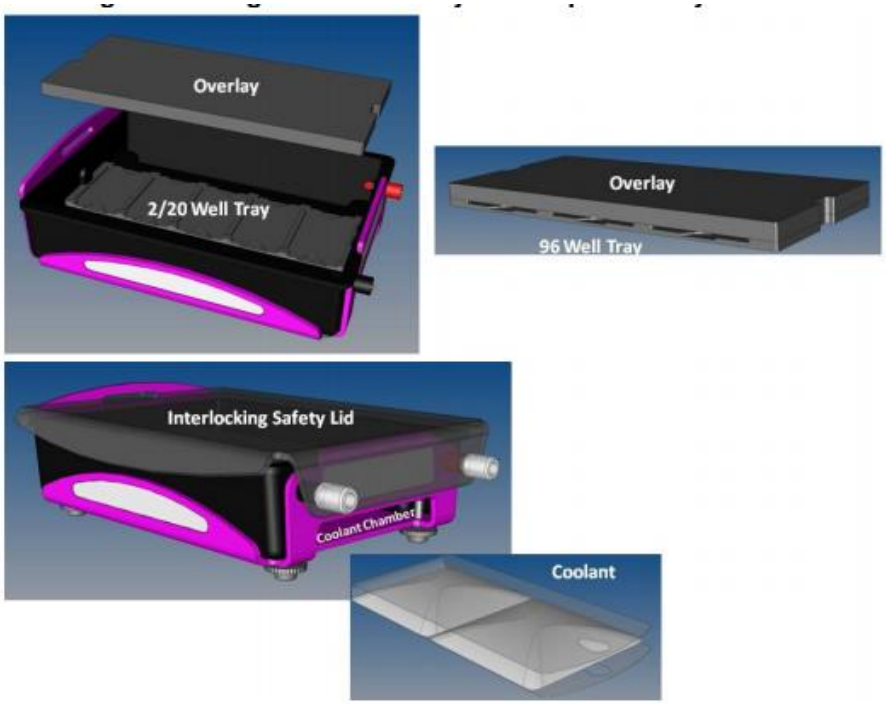

Figure 3. Electrophoresis cuvette

3) Wash the slides with deionized water twice during 5 minutes, with ethanol 70% one time during 5 minutes, and finally with absolute ethanol during 5 minutes once. Let the slides dry in a stove at 37°C.

4) Prepare the TE Buffer (Tris-HCl 10 mM pH 7.5, EDTA 1 mM), and the SYBR GOLD solution (1:10000 dilution of SYBR GOLD in TE buffer ie. 7,5 µL de SYBR GOLD in 75 mL of buffer). This compound is a fluorescent DNA intercalant dye used for the comets visualization.

5) Incubate the slides with the diluted SYBR GOLD during 30 minutes at 4°C in the dark and afterwards, wash them with deionized water.

6) Let the slides dry at room temperature and leave them in the dark during 24 hours.

Third day: Visualization and quantitation using a fluorescent microscope

1) Place the slides below the microscope (inverted fluorescence microscope Leica DMI4000B) objective.

2) Acquire the photographs with manual focus and using the following parameters of the Leica Photo Software photos:

- *Exposition: 370ms*
- *Output: 2,1 X*
- *Saturation: 1,20*
- *Gamma: 1,03*

At least 100 different cells for each experimental condition are needed in order to get reliable results.

3) Analyze the comets with the visual scale analysis. Comets can be classified into different scale analysis taking into account the size of the tail (Figure 4).

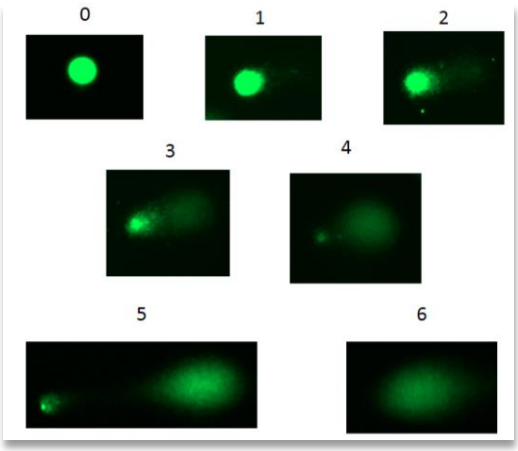

Figure 4. Comet visual scale classification for visual analysis

References

[1] J. P. Blinco, K. E. Fairfull-Smith, B. J. Morrow, and S. E. Bottle, "Profluorescent nitroxides as sensitive probes of oxidative change and free radical reactions," *Aust. J. Chem.*, **2011**, 64, 373–389.

Chapter 9:

General Conclusions

This Doctoral Thesis contrasts the role of 1,3-dicarbonyl compounds as DNA damaging agents to their photoprotective potential. The conclusions of each study are summarized as the following:

As regards the selective photogeneration and photophysical characterization in non-aqueous medium of pyrimidin-5-yl radicals from a 1,3-dicarbonyl precursor derivatives:

- The synthesis of two lipophilic C5 radical precursors, using *tert*-butyl ketone as a photoremovable protecting group, has been developed in a 5 step procedure.
- A new profluorescent probe (AAA-TEMPO) has been designed and synthesized in 4 steps in order to fulfill the following requirements: (*i*) to be excited at wavelengths higher than 350 nm, where DNA does not absorb and (*ii*) to show little if any absorption in the 260−330 nm range in order to not interfere with the absorbance of the *tert*-butyl ketone moiety.
- The photogeneration of lipophilic C5 radicals in non-aqueous medium has been established by radical trapping experiments using TEMPO-based profluorescent probe. Indeed, the irradiation of the photolabile nucleic acid derivatives in the presence of AAA-TEMPO has resulted in an increase of emission, in agreement with the trapping of C5 radical by the paramagnetic probe. Moreover, the formation of the resulting adduct has been confirmed by UPLC-HRMS.
- The laser flash photolysis experiments have evidenced a long lived transient species, which does not decay in the μs range and is centered at 400-420 nm or 350-400 nm for the 5,6-dihydrouridine or 5,6-dihydrothymidine derivatives, respectively.
- These experimental data have been supported by multiconfigurational *ab initio* CASPT2//CASSCF theoretical calculations.

Concerning the evaluation of the potential photosensitizing behavior of an oxidatively generated DNA damage, 5-formyluracil, another 1,3-dicarbonyl derivative:

- It has been evidenced that ForU fulfills the basic requirements to behave as an endogenous photosensitizer. First, it exhibits a red shifted absorption spectrum, with a maximum at *ca.* 297 nm and a tail that reaches up to almost 350 nm by respect to canonical DNA bases extending the active fraction of sunlight. Furthermore it has the ability to populate its triplet excited state (^{3}ForU*) with a E_T value of *ca.* 314 kJ mol^{-1}, making it an appropriate energy donor for a triplet-triplet energy transfer (TTET) to a pyrimidine nucleobase.
- Likewise, the laser flash photolysis experiments reveal a transient species from 320 to 560 nm with a maximum at *ca.* 460 nm and a τ of some μs, which was efficiently quenched by oxygen.
- EPR experiments, using TEMP (2,2,6,6-tetramethylpiperidine) as specific spin trap, confirm the possibility of producing singlet oxygen ($^1O_2$) as a result of ^{3}ForU oxygen quenching.
- The ability of producing photosensitized damage has been studied by means of the synthesis of model Thy-Thy and Cyt-Cyt dyads. These compounds after irradiation in the presence of ForU give rise to the formation of CPDs through TTET. This photosensitized process was tracked down by HPLC, UPLC-HMRS and ^{1}H NMR measurements.
- Finally, the study has been extended to plasmid DNA; this allows establishing the ability of ForU to produce single strand breaks and CPDs.

Related to the development of a new strategy for photoprotection of bioactive molecules taking advantage of the photochemical reactivity of the 1,3-diketo tautomer of the UVA filter avobenzone (AB):

- The design and synthesis of dyads, containing a photosensitive topical drug ((*S*)-KP or DF) and a UVA filter (AB), have been performed in a 2 step procedure taking advantage of the two phenacyl moieties, which is a well-known photoremovable protecting group, present in AB.
- The viability of the controlled photorelease of the drug and its protecting shield, avobenzone, has first been checked upon different solvents (H and non-H donor) and conditions (aerobic and anaerobic). The photorelease process only takes place under H donating conditions (ie. ethanol), which is in agreement with photorelease of phenacyl-like PPG. In addition, it only works under anaerobic conditions evidencing that it takes place through a triplet excited state mediated process.
- Moreover, the photorelease has been achieved using propylene glycol and diethylene glycol as more viscous matrix under aerobic conditions in order to establish a more realistic approach.
- The photorelease of the active ingredients has been followed and quantified by HPLC analysis.
- Triplet excited states of the dyads have been studied by phosphorescence measurements at 77K to determine their energy; but also by laser flash photolysis experiment in ethanol. This allows the characterization of a transient absorption band at 400-420 nm of short lifetime 0.4 µs assigned to the triplet excited state of the dyad by comparison with that of the diketo form of AB.

Concerning the photosafety of the photoactivatable dyad formed between ketoprofen and avobenzone in order to guarantee its harmlessness towards the DNA:

- The transient absorption spectrum of the KP-AB dyad in cyclohexane obtained by laser flash photolysis experiments evidences the triplet excited state of KP *ca.* 525-540 nm and

not that of the AB in its diketo form. By contrast, the transient absorption spectrum in ethanol shows a band at 400 nm that corresponds to AB in its diketo form.

- Moreover, the impact on the cellular membrane has been addressed by UVA irradiation of linoleic acid solutions in the presence of the dyad. The phototoxic potential of the AB-KP dyad has been confirmed by UV-Vis spectrophotometry through the formation of the conjugated dienic hydroperoxides derived from linoleic acid.
- Finally, the comet assay experiments demonstrate that AB-KP dyad does not exhibit a photogenotoxic potential towards cellular DNA since the non-damaged round shape of the cell is still observed after UVA irradiation, if compared to that of KP.

Summary

The 1,3-dicarbonyl functional groups are present in a wide range of compounds. Their photochemistry displays interesting features due to the presence of various isomers that exhibit particular spectroscopic properties or photoreactivity. In this context, the large UVA absorption of the chelated enol isomer of dibenzoylmethanes has been widely used in cosmetic industry for photoprotection purposes. The β-dicarbonyl compounds are also found in the structure of photoreactive thymidine or uridine derivatives bearing a pivaloyl or formyl group at C5 position.

The main objective of this thesis is to contrast the role of these 1,3-dicarbonyl compounds as DNA damaging agents to their photoprotective potential. Thus, on the one hand the properties of β-dicarbonyl compounds as part of the DNA structure have been addressed through the study of C5-pivaloyl substituted dihydropyrimidines as photolabile precursors of carbon centered radicals, but also through the assessment of the DNA oxidatively generated damage, 5-formyl uracil, as a potential intrinsic DNA photosensitizing agent. On the other hand, the diketo isomer of the most representative UVA filter *ie.* 4-*tert*-butyl-4´-methoxydibenzoylmethane, the so-called avobenzone filter, contains two photoremovable phenacyl groups. This has led to the development of a new strategy for photoprotection based on the photorelease of a photosensitizing topical drug together with its protecting UVA filter.

Firstly, 5,6-dihydropyrimidines have been derivatized using a *tert*-butyl ketone photolabile group in order to study the generation of C5-centered radicals in non aqueous media. This is of particular importance as the microenvironment provided by the DNA structure and its complexes with proteins such as histones may not be fully reproduced by aqueous media, and the pyrimidine-derived radical

would be embedded into the complex DNA/RNA system, which constitutes a heterogeneous environment. Thus, laser flash photolysis study in acetonitrile of the designed 1,3-dicarbonyl derivatives gives rise to the formation of the purported 5,6-dihydropyrimidin-5-yl radicals. Their characterization shows long lived transient species, which do not decay in the μs range and are centered at 400-420 nm or 350-400 nm for the 5,6-dihydrouridine or 5,6-dihydrothymidine derivatives, respectively. Moreover, radical generation has also been evidenced by steady state fluorescence experiments by using a profluorescent radical trap (AAA-TEMPO). This probe has been especially designed to fulfill principally two requirements: (*i*) be excited at wavelengths higher than 350 nm, where DNA does not absorb and (*ii*) show little if any absorption in the 260−330 nm range in order to not interfere with the absorbance of the *tert*-butyl ketone moiety. Thus, irradiation of the photolabile nucleic acid derivatives in the presence of AAA-TEMPO results in an increased emission, in agreement with the trapping of C5 radical by the paramagnetic probe. Formation of the resulting adduct has been confirmed by UPLC-HRMS. Experimental data have been corroborated with *ab initio* CASPT2//CASSCF theoretical calculations.

In a second chapter, another 1,3-dicarbonyl derivative of pyrimidine has been investigated. Indeed, the oxidatively generated damage 5-formyluracil (ForU) presents interesting features as a potential intrinsic DNA photosensitizing agent. Thus, spectroscopic studies reveal that ForU has not only an absorption in the UVA/UVB range, where canonical bases barely absorb, but also a triplet excited state (^{3}ForU*) with a lifetime of some μs and with an energy high enough to photosensitize the well-known cyclobutane pyrimidine dimers (CPDs) through triplet-triplet energy transfer. This process has been confirmed by means of the synthesis of model Thy-Thy and Cyt-Cyt dyads, which after irradiation in the presence of ForU have been demonstrated to produce CPDs. Finally, the study extended to plasmid DNA allows establishing the ability of ForU to produce single strand breaks and CPDs.

Next, the attention has been focused on the development of a new strategy for photoprotection of bioactive molecules taking advantage of the photochemical reactivity of the 1,3-diketo tautomer of the UVA filter avobenzone (AB). The selected bioactive compounds are two photosensitive topical non steroidal anti-inflammatory drugs, namely (S)-ketoprofen (KP) and diclofenac (DF). In this context, the diketo tautomer of avobenzone contains two phenacyl moieties, which are well-known photoremovable protecting groups. Thus, a judicious design of a pro-drug/pro-filter dyad allows the photorelease of the drug and its protecting shield, avobenzone. The viability of this controlled release of the active ingredients was checked in different solvents of different H donating properties and viscosity to simulate topical formulation. In addition, laser flash photolysis studies in ethanol allow characterization of a transient absorption band at 400-420 nm assigned to the triplet excited state of the dyad by comparison with that of the diketo form of AB.

Finally, the photosafety of the photoactivatable dyad formed between ketoprofen and avobenzone has been assessed. An interesting result is obtained from the transient absorption spectra of the KP-AB dyad in cyclohexane where, by contrast with ethanol, the observed species is the triplet excited state of KP and not that of the AB in its diketo form. This is of paramount importance in terms of phototoxicity and photogenotoxicity in connection with the widely studied photosensitizing properties of KP. The impact on the cellular membrane has been addressed by UVA irradiation of linoleic acid solutions in the presence of the dyad. Phototoxic potential of the dyad has been evidenced by UV-Vis spectrophotometry through the formation of the conjugated dienic hydroperoxides derived from linoleic acid. However, AB-KP does not exhibit a photogenotoxic potential as demonstrated by comet assay experiments, where by contrast with KP, the non damaged round shape of the cell is still observed after UVA irradiation.

Resumen

Los grupos funcionales 1,3-dicarbonilo están presentes en una amplia gama de compuestos. Su fotoquímica muestra características interesantes debido a la presencia de varios isómeros que presentan propiedades espectroscópicas o de fotorreactividad particulares. En este contexto, la gran absorción en el UVA del isómero enol quelado de los dibenzoilmetanos ha sido ampliamente utilizada en la industria cosmética con fines de fotoprotección. Los compuestos β-dicarbonilicos también se encuentran en la estructura de derivados fotorreactivos de timidina o de uridina que llevan un grupo pivaloilo o formilo en la posición C5.

El objetivo principal de esta tesis es contrastar el papel de dichos compuestos 1,3-dicarbonilicos como agentes que dañan el ADN con respecto a su potencial fotoprotector. Por lo tanto, por un lado, se han abordado las propiedades de los compuestos β-dicarbonilicos como parte de la estructura del ADN mediante el estudio de dihidropirimidinas sustituidas en C5 por una función pivaloilo como precursores fotolábiles de radicales centrados en carbono, pero también a través de la evaluación de un daño oxidativo generado en el ADN, el 5-formil uracilo, como un potencial agente fotosensibilizador intrínseco de la doble hélice. Por otro lado, el isómero dicetona del filtro UVA más representativo, 4-*tert*-butil-4'-metoxidibenzoilmetano conocido como avobenzona, contiene dos grupos fotolábiles de tipo fenacilo. Esto ha llevado al desarrollo de una nueva estrategia de fotoprotección basada en la fotoliberación de un fármaco fotosensiblizante de uso tópico junto con su filtro solar protector del UVA.

En primer lugar, 5,6-dihidropirimidinas han sido derivatizadas utilizando el grupo fotolábil *tert*-butil cetona con el fin de estudiar la generación de radicales centrados en C5 en un medio no acuoso. Esto es de particular importancia ya que el microambiente proporcionado por la estructura del ADN y sus complejos con

proteínas, tales como las histonas, puede no estar completamente reproducido en medios acuosos, y el radical derivado de pirimidina estaría embebido en el complejo sistema ADN / ARN, lo que constituye un ambiente heterogéneo. Por lo tanto, el estudio por fotólisis de destello láser en acetonitrilo de los derivados 1,3-dicarbonilicos diseñados da lugar a la detección de los supuestos radicales 5,6-dihidropirimidin-5-ilo. Su caracterización muestra especies transitorias de vida larga, que no decaen en el rango de μs y están centrados a 400-420 nm o 350-400 nm para los derivados 5,6-dihidrouridina o 5,6-dihidrotimidina, respectivamente. Además, la generación de radicales también se ha evidenciado mediante experimentos de fluorescencia en estado estacionario mediante el uso de una sonda profluorescente (AAA-TEMPO) que atrapa el radical. Esta sonda ha sido especialmente diseñada para cumplir dos requisitos principales: (*i*) excitarse a longitudes de onda superiores de 350 nm, donde el ADN no absorbe y (*ii*) mostrar poca o ninguna absorción en el rango de 260-330 nm para no interferir con la absorbancia de la porción *tert*-butil cetona. Por lo tanto, la irradiación de los derivados fotolábiles del ácido nucleico en presencia de AAA-TEMPO da como resultado un aumento de la emisión, de acuerdo con la captura del radical C5 por la sonda paramagnética. La formación del aducto resultante se ha confirmado mediante UPLC-HRMS. Asimismo, los datos experimentales se han corroborado con cálculos teóricos ab initio CASPT2 // CASSCF.

En un segundo capítulo, otro derivado 1,3-dicarbonílico de la pirimidina ha sido investigado. De hecho, el daño oxidativo 5-formiluracilo (ForU) presenta características interesantes como potencial agente fotosensibilizador intrínseco del ADN. Por lo tanto, los estudios espectroscópicos revelan que ForU no solo tiene una absorción en el rango UVA / UVB, donde las bases canónicas apenas absorben, sino también presenta un estado triplete excitado (^{3}ForU *) con un tiempo de vida de algunos μs y con una energía lo suficientemente alta como para fotosensibilizar la formación de los

conocidos dímeros de pirimidina de tipo ciclobutano (CPDs) a través de una transferencia de energía triplete-triplete. Este proceso ha sido confirmado por medio de la síntesis de díadas modelo Thy-Thy y Cyt-Cyt, ya que después de la irradiación en presencia de ForU se ha demostrado que producen CPDs. Finalmente, el estudio se extendió a ADN plasmídico permitiendo establecer la capacidad de ForU para inducir roturas de cadena simple y CPDs.

A continuación, la atención se ha centrado en el desarrollo de una nueva estrategia para la fotoprotección de moléculas bioactivas aprovechando la reactividad fotoquímica del tautómero 1,3-dicetona de la avobenzona (AB), un filtro del UVA. Los compuestos bioactivos seleccionados son dos fármacos antiinflamatorios no esteroideos de uso tópico con propiedades fotosensibilizantes, (*S*)-ketoprofeno (KP) y diclofenaco (DF). En este contexto, el tautómero dicetona de la avobenzona contiene dos restos fenacilo, que es un grupo protector fotolábil muy establecido. Por lo tanto, un diseño juicioso de una díada profármaco / profiltro permite la fotoliberación del fármaco y de su protector, la avobenzona. La viabilidad de esta liberación controlada de los ingredientes activos se verificó en diferentes disolventes de diferente carácter dador de H y viscosidad para simular la formulación tópica. Además, los estudios de fotólisis de destello láser en etanol permiten la caracterización de una banda de absorción transitoria a 400-420 nm, la cual ha sido asignada al estado excitado triplete de la díada mediante comparación con la de la forma dicetónica de AB.

Finalmente, se ha evaluado la fotoseguridad de la díada fotoactivable formada entre el (*S*)-ketoprofeno y la avobenzona. Se obtiene un resultado interesante a partir de los espectros de absorción transitoria de la díada AB-KP en ciclohexano donde, al contrario que en etanol, la especie observada es el estado excitado triplete del KP y no el de la AB en su forma dicetona. Esto es de suma importancia en términos de fototoxicidad y fotogenotoxicidad en relación con las propiedades fotosensibilizantes ampliamente

estudiadas del KP. El impacto de la díada sobre la membrana celular se ha abordado mediante irradiación UVA de soluciones de ácido linoleico en presencia de la díada. El potencial fototóxico de AB-KP se ha evidenciado mediante espectrofotometría UV-Vis revelando la formación de derivados hidroperóxidos diénicos conjugados del ácido linoleico. Sin embargo, la diada AB-KP no exhibe un potencial fotogenotóxico como lo demuestran los experimentos del ensayo comet, donde a diferencia del KP, la forma redonda no dañada de la célula todavía se observa después de la irradiación UVA.

Resum

Els grups funcionals 1,3-dicarbonil estan presents en una àmplia gamma de compostos. La seua fotoquímica mostra característiques interessants a causa de la presència de diversos isòmers que presenten propietats espectroscòpiques o de fotorreactivitat particulars. En aquest context, la gran absorció en l' UVA de l'isòmer enol quelat dels dibenzoilmetans ha sigut utilitzada àmpliament en la indústria cosmètica amb fins de fotoprotecció. Els compostos β-dicarbonil també és troben en l'estructura de derivats fotorreactius de timidina o d'uridina que porten un grup pivaloil o formil en la posició C5.

L'objectiu principal d'aquesta tesi és contrastar el paper d'aquests compostos 1,3-dicarbonil com a agents que danyen l'ADN respecte al seu potencial fotoprotector. Per tant, d'una banda, les propietats dels compostos β-dicarbonil com a part de l'estructura de l'ADN s'han abordat mitjançant l'estudi de 5,6-dihidropirimidines substituïdes en C5 per un grup pivaloil com a precursors fotolàbils de radicals centrats en carboni, però també a través de l'avaluació del dany oxidatiu generat en l'ADN, el 5-formil uracil, com un potencial agent fotosensibilitzador intrínsec de l'ADN. D'altra banda, l'isòmer dicetona del filtre UVA més representatiu, 4-*tert*-butil-4'-metoxidibenzoilmetà conegut com avobenzona, conté dos grups fotolàbils de tipus fenacil. Açò ha portat al desenvolupament

d'una nova estratègia de fotoprotecció basada en el fotoalliberament d'un fàrmac tòpic amb propietats fotosensibilitzants juntament amb el seu filtre protector de l'UVA.

En primer lloc, 5,6-dihidropirimidines han sigut derivatitzades utilitzant el grup fotolàbil *tert*-butil cetona amb la finalitat d'estudiar la generació de radicals centrats en C5 en un mitjà no aquós. Açò és de particular importància ja que el micró ambient proporcionat per l'estructura de l'ADN i els seus complexos amb proteïnes, tals com les histones, pot no estar completament reproduït en mitjans aquosos, i el radical derivat de pirimidina estaria embegut en el complex sistema ADN / ARN, la qual cosa constitueix un ambient heterogeni. Per tant, l'estudi de fotòlisi de flaix làser en acetonitril dels derivats 1,3-dicarbonil dissenyats dóna lloc a la formació dels suposats radicals 5,6-dihidropirimidin-5-il. La seua caracterització mostra espècies transitòries de vida llarga, que no decauen en el rang de μs i estan centrats a 400-420 nm o 350-400 nm per als derivats 5,6-dihidrouridina o 5,6-dihidrotimidina, respectivament. A més, la generació de radicals també s'ha evidenciat mitjançant experiments de fluorescència en estat estacionari mitjançant l'ús d'una sonda profluorescent (AAA-TEMPO) que atrapa el radical. Aquesta sonda ha sigut especialment dissenyada per a complir principalment dos requisits: (*i*) excitar-se a longituds d'ona superiors de 350 nm, on l'ADN no absorbeix i (*ii*) mostrar poca o cap absorció en el rang de 260-330 nm per a no interferir amb l'absorbància de la porció *tert*-butil cetona. Per tant, la irradiació dels derivats fotolàbils d'àcid nucleic en presència de AAA-TEMPO dóna com resultat un augment de l'emissió, d'acord amb la captura del radical C5 per la sonda paramagnètica. La formació del adducte resultant s'ha confirmat mitjançant UPLC-HRMS. Així mateix, les dades experimentals s'han corroborat amb càlculs teòrics ab initio CASPT2 // CASSCF.

En un segon capítol, un altre derivat 1,3-dicarbonil de la pirimidina ha sigut investigat. De fet, el dany oxidatiu 5-formiluracil

(ForU), presenta característiques interessants com a potencial fotosensibilitzador intrínsec de l'ADN. Per tant, els estudis espectroscòpics revelen que ForU no solament té una absorció en el rang UVA / UVB, on les bases canòniques amb prou faenes absorbeixen, sinó també presenta un estat triplet excitat (^{3}ForU*) amb un temps de vida d'alguns μs i amb una energia prou alta com per a fotosensibilitzar la formació dels coneguts dímers de pirimidina de tipus ciclobutà (CPDs) a través d'una transferència d'energia triplet-triplet. Aquest procés ha sigut confirmat per mitjà de la síntesi de diades model Thy-Thy i Cyt-Cyt, que després de la irradiació en presència de ForU s'ha demostrat que produeixen CPDs. Finalment, l'estudi es va estendre a ADN plasmídic permetent establir la capacitat de ForU per a produir trencaments de cadena simple i CPDs.

A continuació, l'atenció s'ha centrat en el desenvolupament d'una nova estratègia per a la fotoprotecció de molècules bioactives aprofitant la reactivitat fotoquímica del tautòmer 1,3-dicetona del filtre de l'UVA Avobenzone (AB). Els compostos bioactius seleccionats són dos fàrmacs antiinflamatoris no esteroïdals d'ús tòpic amb propietats fotosensibilizants, (*S*)-ketoprofè (KP) i diclofenac (DF). En aquest context, el tautòmer dicetona de l'avobenzona conté dues fraccions fenacil, que es un grup protector fotolàbil ben conegut. Per tant, un disseny judiciós d'una diada profàrmac / profiltre permet el fotoalliberament del fàrmac i del seu escut protector, l'avobenzona. La viabilitat d'aquest alliberament controlat dels ingredients actius es va verificar en diferents dissolvents de diferent caràcter dador d'hidrogen i viscositat per a simular la formulació tòpica. A més, els estudis de fotòlisi de flaix làser en etanol permeten la caracterització d'una banda d'absorció transitòria a 400-420 nm, la qual ha sigut assignada a l'estat excitat triplet de la diada mitjançant comparació amb la de la forma dicetònica de AB.

Finalment, s'ha avaluat la fotoseguretat de la diada fotoactivable formada entre el (*S*)-ketoprofè i l'avobenzona. S'obté

un resultat interessant a partir dels espectres d'absorció transitòria de la diada KP-AB en ciclohexà on, al contrari que en etanol, l'espècie observada és l'estat excitat triplet del KP i no el de la AB en la seua forma dicetònica. Açò és de summa importància en termes de fototoxicitat i fotogenotoxicitat en relació amb les propietats fotosensibilitzants àmpliament estudiades del KP. L'impacte sobre la membrana cel·lular s'ha abordat mitjançant la irradiació UVA de solucions d'àcid linoleic en presència de la diada. El potencial fototòxic de la diada s'ha evidenciat mitjançant espectrofotometria UV-Vis revelant la formació de derivats hidroperòxids diènics conjugats de l'àcid linoleic. No obstant açò, la diada AB-KP no exhibeix un potencial fotogenotòxic com ho demostren els experiments de l'assaig comet, on a diferència del KP, la forma redona no danyada de la cèl·lula encara s'observa després de la irradiació UVA.

Publications Related to this Doctoral Thesis

I. Aparici-Espert, A. Francés-Monerris, G. M. Rodríguez-Muñiz, D. Roca-Sanjuán, V. Lhiaubet-Vallet, and M. A. Miranda "A combined experimental and theoretical approach to the photogeneration of 5,6-dihydropyrimidin-5-yl radicals in non-aqueous media," *J. Org. Chem.,* **2016**, 81, 4031-4038.

I. Aparici-Espert, M. C. Cuquerella, C. Paris, V. Lhiaubet-Vallet and M. A. Miranda "Photocages for protection and controlled release of bioactive compounds," *Chem. Commun.,* **2016**, 52, 14215-14218.

I. Aparici-Espert, G. Garcia-Lainez, I. Andreu, M. A. Miranda and V. Lhiaubet-Vallet, "Oxidatively generated lesions as internal photosensitizers for pyrimidine dimerization in DNA," *ACS Chem. Biol.,* 2018, 13, 542−547.

I. Aparici-Espert, V. Lhiaubet-Vallet and M. A. Miranda, "Sunscreen-based photocages for topical drugs: A photophysical and photochemical study of a diclofenac-avobenzone dyad," *Molecules,* **2018**, 23, 673.

Other publications

Ming-De Li, Z. Yan, R. Zhu, D. L. Phillips,I. Aparici-Espert, V. Lhiaubet-Vallet, and M. A. Miranda "Enhanced drug photosafety by interchromophoric interaction due to intramolecular charge separation," *Chem. Eur. J.*, **2018**, 24, 1–7.